Plasticity of Antioxidant Defense Pathways in Response to Aging and Cadmium in Glutathione-Deficient Mice

Christopher M. Schaupp

A dissertation
submitted in partial fulfillment of the
requirements for the degree of

Doctor of Philosophy

University of Washington
2017

Reading Committee:

Terrance J. Kavanagh, Chair
David L. Eaton
Peter S. Rabinovitch

Program Authorized to Offer Degree:
Environmental and Occupational Health Sciences – Public Health

University of Washington

Abstract

Plasticity of Antioxidant Defense Pathways in Response to Aging and Cadmium in Glutathione-Deficient Mice

Chair of the Supervisory Committee:
Professor Terrance J. Kavanagh
Department of Environmental and Occupational Health Sciences

The ability to maintain cellular homeostasis during aging is an important determinant of organismal health throughout the lifespan. Understanding key pathways that govern homeostatic responses to endogenous and exogenous stressors is an important goal in aging research. The Nrf2 (nuclear factor erythroid 2-related factor 2; NFE2L2)/Keap1 (Kelch-like erythroid cell-derived protein with CNC homology [ECH]-associated protein 1) signaling pathway is one of the most important cellular defense and survival pathways, and has been shown to interact with a myriad of other signaling pathways, including those controlling xenobiotic metabolism, cellular growth, proliferation and nutrient sensing (Chartoumpekis and Kensler, 2013). Nrf2 can modulate the expression of genes involved in gluconeogenesis, fatty acid β-oxidation and lipogenesis, and can enhance (and be enhanced by) the effects of caloric restriction, a regimen that is known to promote longevity in many species (Fontana and Partridge, 2015; Kulkarni et al., 2013; Ruetenik and Barrientos, 2015; Slocum et al., 2016). In this regard, Nrf2 and its orthologs have been shown to decrease aging associated pathology and increase longevity in a number of organisms (Bruns et al., 2015; Lewis et al., 2015; Rahman et al., 2013; Sykiotis et al., 2011).

Among the most important Nrf2 regulated genes are glutamate cysteine ligase catalytic (GCLC) and modifier (GCLM) subunits, which are critical for the synthesis of the antioxidant tripeptide glutathione (GSH), a free radical scavenger and cofactor for many antioxidant enzymes (Franklin et al., 2009). *Gclm* null mice are a model of chronic GSH deficiency, and have modified expression of a number of antioxidant genes, including those regulated by Nrf2 (Chen et al., 2012; Haque et al., 2010; Kendig et al., 2011), presumably to compensate for their low GSH levels. Moreover, because *Gclm* null mice appear to have chronic Nrf2 activation, they exhibit resistance to some but not all environmental stressors (Chen et al., 2012; McConnachie et al., 2007), including ozone (Johansson et al., 2010), diesel exhaust (Weldy et al., 2011), and CdSe/ZnS quantum dot nanoparticles (McConnachie et al., 2013). Importantly, *Gclm* null mice are approximately 20% leaner than *Gclm* wild-type mice, appear resistant to high fat diet-induced weight gain, are more glucose-tolerant and insulin-sensitive than *Gclm* wild-type mice (Kendig et al., 2011; Yang et al., 2002), and may be resistant to the development of Type II diabetes mellitus (T2DM), a disease of major public health importance associated with aging. While these resistant phenotypes have been shown to occur in younger (10 week old) *Gclm* null mice, it is unclear if they persist with aging.

Because Nrf2 signaling may be attenuated with aging (Rahman et al., 2013; Zhang et al., 2012a), the resistance of young *Gclm* null mice against metabolic and environmental stress may not persist with age. Being both GSH deficient and Nrf2 inefficient, older *Gclm* null mice may show greater susceptibility to exogenous stressors, such as cadmium. This model toxicant has been chosen because Cd has been associated with the development of type II diabetes mellitus (T2DM) in several species (Edwards

and Ackerman, 2016) and is known to accumulate in pancreatic β-cells, causing their dysfunction (i.e. impaired insulin release) (El Muayed et al., 2012), in addition to its more canonical role as a oxidative stress-inducing heavy metal.

In this work, we addressed whether aging compromises the favorable phenotype of increased Nrf2 activity and improved glucose homeostasis observed in younger *Gclm* null mice, and if so, whether such compromise was due to attenuation of Nrf2 signaling with aging, which has been reported by others to occur in flies, mice, and rats (Rahman et al., 2013; Shih and Yen, 2007; Suh et al., 2004; Zhang et al., 2012a). The main thrust of this work was to confirm existing data on the differences in Nrf2 activity and glucose homeostasis between young *Gclm* wild-type and null mice, and to add to these data by examining the effects of aging and cadmium exposure on these phenotypes.

In response to aging and acute cadmium administration, we found *Gclm* null mice maintain improved glutathione redox homeostasis, increased Nrf2 target gene expression and inducibility, and improved parameters of glucose homeostasis, relative to *Gclm* wild-type mice. These unexpected findings support the notion that chronic adaption to severely compromised glutathione levels, primarily via upregulation of Nrf2 stress responses, persists throughout the lifespan. This stands in contrast to the prevailing literature suggesting that compensatory cytoprotective responses (particularly antioxidant defense) decline with age. This work supports the notion that pharmacologic interventions to upregulate the Nrf2 pathway could improve late-life insulin sensitivity, glucose homeostasis and promote an improved healthspan.

Table of Contents

List of Figures

Acknowledgements

This work would not have been possible without the support from my colleagues at the University of Washington, Oregon State University, and Montana State University. Thanks especially to all the members of the Kavanagh lab, past and present, who have helped guide me through this maze.

Thanks to my "Dream Team" of dissertation committee members, Drs. Karin E. Bornfeldt, David L. Eaton, Terrance J. Kavanagh, David J. Marcinek, and Peter S. Rabinovitch, for all your insights, suggestions, and patience.

I would also like to recognize the following organizations and individuals for providing financial support for this work, and travel funds for sharing the research presented herein at professional meetings:

National Institute on Aging

National Institute of Environmental Health Sciences

Society of Toxicology

University of Washington Graduate School

UW Department of Environmental and Occupational Health Sciences

UW Nathan Shock Center

UW Genetic Approaches to Aging Training Grant

Bruce Kelman, Ph.D.

Dedication

What a journey. I can't begin to adequately express my gratitude to all those who have helped me along the way. It truly does seem like just yesterday that I packed up the trailer with my dad and headed for Seattle, giving in to the voices telling me to "Go West, young man." I have been incredibly fortunate to have so many wonderful, helpful people in my life. I cannot envision a better community to help me grow from that proverbial young man.

To my parents, Michael and Marcia: I cannot thank you enough for all the love, support, and unwavering belief you have provided me over the years, even during that awful middle school era! Cliché as it might be, I truly would not be who I am today without both of you. Living across the country has been difficult, but just remember—I gave you a reason to visit the Pacific Northwest!

Knut, sadly you're not around to see this day. I miss you and can't really articulate what it meant to have you around to talk to and visit with. Thanks for being such a great, supportive friend. Hope that you're at peace.

Uncle Mitch, though we don't see each other very often anymore, I want you to know that you were the motivating force behind my decision to become an environmental health scientist. I'll always hold close to my heart those times at the Taylor farm where I was educated on barns, tractors, cars, football, Neil Young, and native Wisconsin flora and fauna, and all the great writings you introduced me to, namely 'A Silent Spring,' and, of course, 'A Sand County Almanac.' You helped ignite that fierce green fire within.

To Ellyn, who will never know how much she means to me. Thank you for being a steadying influence in my life and the best co-adventurer a boy could ask for. Looking forward to exploring as much of this beautiful country as I can with you! Particular thanks for agreeing to that hike during our last semester at Luther. Worked out pretty well, wouldn't you say?

Dianne and Collin—though I'm sure he knows it, Terry is incredibly lucky to have both of you. Thanks for taking me under your wings and providing advice and laughs along the way! Also special thanks to David for you help and friendship. You guys are the best!

Dave Eaton, from the beginning you have been an excellent teacher and the go-to person for all things toxicology. Writing a review and book chapter together was a great honor. I'm privileged to have worked with you. The UW Graduate School is fortunate to call you Dean.

Before I wax poetic for too much longer, I would be remiss if I failed to recognize my mentor and friend, Terry Kavanagh. TK, you are one of a kind. Over these past six years, I've come to the conclusion that if there were one word I would choose to describe you, it would be 'genuine.' Genuinely nice, genuinely kind, genuinely funny, genuinely intelligent, I could keep going on. There is no so-called 'curtain' to pull back on your personality—what you see is what you get, and that's a great thing! Your passion for research and commitment to science (and I guess casting a line, too) is so inspiring. I'll miss talking about the 'toots and the twigs.' Thank you for being such a great role model, and for welcoming me into your lab and life!

Finally, thanks to all of my friends and anyone I haven't explicitly mentioned here. You know who you are. I've gotten here because of you; thank you for making my life great!

Chapter 1: Introduction

1.1. Redox Homeostasis and glutathione.

At the most basic level, redox homeostasis refers to a functional balance between reduction and oxidation (i.e. pro- and anti-oxidant molecules) within the cell. Rather than having a defined numerical value, redox homeostasis exists on a spectrum, which varies depending on cell and tissue type. This is important, because cells require a fair amount of 'redox buffering capacity'(e.g., intracellular antioxidants) to deal with the millions of oxidative chemical reactions occurring at any given time. Imbalances in redox homeostasis are often associated with cellular dysfunction.

Tipping the balance towards an overly oxidative state (oxidative stress) is associated with macromolecular damage, aging, and multiple disease states, including cardiovascular disease, metabolic dysfunction, neurodegeneration, pulmonary fibrosis, etc. (Berlett and Stadtman, 1997; Betteridge, 2000; Bhatti et al., 2017; Cheresh et al., 2013; Coyle and Puttfarcken, 1993; Dhalla et al., 2000; Jadeja et al., 2017; Roberts and Sindhu, 2009; Sohal and Weindruch, 1996; Uttara et al., 2009). Cells are under constant barrage from oxidants. Reactive oxygen species (ROS), such as superoxide and hydroxyl radicals, are some of the most common oxidants, and are regularly produced as a result of cellular respiration. Oxidative stress can also contribute significantly to the formation of other damaging molecules or states, such as advanced glycation end products (AGEs) and protein carbonylation, which can in turn stimulate production of ROS, compounding the state of oxidative stress (Coughlan et al., 2009; Guimaraes et al., 2010; Yan et al., 2008).

Conversely, an overly reductive state (reductive stress) is also problematic,

potentially leading to impaired signal transduction, abnormal cell growth and differentiation, and defective host defense—processes which require oxidants (D'Autréaux and Toledano, 2007; Ray et al., 2012; Veal and Day, 2011; Winterbourn and Kettle, 2013). While the importance of low-level oxidants for normal cellular function is becoming more readily recognized, oxidative stress remains more of a concern than reductive stress, as evidenced by the fact that the redox state of most mammalian cell types is slightly reduced at equilibrium. The sheer abundance of highly-conserved enzymes which exist to detoxify oxidative molecules, such as catalase, superoxide dismutases (SODs), glutathione *S*-transferases (GSTs), glutathione peroxidases (GPXs) etc. also point to the importance of combating oxidation in all types of life, from archaea, to prokaryotes, to eukaryotes.

Two principal thiol-based redox buffering systems exist within mammalian cells: the thioredoxin (Trx) and glutathione (GSH) systems (Lu and Holmgren, 2014). These systems use redox-sensitive cysteine residues to control their functions, of which there are many, perhaps the most important being their role as antioxidants. These systems are similar in a number of aspects, including that both have enzymes for regenerating reduced cysteine residues (Trx uses thioredoxin reductase (TrxR), and GSH uses glutathione reductase (GR)). TrxR1 and GR are dependent on NADPH pools for reducing power. Within mammalian cytosol and nuclei, the thioredoxin system provides an electron to Trx-dependent peroxidases (Prx), which can remove ROS, similar to the action of glutathione peroxidase (GPx1) (Lu and Holmgren, 2014). Under stress, GSH can regulate protein function by *S*-glutathionylation through glutaredoxins (Grx). Both systems are important for "recharging" ribonucleotide reductase (RNR), a protein

essential for DNA synthesis. In addition to sharing overlapping functions, there is significant crosstalk between the GSH and Trx systems. Under conditions where TrxR is unable to provide reducing equivalents to Trx, GSH and Grx can provide electrons to Trx, and the reverse is also true (i.e. the Trx system can reduce glutathione disulfide (GSSG), the oxidized form of GSH), providing a basis for the redundancy of these systems (Du et al., 2012; Tan et al., 2010). The duality of these systems in higher organisms points to their extreme importance in maintaining mammalian cellular homeostasis, proliferation, and defense.

1.2. *Gclm* null mouse model.

Though the Trx and GSH systems share many similarities, they do diverge in some important ways. The work presented herein focuses on the GSH system. Glutathione is an abundant, low molecular weight antioxidant present within mammalian cells at millimolar levels. GSH serves several vital functions, including detoxification, free radical scavenging, maintenance of protein redox status, providing a reservoir for cysteine, modulating critical processes such as DNA synthesis, and protein modification (*S*-glutathionylation) (Franklin et al., 2009; McConnachie et al., 2007).

Glutathione is a tripeptide comprised of the amino acids glutamate, cysteine, and glycine, and is synthesized *de novo* using a two-step, ATP-dependent enzymatic process (Figure 1) (Meister and Anderson, 1983). The first, and rate-limiting, step involves the conjugation of glutamate and cysteine by the enzyme glutamate-cysteine ligase (GCL; also known as γ-glutamylcysteine synthetase) to form gamma-glutamylcysteine (γ-GC)

(Franklin et al., 2009; Meister and Anderson, 1983). GCL is comprised of two subunits: GCLc and GCLm. GCLc ("c" for catalytic subunit, also referred to as the heavy chain

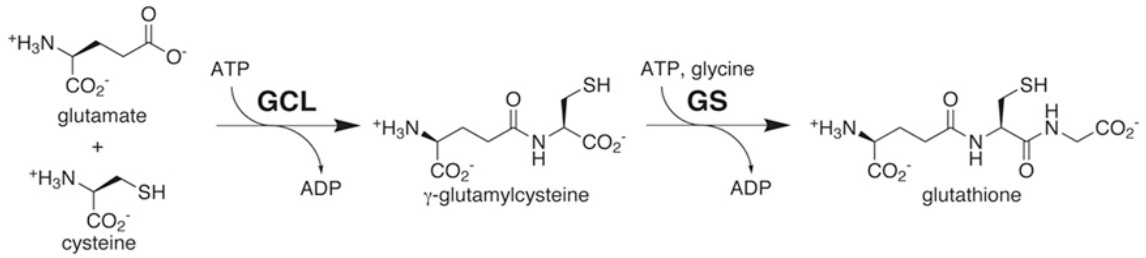

Figure 1.1. Mammalian glutathione biosynthesis pathway.

subunit) provides all the catalytic activity for GCL, while GCLm ("m" for modifier or modifying subunit, also known as the light chain subunit) essentially allows the conjugation of Glu and Cys to occur more efficiently and quickly by lowering the K_m for glutamate and ATP, while also increasing the K_i for GSH feedback inhibition (Franklin et al., 2009). The second enzymatic step of GSH biosynthesis is the conjugation of glycine to γ-GC by the enzyme glutathione synthetase (GS). GSH can also regulate its own production through negative feedback inhibition of GCL activity when cellular GSH levels are sufficient.

Functional differences in GCL expression and activity in humans exist. Though instances in which endogenous GSH levels are severely compromised (i.e. GCL deficiency) are exceedingly rare (Ristoff and Larsson, 2007) such cases are associated with hemolytic anemia, metabolic acidosis, 5-oxoprolinuria, and susceptibility to infection (Beutler et al., 1990; Ristoff and Larsson, 2007). More commonly, polymorphic variation in the human *GCLC* and *GCLM* genes results in "less severe" outcomes, being associated with acetaminophen toxicity, stroke, schizophrenia, myocardial infarction, impaired mercury excretion, asthma, pulmonary fibrosis, and diabetes, among others

(Baum et al., 2007; Bekris et al., 2005; Custodio et al., 2005; McConnachie et al., 2007; McKone et al., 2006; Polonikov et al., 2007; Tosic et al., 2006).

Given the importance of GSH in the cell, and its clinical relevance to disease, animal models of altered GCL activity have been created to more fully elucidate molecular and physiological processes involving GSH. Homozygous deletion of the *Gclc* gene in mice results in embryonic lethality (Dalton et al., 2000). However, mice with homozygous deletion of the murine *Gclm* gene (*Gclm* null mice) are healthy and viable (McConnachie et al., 2007; Yang et al., 2002). *Gclm* null mice display a fascinating phenotype. Across tissues, young *Gclm* null mice display low levels of GSH (~10-20%) compared to their *Gclm* wild-type counterparts (McConnachie et al., 2007). (*Gclm* heterozygotes have approximately 70% of normal GSH levels.) Given GSH's central role in cellular redox homeostasis and antioxidant defense, one would expect *Gclm* null mice to be sensitive to pathophysiological conditions involving environmental and oxidative stress. While this holds true for some stressors which specifically require the GSH molecule for detoxification, such as acetaminophen-induced liver injury (McConnachie et al., 2007), *Gclm* null mice are unexpectedly resistant to many stressors, including ozone, diesel exhaust, certain nanoparticle exposures, methionine and choline-deficient (MCD) diet-induced nonalcoholic steatohepatitis (NASH)-like liver injury, and 2,3,7,8-tetrachlorodibenzodioxin (TCDD)-induced steatosis (Chen et al., 2012; Cole et al., 2016; Haque et al., 2010; Johansson et al., 2010; McConnachie et al., 2013; Weldy et al., 2011). In contrast, *Gclm* heterozygous mice are more sensitive than *Gclm* wild-type and null mice to some of the aforementioned stressors. It should be noted that some of these findings may be gender-dependent (Cartwright et al., 2016).

Why would severely glutathione-deficient mice be paradoxically resistant to oxidative stressors? The answer likely boils down to *Gclm* null mice having compensated for chronic low GSH levels by upregulating a number of genes involved in antioxidant response and detoxification. Many of these genes are controlled by the activity of the transcription factor Nrf2, and consistent with this, the most highly upregulated pathway in the livers of *Gclm* null mice is the Nrf2/Keap1 pathway (McConnachie et al., 2007). The overexpression of Nrf2-regulated genes in the livers of *Gclm* null mice, such as *Gclc, Gsr, Gstm1, Nqo1, Hmox1, Trx,* and *Cbr3*, likely allows these mice to maintain antioxidant response capacity in the face of low GSH. (This hypothesis also helps to explain why *Gclm* heterozygotes are often more susceptible to exogenous stress—they have diminished GSH levels, but not to a severe enough degree to have chronically increased homeostatic and antioxidant defense systems.) Interestingly, the Nrf2 pathway is also highly increased in a related mouse model of chronic thiol insufficiency, conditional hepatic knockdown of *Txnrd1 (*Bondareva et al., 2007; Suvorova et al., 2009). In fact, both *Txnrd1* and *Gclm* null mice share the same most highly upregulated gene, *Cbr3*, whose endogenous function remains unresolved (Bondareva et al., 2007; Schaupp et al., 2015). Similar compensatory responses to *Gclm* and *Txnrd1* deletions in mice further highlight the interplay between the Trx and GSH systems.

In addition to their surprising resistance to exogenous stressors, *Gclm* null mice also display an altered metabolic phenotype, particularly with regard to glucose homeostasis. Previous work has shown that compared to young *Gclm* wild-type mice, young *Gclm* null mice are leaner, more glucose tolerant and insulin sensitive, have a higher basal metabolic rate, and are resistant to high-fat diet-induced diabetes, obesity,

and steatosis (Kendig et al., 2011; Lavoie et al., 2016). These differences have been partially attributed to reduced expression of lipid biosynthesis genes in *Gclm* null livers, including *Fasn*, *Srebf1*, *Srebf2*, *Ppara*, and *Ppargc1a* (Kendig et al., 2011). However, this research did not investigate the contributions of the Nrf2 pathway in modulating energy homeostasis of *Gclm* null mice.

Because *GCLC* and *GCLM* variants in humans often result in only modestly compromised GSH levels, others have posited that *Gclm* heterozygous mice represent a model with more direct clinical relevance (Weldy et al., 2012). However, while an admittedly extreme model, mice with homozygous *Gclm* ablation are potentially more useful than *Gclm* heterozygotes for studying how the systems responsible for controlling responses to endogenous and exogenous stress (e.g., Nrf2) may be perturbed under conditions of co-exposure, gender, age, etc., because *Gclm* null mice are highly dependent on these systems to maintain normal cellular homeostasis.

1.3. Cellular antioxidant systems.

The Nrf2/Keap1 antioxidant system is an important cellular defense pathway for protecting against oxidative and/or electrophilic stress (Kensler et al., 2007). Nrf2's importance is highlighted by its conservation across vertebrates—compared to human Nrf2, mouse Nrf2 has "DNA and protein homology scores of 83.4% and 82.5%, respectively; rat Nrf2, 84% and 83%; cow Nrf2, 91% and 89%; dog Nrf2, 89.4% and 88.9%; chicken Nrf2, 72% and 67%; and zebrafish Nrf2, 55% and 49%" (Ma, 2013). Nrf2 is a basic leucine zipper transcription factor which regulates a battery of antioxidant

and detoxification (phase II) genes through a *cis*-acting DNA element called the antioxidant, electrophilic, or xenobiotic response element (ARE, EpRE, or XRE) (He and Ma, 2009). Mutational and deletion analyses have identified the consensus ARE regulatory motif to be 5'-TGACNNNGC-3' (Malhotra et al., 2010). Under basal conditions, Nrf2 is in a state of constant production and degradation (via ubiquitination), being repressed in the cytosol by the Keap1 protein (Itoh et al., 2003). Three critical cysteine residues on Keap1 (Cys 151, Cys 273, and Cys 288) can be modified by electrophilic/oxidative insult to induce dissociation of Nrf2 (Zhang and Hannink, 2003). Upon electrophilic or oxidative stress, the Nrf2 protein is thus not ubiquinitated and becomes stabilized, and a nuclear localization epitope is revealed, allowing translocation to the nucleus. Once in the nucleus, Nrf2 binds to AREs, usually in the 5' untranslated region upstream of antioxidant response genes, it recruits binding partners (e.g., sMaf, CBP/p300), and initiates transcription of target genes (Figure 1.2). Acetylation/deacetylation of Nrf2 regulates its nuclear export via two main pathways: the GSK3β-Fyn pathway and Keap1-mediated export (Kaspar and Jaiswal, 2011; Kawai et al., 2011).

Other non-canonical modes of Nrf2 regulation are also important. Bach1 appears to repress Nrf2-regulated gene expression by directly competing with Nrf2 for binding to AREs in the promoter region of these genes (Dhakshinamoorthy et al., 2005; Sun et al., 2004; Zhang et al., 2012a). c-Myc also negatively regulates Nrf2 gene expression, as demonstrated in 2010 by Forman and colleagues, who showed that silencing c-Myc expression could result in elevated mRNA expression of Nrf2-regulated genes and ARE-driven reporter constructs as well as an increased half-life of Nrf2 protein (Levy and

Forman, 2011; Zhang et al., 2012a).

Many Nrf2-regulated gene products (e.g., *Nqo1, Gclc, Gclm,* multiple *GSTs, UGTs, MRPs, Hmox1, Txnrd1, Gsr, Gpx1, Prx1*) eliminate reactive oxidants and electrophiles through conjugative reactions and by enhancing cellular antioxidant capacity (He and Ma, 2009; Kensler et al., 2007). Nrf2 also controls the expression of cellular NADPH-regenerating enzymes, including glucose 6-phosphate dehydrogenase, 6-phosphogluconate dehydrogenase, and malic enzyme (Kensler et al., 2007), and genes involved in glucose metabolism, purine biogenesis and fatty acid oxidation (Harder et al., 2015). In addition to directly regulating the expression of the aforementioned cytoprotective genes, there is a great deal of crosstalk between Nrf2/Keap1 and other cellular signaling pathways, including those involved in inflammation (NF-κB), autophagy, apoptosis (MAPK), energy metabolism (PGC1α, PPARs), nutrient sensing (mTOR, AMPK), and development (Notch) (Bendavit et al., 2016; Cho et al., 2010; Jiang et al., 2015; Joo et al., 2016; Sun et al., 2009; Wakabayashi et al., 2016; Wardyn et al., 2015).

Given Nrf2's importance in maintaining cellular homeostasis, dysregulation of this pathway (including Nrf2 polymorphisms) and its target genes is, unsurprisingly, implicated in myriad human disease states, including Alzheimer's disease, chronic kidney disease, chronic liver injury, chronic obstructive pulmonary disease, Friedreich's ataxia, multiple sclerosis, non-alcoholic steatohepatitis, hypertension, Parkinson's disease, and many types of cancer (Al-Sawaf et al., 2015). Thus, Nrf2 has become an attractive therapeutic target. Many Nrf2 'therapeutics,' such as sulforaphane, curcumin, bardoxolone methyl (CDDO-Me), and dimethylfumarate, exert their effects through low-

level electrophilic stimulation. Therapeutic interventions targeting the Nrf2 pathway have had mixed results, but have shown particular promise in neurodegenerative disease. As an example, dimethylfumarate has been recently approved by the United States Food and Drug Administration for the treatment of multiple sclerosis, and has shown promise in mouse models of Huntington's disease (Ellrichmann et al., 2011; Harder et al., 2015).

The (to this point) murky legacy of interventions targeting Nrf2 in disease is perhaps not unexpected, given Nrf2's interaction with, and reliance on, multiple other cellular signaling and homeostatic pathways. Rarely do perturbations involving a master regulator, such as Nrf2, not have unintended effects. Because of Nrf2's importance in multiple types of disease, there is little doubt that interventions targeting Nrf2 will continue to be explored in the future, which will require researchers to more fully elucidate the molecular underpinnings of Nrf2 in aging and disease.

1.4. Theories of aging.

Over the years, many different theories have been proposed to explain why organisms age (Hayflick, 1998; López-Otín et al., 2013). Perhaps the most famous of these, and the first to gain real traction and attention, was the 'free radical theory of aging,' posited in 1957 by Denham Harman (Harman, 1957). Following Harman's proposition, researchers continued to develop singular theories to decode the aging process (Jin, 2010; López-Otín et al., 2013; Warner et al., 1987; Weinert and Timiras, 2003). None of these theories are without their flaws, and the prevailing view now among

scientists is more nuanced—that aging is a complex, multifactorial process, in which different elements are inextricably linked. Many aging researchers also recognize that both genetic *and* environmental factors (i.e. 'programmed' vs. 'error' theories) contribute to the aging process (Weinert and Timiras, 2003). López-Otín and colleagues provide a good précis of the current prevailing 'hallmarks' of aging—genomic instability, telomere attrition, epigenetic alterations, loss of proteostasis, deregulated nutrient sensing, mitochondrial dysfunction, cellular senescence, stem cell exhaustion, and altered intercellular communication (López-Otín et al., 2013). These hallmarks of aging can be further divided into three categories: primary hallmarks, antagonistic hallmarks, and integrative hallmarks. Oxidative stress (ROS in particular) would fall into the antagonistic category, because it has opposing effects, depending on intensity—at low levels, it is beneficial for cell signaling and development, but at high levels, it can cause cellular damage and promote aging (López-Otín et al., 2013).

Because scientists now realize that a singular theory of aging is overly simplistic, it would be easy to dismiss Harman's original 'free radical' postulate, but doing so would fail to acknowledge that some of the ideas therein are still accepted by the aging research community today, namely that (1) an imbalance in anti-oxidants and oxidants occurs with aging, resulting in the accumulation of oxidatively damaged macromolecules, and (2) accumulating oxidative damage causes a 'degenerative aging' phenotype (Zhang et al., 2015). Evidence for and against the free radical theory of aging exists. Some of the strongest support comes from mammalian transgenic studies, particularly genetically engineered MCAT mice, in which human catalase (which converts hydrogen peroxide to water and oxygen, and is normally expressed in the peroxisome) is localized to

mitochondria (Schriner et al., 2005). MCAT mice display significantly longer lifespans, and reduction in a number of age-related complications, including cataract development and cardiac pathology, compared to wild-type counterparts (Dai et al., 2017; Schriner et al., 2005). Murine overexpression of another important redox molecule, human TRX, also resulted in extended median and maximum life span, and resistance to oxidative stress, compared to wild-type mice (Mitsui et al., 2002). Overexpression studies of other antioxidant genes, including *Prx3, Prx4, Prx6, Sod1, Sod2*, and *Gpx4*, in mice have shown negligible lifespan changes (Perez et al., 2009). However, deletions of *Gclc, Prx1, Prx2, Sod1, Sod2*, and *Txnrd1* either reduce lifespan or are embryonic lethal (Hamilton et al., 2014). These studies have many caveats, namely that they are generally only indirect tests of the free radical theory of aging, and do not account for redundancy and compensation that may occur as a result of antioxidant system perturbation. In addition, these experiments take place in highly controlled environments, and cannot account for cumulative lifetime exposures to various agents that may accelerate the aging process—organisms in the wild do not live in 'bubbles' (Salmon et al., 2010).

Variations on Harman's original proposal have been presented. Some, such as the mitochondrial free radical theory, modify the original theory slightly, specifying that *mitochondrial* free radicals, produced as by-products during normal metabolism, cause oxidative damage, and accumulation of this damage is the main driving force in the aging process (Sanz and Stefanatos, 2008). Recently, NADH/NAD+ imbalance has been discussed as a central driver of the aging process (Imai, 2016; Li et al., 2017a). It seems unlikely that free radicals, central reducing modulators (i.e. $NADPH/NADP^+$, $NADH/NAD^+$, GSH/GSSH, $Trx\text{-}(SH)_2/Trx\text{-}S_2$), and redox reactions can be separated

from one another. Thus, others espouse a more holistic reworking of the free radical theory—one which does not attempt to dismiss, but rather, consolidate prevailing aging theories centered around redox biology. The 'redox theory of aging' is one such example, which asserts:

> "[A]ging is a decline in plasticity of the genome-exposome interaction that occurs as a consequence of execution of differentiation and exposure memory systems. This includes compromised mitochondrial and bioenergetic flexibility, impaired food utilization and metabolic homeostasis, decreased barrier and defense capabilities and loss of reproductive fidelity and fecundity…this redox theory is not exclusively limited to redox reactions, but rather emphasizes the key role of electron transfer in supporting central energy currencies (ATP, phosphorylation, acetylation, acylation, methylation and ionic gradients across membranes), and providing the free energy to support metabolism, cell structure, biologic defense mechanisms and reproduction" (Jones, 2015).

Working under this assertion, it would follow that an uncompromised ability to maintain redox homeostasis in response to endogenous and exogenous stressors is essential for delaying aging.

Central to the basis of the work presented in this thesis are studies demonstrating that the ability to respond to redox stress (i.e. Nrf2 activation) declines with age, and that improved expression and responsiveness is correlated with longevity (Bruns et al., 2015;

Kubben et al., 2016; Lewis et al., 2015; Nobrega-Pereira et al., 2016; Shih and Yen, 2007; Suh et al., 2004; Zhang et al., 2012a). If antioxidant responsiveness is indeed blunted with age, we hypothesize that *Gclm* null mice would be especially susceptible to exogenous oxidative stressors in old age compared to wild-type counterparts.

1.5. Interplay of Nrf2 and diabetes.

An important role for Nrf2 in diabetes is supported by many studies. First, circulating Nrf2 mRNA is decreased in patients with type II diabetes mellitus (T2DM) (Siewert et al., 2013), and second, studies in mice have demonstrated that mild Nrf2 overexpression or activation via small molecule Nrf2 stimulators (e.g., sulforaphane) can prevent T2DM onset (Dieter, 2015). Because oxidative stress is believed to contribute significantly to TD2M progression, it follows that reducing oxidative insult via activation of antioxidant pathways could potentially prevent or delay the onset of TD2M. Additionally, hyperglycemia (a clinical characteristic of T2DM) is associated with ROS and AGE production, creating a feedback loop of increasing oxidative stress (Friedman, 1999; Schulze et al., 2004; Tan et al., 2007; Yao and Brownlee, 2010; Yu et al., 2006). While acute hyperglycemia has been shown to increase Nrf2 activity, a state of chronic high blood sugar dampens Nrf2 signaling (He et al., 2012; He and Ma, 2009; Ramprasath and Selvam, 2013; Tan et al., 2011). Complications of long-term T2DM include cardiovascular, renal, and neuropathic sequelae—states associated with oxidative stress.

There is conflicting data on the role of Nrf2 on T2DM in animal models. Murine knockdown of Keap1 induces a T2DM-like phenotype, and constitutive Nrf2 activation

has been shown to exacerbate metabolic dysfunction and increase sensitivity to high-fat diet-induced obesity (Xu et al., 2012; Yore et al., 2011; Zhang et al., 2012b). However, Uruno and colleagues showed that hypomorphic *Keap1* knockdown suppressed T2DM onset (Uruno et al., 2013). They found that when *Keap1flox*$^{/-}$ mice were crossed with leptin receptor-deficient diabetic *db/db* mice, circulating glucose levels decreased through improved insulin secretion and sensitivity (Uruno et al., 2013). *Keap1flox*$^{/-}$ also prevented HFD-induced diabetes and obesity, at least partially through suppression of hepatic gluconeogenesis (Uruno et al., 2013). Furthermore, oral administration of CDDO-Im (a potent NRf2 activator) attenuated diabetes in *db/db* mice by protecting β-cells and improving insulin sensitivity (Uruno et al., 2013). Interestingly, preliminary data from the Kavanagh lab suggests that crossing *db/db* mice with *Gclm* null mice results in significant weight reduction and decreased serum triglycerides, relative to *db/db* mice with unmodified *Gclm* status (unpublished data). Other *in vitro* and *in vivo* mouse and rat studies have shown Nrf2 activation can reduce glomerular injury and cardiomyopathy in diabetic mice (Bai et al., 2013; Bitar and Al-Mulla, 2011; Li et al., 2011).

While Nrf2 remains an attractive therapeutic target for T2DM (de Haan, 2011; Tan and de Haan, 2014), animal studies suggest a delicate balance in antioxidant activity is needed to maintain normal glucose homeostasis. This was highlighted in a recent clinical trial targeting Nrf2—Bardoxolone Methyl Evaluation in Patients With Chronic Kidney Disease and Type 2 Diabetes: the Occurrence of Renal Events (BEACON), which was terminated prematurely in phase III due to severe adverse toxicities, including albuminuria, hypertension, and heart failure (de Zeeuw et al., 2013). Bardoxolone methyl, a synthetic triterpenoid derived from oleanolic acid, is known to be a potent Nrf2

inducer, and its anti-cancer and anti-inflammatory properties have been studied extensively in laboratory models (Dinkova-Kostova et al., 2005; Patlolla and Rao, 2012; Yates et al., 2007). However, there are over 500 off-target, candidate binding proteins for bardoxolone methyl, so it is quite possible that improved specificity may have mitigated the safety concerns associated with its clinical use (Wang et al., 2014; Yore et al., 2011). Additionally, the patients in the BEACON study had late-stage chronic kidney disease and/or advanced TD2M, and thus, the prospect of significant disease regression was unlikely. Regardless, further investigation into the role of Nrf2 in diabetes and its potential use as a therapeutic target is necessary.

1.6. Cadmium as a model toxicant.

Cadmium is a ubiquitous toxicant with environmental health relevance. A transition metal used in the battery and electroplating industries, it is also notably important for use in colored glass manufacturing and biotechnology. Tobacco smoking is the source of greatest exposure to cadmium. Smoking roughly doubles cadmium body burden in comparison to not smoking (ATSDR, 2011). For nonsmokers, the primary source of cadmium exposure is dietary. In general, leafy vegetables such as lettuce and spinach, potatoes and grains, peanuts, soybeans, and sunflower seeds contain relatively high levels of cadmium; these plants readily absorb and accumulate cadmium from the soil (ATSDR, 2011). Cadmium is consequently an unwanted contaminant formed in the preparation of fertilizers made from sewage sludge, decomposing plant material and other waste streams. Fish consumption may also be a significant source of cadmium,

especially of high trophic level species. The average daily intake of Cd is estimated to range from 8 to 25 μg (Jarup and Akesson, 2009). In addition to food, exposure to cadmium may occur via the air and water. Occupational exposure to cadmium is also important, where the major route of exposure is inhalation of dust and/or fumes resulting from smelting and electroplating.

Chronic, low-level oral exposure to cadmium is associated with renal toxicity, while acute, high-level exposure is associated with hepatotoxicity (Klaassen et al., 2008; Wu et al., 2012). The U.S. Department of Health and Human Services and the International Agency for Research on Cancer have categorized cadmium as a human carcinogen, due to its potential to induce pulmonary tumors (ATSDR, 2011; Waalkes, 2003). The mechanisms that underlie Cd toxicity include induction of oxidative and endoplasmic reticulum stress, inflammation, genotoxicity, and interference with the biochemical functions of essential metals (e.g., zinc) (Klaassen et al., 2008; Tinkov et al., 2017).

Oxidative stress (or more specifically, the production of ROS) is known to play a critical role in cadmium-induced hepatotoxicity. Cd-induced ROS can produce lipid peroxidation, and result in damage to other macromolecules, such as DNA and proteins (Klaassen et al., 2009; Liu et al., 2009; Oh and Lim, 2006; Waalkes and Goering, 1990). While induction of Nrf2-regulated metal-binding proteins called metallothioneins is the canonical cadmium detoxification pathway, the immediate line of defense against cadmium toxicity is the binding of Cd to sulfhydryls of GSH (Delalande et al., 2010; Fuhr and Rabenstein, 1973; Klaassen et al., 2009; Singhal et al., 1987; Stillman et al., 1987). This is especially important to emphasize given that protein production resulting

from gene response to an environmental stress generally occurs on the timescale of minutes to hours (de Nadal et al., 2011). Thus, in an acute, high-dose heavy metal exposure scenario, the availability of GSH to quench Cd cations is an important determinant in the severity of hepatic cadmium toxicity (Hassoun and Stohs, 1996).

Increasing evidence points toward associations between cadmium exposure and diabetic-like phenotypes. T2DM is characterized by decreased insulin sensitivity, altered glucose transport, and β-cell dysfunction (Petersen et al., 2017). Chronic exposure to cadmium in mice and rats has been shown to induce insulin resistance, increase the expression of gluconeogenic enzymes, and decrease glucose transport by downregulation of Glut4 receptors (Edwards and Ackerman, 2016; Han et al., 2003; Merali and Singhal, 1975; Rajanna et al., 1984; Tinkov et al., 2017; Trevino et al., 2015). In both laboratory mammals and humans, cadmium has been shown to accumulate in β-cells and induce pancreatic islet dysfunction, potentially through disruption of calcium channels and/or oxidative stress (Edwards and Prozialeck, 2009; El Muayed et al., 2012; Gavazzo et al., 2005; Kurata et al., 2003; Lei et al., 2007; Merali and Singhal, 1980; Nilsson et al., 1986; Sato et al., 1997). In humans, early life exposure to cadmium is associated with low birth weight and susceptibility to obesity and metabolic syndrome later in life (Park et al., 2017). Some human observational studies demonstrate a positive association between early to mid-life cadmium exposure and obesity, in addition to cardiovascular disease or metabolic syndrome (Lee and Kim, 2013; Li et al., 2017b; Pizzino et al., 2014). Blood and urinary cadmium levels from the have been found to be significantly associated with impaired fasting glucose and pre-diabetes (Nie et al., 2016; Schwartz et al., 2003; Wallia et al., 2014). However, these observations do not always hold, likely owing to the

complex nature of metal exposure, which can be influenced/confounded by genetic susceptibility, dose, timing, co-exposure with other metals, and other factors such as smoking status (Menke et al., 2016). Nonetheless, there is sufficient evidence to suggest that in addition to being a carcinogen, cadmium may act as a 'diabetogen,' exerting its effects (at least partially) via induction of oxidative stress and disruption of islet β-cell function (Chang et al., 2013; Chen et al., 2009; Cuypers et al., 2010).

1.7. Rationale, hypotheses, and specific aims.

Glutathione is an important antioxidant and co-factor for combating exogenous stresses—mice with severely compromised (but not complete absence of) GSH levels (i.e. *Gclm* null mice) compensate by increasing expression and activity of the Nrf2/Keap1 cytoprotective pathway. As a result, young *Gclm* null mice display increased resistance to many stressors, an overall favorable metabolic profile, and resistance to diabetes and obesity. However, to date, no study has investigated the influence of aging on the *Gclm* null phenotype. Because previous work suggests that an organism's ability to respond to oxidative stress and maintain glucose homeostasis declines with age, we hypothesized that *Gclm* null mice would be uniquely susceptible to age-related dysfunction of the cellular stress pathway Nrf2. Cadmium chloride was employed as an exogenous stressor to test both resistance to oxidative insult and favorable parameters of glucose homeostasis.

These data will serve to significantly augment the current literature surrounding responsiveness of the Nrf2 system with aging. As such, the specific aims of this

dissertation are to: **(1) Determine if *Gclm* genotype status predicts susceptibility or resistance to Cd-induced toxicity relative to wild-type mice, and whether this effect is age-dependent,** and **(2) determine if improved parameters of glucose and metabolic homeostasis observed in young *Gclm* null mice relative to wild-type mice (i.e. insulin sensitivity, glucose tolerance, lean phenotype) are maintained through old age.**

Chapter 2

Glutathione redox homeostasis and antioxidant system plasticity in *Gclm* mice in response to age and cadmium.

2.1. Introduction

Numerous laboratory and clinical studies have contributed to a scientific consensus that aging alters glutathione redox homeostasis, shifting the cell to a more pro-oxidative state (Brandes et al., 2013; Calabrese et al., 2010; Feleciano and Kirstein, 2016; Giustarini et al., 2006; Liu et al., 2004; Maher, 2005; Rebrin and Sohal, 2008; Toroser and Sohal, 2007). At the biochemical level, data indicate perturbation of GCL catalysis, increased oxidized glutathione, and accumulation of L-homocysteine from the transsulfuration pathway contribute to altered GSH redox homeostasis and may adversely affect *de novo* glutathione biosynthesis during aging (Toroser and Sohal, 2007). However, cells are resilient, and there are redundant pathways which can offset changes to the redox state (Du et al., 2012). Importantly, age-induced changes in glutathione redox homeostasis are often accompanied by decreased antioxidant enzyme activity—the effects of altered GSH redox homeostasis and reduced cytoprotective pathway responsiveness likely influence each other and are difficult to separate.

Among antioxidant pathways, Nrf2/Keap1 functions as a critical regulator of the cell's defense against endogenous and exogenous stress by controlling the expression of many cytoprotective proteins (Lau et al., 2010; O'Connell and Hayes, 2015). Many studies have investigated changes in Nrf2/Keap1 activity, including in its nuclear level and binding to the EpRE transactivation motif, in older organisms (Lewis et al., 2015;

Shih and Yen, 2007; Suh et al., 2004; Zhang et al., 2015). Although variability exists with regards to the effects of age on the basal expression of these enzymes, there is general agreement that the ability to induce these enzymes by electrophiles declines with age. Accumulating data suggest that this age-dependent decline in the antioxidant enzyme response is caused by declining efficiency of Nrf2/EpRE signaling (Zhang et al., 2015; Zhang et al., 2012a). Data from Henry Forman and colleagues, in which they studied Nrf2 activation in response to nanoparticles, found that although the basal Nrf2 level was increased in 21-month compared to 6-month mice, Nrf2/EpRE activation and further induction of Nrf2 target genes were lost in the liver, lung, and cerebellum in late middle-aged mice (21 months) compared with that of young adults (6 months) (Zhang et al., 2012a). Their work provides convincing evidence that Nrf2 activity/responsiveness to electrophilic/oxidative stressors decreases with age, making cells more susceptible to deleterious insult. Thus, although *Gclm* null mice may very well maintain elevated basal expression of Nrf2-regulated genes into old age, we predict that *Gclm* null mice will be more susceptible to an exogenous exposure that induces oxidative stress, such as cadmium, due to decreased Nrf2 responsiveness, relative to wild-type mice, with age.

We hypothesize that young *Gclm* null mice will be resistant to Cd-induced hepatotoxicity and perturbation of metabolic and redox homeostasis relative to wild-type mice due to increased Nrf2 activity, but this trend will reverse with age, and *Gclm* null mice will become more sensitive to Cd-induced toxicity relative to wild-type mice due to a decline in responsiveness of the Nrf2 system.

To test this hypothesis, we quantified hepatic glutathione redox homeostasis in *Gclm* wild-type (WT), heterozygous (Het), and null (KO) mice, via quantitation of total

GSH, GSSG, and % GSSG , and examined expression of Nrf2-regulated genes at the transcriptional and protein levels in *Gclm* WT, Het, and null mice into 24+ months of age by treatment.

2.2. Materials & Methods

Reagents

All reagents were purchased from Life Technologies (Carlsbad, CA) and/or Sigma-Aldrich (Saint Louis, MO), unless otherwise noted.

Establishment of an Aging Gclm *Mouse Colony*

We performed all animal experiments in accordance with the National Institutes of Health Guide for the Use and Care of Laboratory Animals (NRC, 2011) and with the approval of the University of Washington Institutional Animal Care and Use Committee (IACUC; protocol #2384-08). We made all efforts to minimize animal distress and suffering. *Gclm* null mice were derived by homologous recombination techniques in mouse embryonic stem (ES) cells, as previously described (McConnachie et al., 2007).

Eight cohorts of male *Gclm* wild-type, heterozygous, and null mice were established representing four ages (10-13 weeks, 6 months, 18 months, and 24+ months) and two treatments (saline and 2 mg/kg cadmium chloride, i.p. injection), with an n of 5-6 for each age, genotype, and treatment.

Experimental Design

Once mice reached the desired age (10-13 weeks, 6 months, 18 months, or 24+ months), baseline measurements of glucose homeostasis were initiated; no longer than two weeks post-baseline measurements were mice sacrificed.

Treatments

One week following baseline GTT and ITT measurements, mice were intraperitoneally injected with either 0.9% sterile saline for animal injection, or 2 mg/kg cadmium chloride in sterile saline (0.9% sodium chloride injection, USP; injection volume of 100-200 µl). Due to the dearth of toxicology studies examining acute heavy metal treatments (particularly cadmium) in aged mice, we performed a small dose-escalation study to determine an appropriate sublethal dose using 20 month old *Gclm* mice. We wanted to select an acute dose which also allowed us to perform functional tests of glucose homeostasis following dosing and prior to sacrifice. Based on our internal dose escalation study, and literature review of LD_{50} values for oral $CdCl_2$ administration in different strains of laboratory mice (ranging from 5 to 183 mg/kg), a 2 mg/kg $CdCl_2$ dose of cadmium chloride was chosen (ATSDR, 2011; Basinger et al., 1988; Zhao et al., 2006). Ideally, a chronic dosing regimen would have been used to interrogate the effect of cadmium exposure. However, mice in some of the cohorts had already aged significantly, which precluded us from beginning a chronic dosing protocol.

Twenty-four hours post-dosing, GTT measurements were taken, and 48 hours post-injection, ITT measurements were recorded as previously described (Kendig et al., 2011; Lavoie et al., 2016). Mice were then sacrificed the following morning (~66-72

hours post-dosing). The aforementioned tests and timepoints were designed and chosen to maximize the data collected from each mouse without causing undo harm, while minimizing the number of mice needed.

Necropsies

Animals were sacrificed by placing them under CO_2 narcosis, followed by cervical dislocation. Fresh blood was obtained via heart puncture and collected in plasma separator tubes, placed on ice, centrifuged at 8000 rpm for 10 minutes at room temperature, then stored at -20°C. Following blood collection, tissues were collected and either flash frozen in liquid nitrogen, fixed in 10% neutral buffered formalin, and/or embedded in OCT. Tissues collected include liver, kidney, spleen, duodenum, testes, abdominal and epididymal fat, heart, lung, brain, eye, and gastrocnemius muscle.

Protein Isolation

Total protein concentration in S9 liver homogenate fractions was determined using the Bio-Rad Protein Assay Dye Reagent (Bio-Rad Laboratories Inc., Hercules, CA), in 96-well microtiter plates, following the manufacturer's protocol, a modified version the Bradford assay (Bradford, 1976).

Measurement of Glutathione Redox Homeostasis

Immediately following heart puncture and collection of left and right median lobes of the liver, the right anterior and posterior liver lobes were collected and homogenized in either 1:10 weight:volume of 2 mM N-ethylmaleimide (NEM) for the

GSSG fraction, or monobromobimane (MBB) for the GSH fraction, in mitochondrial isolation buffer (210 mM sucrose, 2 mM EGTA, 40 mM NaCl, 30 mM HEPES; pH=8). Samples were allowed to rock for 4 hours at RT in the dark. They were then prepared as previously described, with GSH and GSSG content measured by HPLC (Siegel et al., 2013). GSH and GSSG levels were then normalized to protein concentrations.

RNA Isolation

Total RNA was extracted from RNAlater®-stabilized liver and kidney samples with the miRNeasy Mini Kit (Qiagen, Venlo, The Netherlands).

Multiplex PCR specific target amplification

cDNA samples were pre-amplified following Fluidigm's (South San Francisco, CA) Specific Target Amplification (STA) protocol, to increase target gene template cDNA for gene expression reactions. Reactions were conducted in 5 µl volumes containing 1.25 µl diluted cDNA, 1.25 µl of 0.2X pooled TaqMan assay mix, and 2.5 µl of TaqMan PreAmp Master Mix 2X (Applied Biosystems Inc.). Pre-amplified PCR products were then diluted 1:5 with DNA Suspension Buffer (10 mM Tris, pH 8.0, 0.1 mM EDTA).

RT- PCR for measurement of antioxidant and energy homeostasis gene expression

Fluidigm GE Dynamic Array 96.96 plates were primed on the Fluidigm IFC Controller prior to loading. Four µl of each 10X assay mix were loaded onto each assay well and 5 µl of each Sample Pre-Mix were loaded onto each sample well of the GE

Dynamic Array (Fluidigm). Assays were run in triplicate. The GE Dynamic Array was loaded onto the IFC Controller before thermocycling with the following profile: 98°C for 40s followed by 40 cycles, consisting of 95°C for 10s and 60°C for 40s. Data were collected using the Fluidigm BioMark Data Collection Software 2.1.1 and analyzed using the Fluidigm Real-Time PCR Analysis Software 1.1.0.

Semi-quantitative Analysis of Protein Expression

Western immunoblotting was performed using standard techniques, as previously reported (McConnachie et al., 2007). Briefly, ~15 μg protein per sample were separated by electrophoresis using 12% Tris-Glycine mini-gels in a Novex XCell *SureLock* Mini-Cell (Life Technologies, Carlsbad, CA). Following electrophoresis, proteins were transferred to polyvinylidine difluoride (PVDF) membranes (Immobilon-P, Millipore, Billerica, MA). Membranes were blocked with 5% milk in the appropriate buffer and incubated with primary antibodies raised against Gclc (1:20,000; rabbit polyclonal antisera, as described previously (McConnachie et al 2007), Gclm (1:1000; rabbit polyclonal antisera (McConnachie et al 2007)), Cbr3 (1:1000 dilution; rabbit polyclonal antisera; Gary F. Merrill, Oregon State University, unpublished), β-actin (1:1000 dilution; Cell Signaling, Beverly, MA), Nqo1 (1:1000 dilution; rabbit polyclonal; Abcam, Cambridge, UK), and Gstm1 (1:2000; rabbit polyclonal; Abbexa, Cambridge, UK).

Protein expression was normalized to the expression of the loading control, β-actin. Following a brief wash, membranes were incubated with horseradish peroxidase-conjugated secondary goat anti-rabbit IgG antibody (Millipore, Billerica, MA), and protein expression was detected using an enhanced chemiluminescence system (GE

Healthcare UK, Buckinghamshire, UK) with X-ray film exposure. The optical densities of the appropriate-sized bands were then analyzed using NIH Image J software v1.48 (National Institutes of Health, Bethesda, MD). The optical density of each band was adjusted to the density of the β-actin band. Quantification and statistical analyses are the result of three independent experiments.

Statistical Analyses

Data are expressed as the mean and SEM, unless otherwise noted. Data were analyzed by one- or two-way ANOVA, followed by a Dunnett's post hoc test, or a Student's *t*-test (for pair-wise comparisons) using a statistical software package (Prism, GraphPad, Inc., San Diego, CA). Differences yielding a *p* value of less than 0.05 were considered statistically significant.

2.3. Results

Glutathione redox homeostasis

Three parameters were measured via HPLC to examine changes in glutathione redox status with aging and cadmium treatment in the livers of *Gclm* mice: total glutathione (GSH), oxidized glutathione (GSSG), and percent oxidized glutathione (%GSSG). In saline and cadmium treated mice, a general trend of decreasing total GSH, and increasing GSSG and %GSSG was observed with age (Figures 2.1 – 2.12). There was a significant effect of age on total GSH and GSSG in all *Gclm* genotypes (Figures 2.6 – 2.8, 2.10 – 2.12). However, while age had a significant effect on %GSSG in *Gclm* WT and Het mice (Figures 2.2, 2.3), *Gclm* null mice did not show an overall increase in %GSSG with age (Figure 2.4). Two-way ANOVA confirmed that age had a significant effect on %GSSG in WT and Het mice ($p<0.0001$, n=6 mice/group), but not in null mice ($p=0.1586$, n=6 mice/group) (Figures 2.2 – 2.4). While the trends in total GSH and GSSG are important to consider, percent GSSG is an integrated measure and potentially more reflective of an organism's ability to maintain redox homeostasis.

We also investigated temporal changes in glutathione redox status by examining GSH, GSSG, and %GSSG at 8 hr post saline or cadmium dosing in 24+ month old *Gclm* mice, comparing these values to those observed at ~72 post-dosing (i.e. data shown in Figures 2.1 – 2.12). In all *Gclm* genotypes, GSSG decreased, total GSH increased, and %GSSG decreased at 8 hr, relative to 72 hr (Figures 2.13 – 2.15). Interestingly, *Gclm* null mice restored GSSG, GSH, and %GSSG to saline levels by 72 hr post-Cd (Figures 2.13 – 2.15). *Gclm* WT and Het mice, however, did not fully restore %GSSG levels to 72 hr

saline levels (Figures 2.13 – 2.15), suggesting that *Gclm* null mice are able to maintain GSH redox more efficiently, even after $CdCl_2$ treatment, at 24+ months of age, compared to WT and Het mice.

RT-PCR for measurement of antioxidant and energy homeostasis gene expression

We quantified hepatic mRNA expression of eight Nrf2-regulated genes— *Gclc, Gclm, Cbr3, Gstm1, Hmox1, Mt1, Mt2,* and *Nqo1*—from 6 and 24+ month saline and cadmium-treated *Gclm* WT, Het, and null mice. Analysis revealed significantly increased mRNA expression of *Cbr3, Gclc, Gstm1,* and *Nqo1* in saline-treated null mice at both 6 and 24+ months (Figure 2.16, panels C, I, K, O). Curiously, following cadmium treatment of 6 month old mice, none of these genes were overexpressed in null mice relative to WT (Figure 2.16, panels D, J, L, P). However, at 24+ months, cadmium treatment significantly increased expression of all genes examined (except *Gclc* and *Gclm*) in *Gclm* null mice, including *Mt1*, *Mt2*, and *Hmox1*, which were not differentially expressed in null mice following saline treatment (Figure 2.16, panels F, H, J, L, N, P). Interestingly, *Cbr3, Gstm1,* and *Nqo1* are significantly repressed following cadmium treatment in *Gclm* null mice at 6 months (Figure 2.16; analysis not shown here). Further investigation into this phenomenon is warranted.

These data suggest that following acute exposure to cadmium chloride, Nrf2 inducibility is retained in 24+ month *Gclm* null mice, relative to WT and Het counterparts (Figure 2.16).

Western immunoblot analysis of Nrf2-regulated protein expression

Five canonical Nrf2-regulated proteins—Gclc, Gclm, Cbr3, Nqo1, and Gstm1—were examined in liver homogenates for expression at 6 and 24+ months in *Gclm* mice of all genotypes following saline or cadmium treatment. All of these proteins (except for Gclm) are quite clearly overexpressed in nulls relative to WT and Het mice (Figure 2.17). As expected, Gclm expression was highest in WT mice, with about 50-60% expression in Het mice, and essentially no expression in null mice (any densitometry values in null mice resulted from background).

Densitometry analysis revealed that following saline treatment, Cbr3 and Nqo1 were significantly upregulated in null mice at 6 and 24+ months, with a similar, but not significant, trend observed for Gclc and Gstm1 (Figure 2.18, panels A, E, G, I). Following cadmium treatment, Gclc, Cbr3, and Nqo1, were significantly induced in 6 month old *Gclm* null mice, (the only exception being Gstm1, which did not reach statistical significance, but still followed the overall trend) (Figure 2.18, panels B, F, H, J). In 24+ month old cadmium-treated mice, Gclc, Cbr3, Nqo1, and Gstm1 were all significantly overexpressed in *Gclm* nulls, relative to WT and Het (Figure 2.18, panels B, D, F, H, J)**.**

2.4. Discussion

In this aim, we first examined the effect that aging had on hepatic redox homeostasis in mice with varying levels of glutathione. The results do not support the

hypothesis that age would have a more detrimental effect on redox homeostasis and Nrf2 activity in *Gclm* null mice compared to wild-type and heterozygous counterparts, as proposed in Aim 1. In fact, the opposite appears to occur—*Gclm* null mice retain high expression of Nrf2 regulated proteins into old age, and, importantly, this system remains responsive to exogenous stress (Figures 2.16, 2.17, 2.18). This finding stands in direct contrast to the prevailing literature suggesting that Nrf2 activity and responsiveness declines in mice with age (Zhang et al., 2015; Zhang et al., 2012a).

The unexpected ability of *Gclm* null mice to maintain hepatic glutathione redox status may be explained by elevated glutathione reductase (Gsr) activity (i.e. increased ability to recycle GSSG to GSH. While not directly tested here, previous microarray data suggests that Gsr activity is higher in the livers of *Gclm* null mice (Haque et al., 2010). Importantly, Gsr requires NADPH to carry out the two-electron enzymatic reduction of GSSG. Thus, *Gclm* null mice must also be maintaining sufficient NADPH pools (or other reducing equivalents) into old age. The primary NADPH-generating pathway in mammals is the pentose phosphate shunt (PPP), in which the nucleotide synthesis precursor ribose-5-phosphate is produced from glucose-6-phosphate, and NADPH is generated as a consequence. Glucose-6-phosphate dehydrogenase (G6PD) is a major enzyme in this pathway, and previous work from the Kavanagh lab showed that G6PD mRNA is increased approximately 1.5 to 2-fold in *Gclm* null mouse livers, relative to *Gclm* wild-type (unpublished data). Further investigation into PPP activity and reducing-equivalent pools in *Gclm* mice (and how age and cadmium affect them) is warranted.

The data presented here provides strong support that the compensatory upregulation of Nrf2/Keap1 in *Gclm* null mice remains active into old age. However,

another potential explanation could be that alternative pathways which partially overlap in function or share complementary roles with Nrf2 (e.g., NF-κB, HIF1) are active into old age, and are able to "pick up the slack" of reduced Nrf2 activity in these mice. Another factor to consider is that our "old" (24+ months) mice may not have progressed to an age where Nrf2 activity declines. A well-known confounding variable in murine aging studies is genetic background. However, a study that has guided our first hypothesis studied mice with the same background as *Gclm* mice—male C57BL/6J—and found that Nrf2 activity was significantly impaired at only 18-21 months of age in response to chronic ambient nanoparticle exposure (Zhang et al., 2012a). In light of this, the idea that 24+ month *Gclm* mice are not "old enough" is unlikely. While it is possible that the mice that reached 24+ months of age represent healthy survivors, when overall survival is assessed, there were two, six and three premature deaths (i.e. did not reach 24 months of age, or were culled because of morbidity) for WT, Het and null mice, respectively. Most of these mice did have hepatomegaly, splenomegaly, or both (likely lymphoma), and this was not genotype dependent.

Finally, we observed only a marginal effect of $CdCl_2$ treatment on glutathione redox with age. Though our dosing regimen (single intraperitoneal injection) would be classified as acute, the mild dose used (2 mg/kg) was specifically chosen to allow for functional testing of glucose homeostasis 24 and 48 hours post-dosing (see **Chapter 3**), which is stressful and requires mice to maintain a relatively normal phenotype. A dearth of literature exists relating to acute heavy metal dosing in age, and though a dose escalation study was performed to help in this regard, we did not have enough extra aged *Gclm* mice allocated for this purpose. A different dose, or range of doses, may have been

more optimal for this experiment. In addition, glutathione redox status and Western blotting analysis of redox-sensitive proteins was mainly observed at 72 hr post-dosing, which may have masked some of the effects of cadmium treatment. We attempted to address this by administering cadmium to a small cohort of 24+ month mice and sacrificing at 8 hr post-dosing (Figures 2.13 – 2.15). Data from the 8 hr cohorts support the broader finding that GSH redox is maintained in the null mice at 24+ months of age.

2.5. Figures

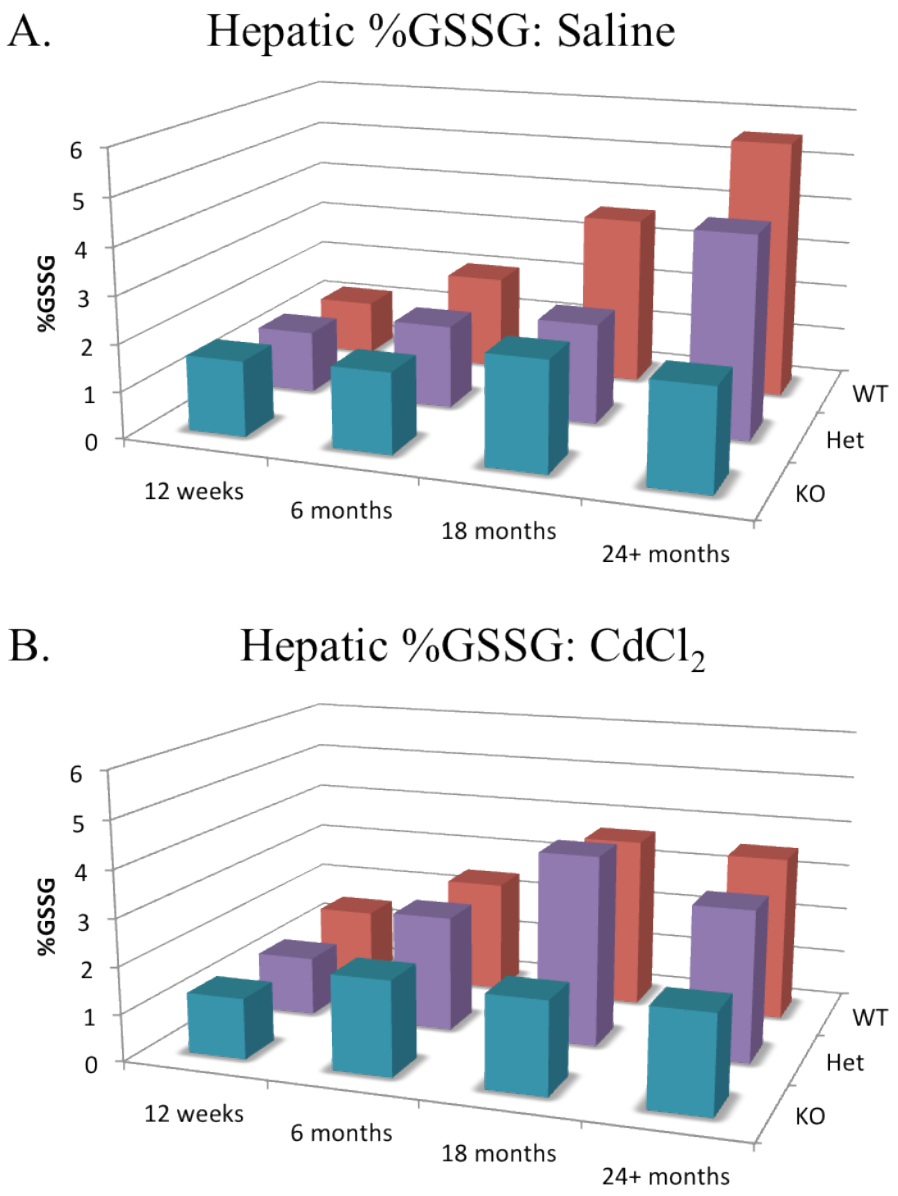

Figure 2.1. Hepatic % GSSG in (A) saline and (B) cadmium treated *Gclm* WT, Het, and null mice at 12 weeks, and at 6, 18, and 24+ months (n=6 mice/group).

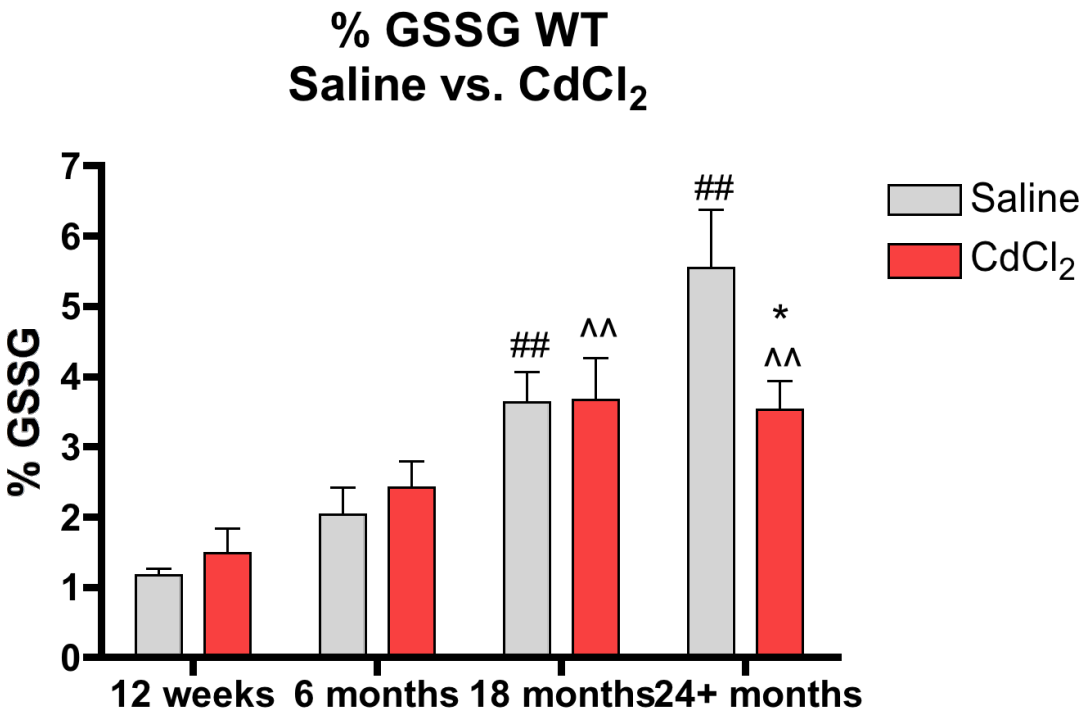

Figure 2.2. Hepatic % GSSG in saline and cadmium treated *Gclm* WT mice at 12 weeks, and at 6, 18, and 24+ months (n=6 mice/group). Data analyzed using One- and Two-Way ANOVA. # = Dunnett's for saline by age: $^{\#}p<0.05$, $^{\#\#}p<0.01$, $^{\#\#\#}p<0.001$; ^ = Dunnett's for $CdCl_2$ by age: $^{\wedge}p<0.05$, $^{\wedge\wedge}p<0.01$, $^{\wedge\wedge\wedge}p<0.001$; * = Two-Way ANOVA for age and treatment (with Bonferroni correction): $^{*}p<0.05$, $^{**}p<0.01$, $^{***}p<0.001$.

<u>One-Way ANOVA</u>
Saline: $p<0.0001$
$CdCl_2$: $p=0.0051$
<u>Two-Way ANOVA</u>
Interaction: $p=0.0413$
Treatment: $p=0.3245$
Age: $p<0.0001$

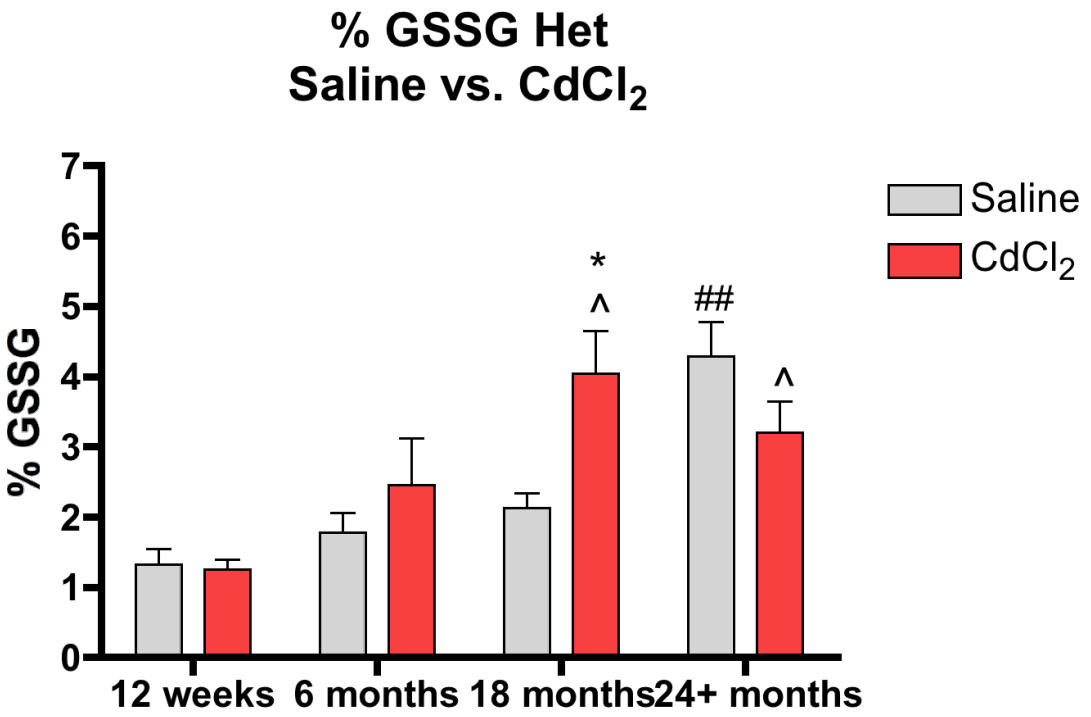

Figure 2.3. Hepatic % GSSG in saline and cadmium treated *Gclm* Het mice at 12 weeks, and at 6, 18, and 24+ months (n=6 mice/group). Data analyzed using One- and Two-Way ANOVA. # = Dunnett's for saline by age: $^{\#}p<0.05$, $^{\#\#}p<0.01$, $^{\#\#\#}p<0.001$; ^ = Dunnett's for $CdCl_2$ by age: $^{\wedge}p<0.05$, $^{\wedge\wedge}p<0.01$, $^{\wedge\wedge\wedge}p<0.001$; * = Two-Way ANOVA for age and treatment (with Bonferroni correction): $^{*}p<0.05$, $^{**}p<0.01$, $^{***}p<0.001$.

<u>One-Way ANOVA</u>
Saline: $p<0.0001$
$CdCl_2$: $p=0.0072$
<u>Two-Way ANOVA</u>
Interaction: $p=0.0098$
Treatment: $p=0.2367$
Age: $p<0.0001$

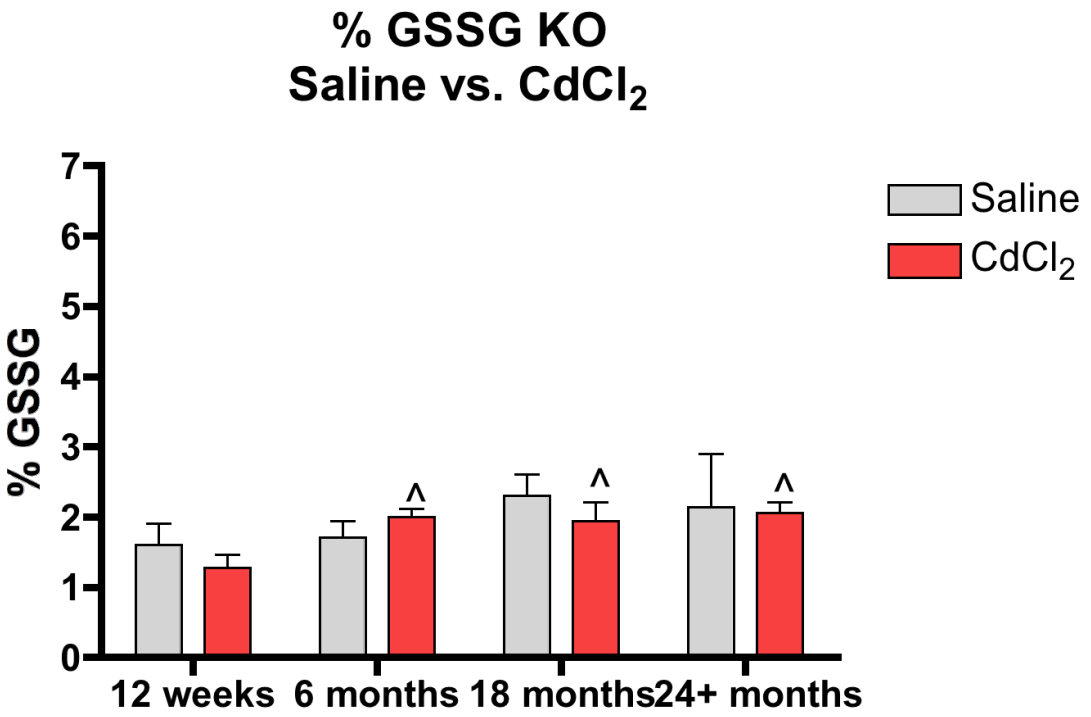

Figure 2.4. Hepatic % GSSG in saline and cadmium treated *Gclm* null mice at 12 weeks, and at 6, 18, and 24+ months (n=6 mice/group). Data analyzed using One- and Two-Way ANOVA. # = Dunnett's for saline by age: $^{\#}p<0.05$, $^{\#\#}p<0.01$, $^{\#\#\#}p<0.001$; ^ = Dunnett's for $CdCl_2$ by age: $^{\wedge}p<0.05$, $^{\wedge\wedge}p<0.01$, $^{\wedge\wedge\wedge}p<0.001$; * = Two-Way ANOVA for age and treatment (with Bonferroni correction): $^{*}p<0.05$, $^{**}p<0.01$, $^{***}p<0.001$.

<u>One-Way ANOVA</u>
Saline: p=0.6440
$CdCl_2$: p=0.0199
<u>Two-Way ANOVA</u>
Interaction: p=0.7457
Treatment: p=0.6241
Age: p=0.1586

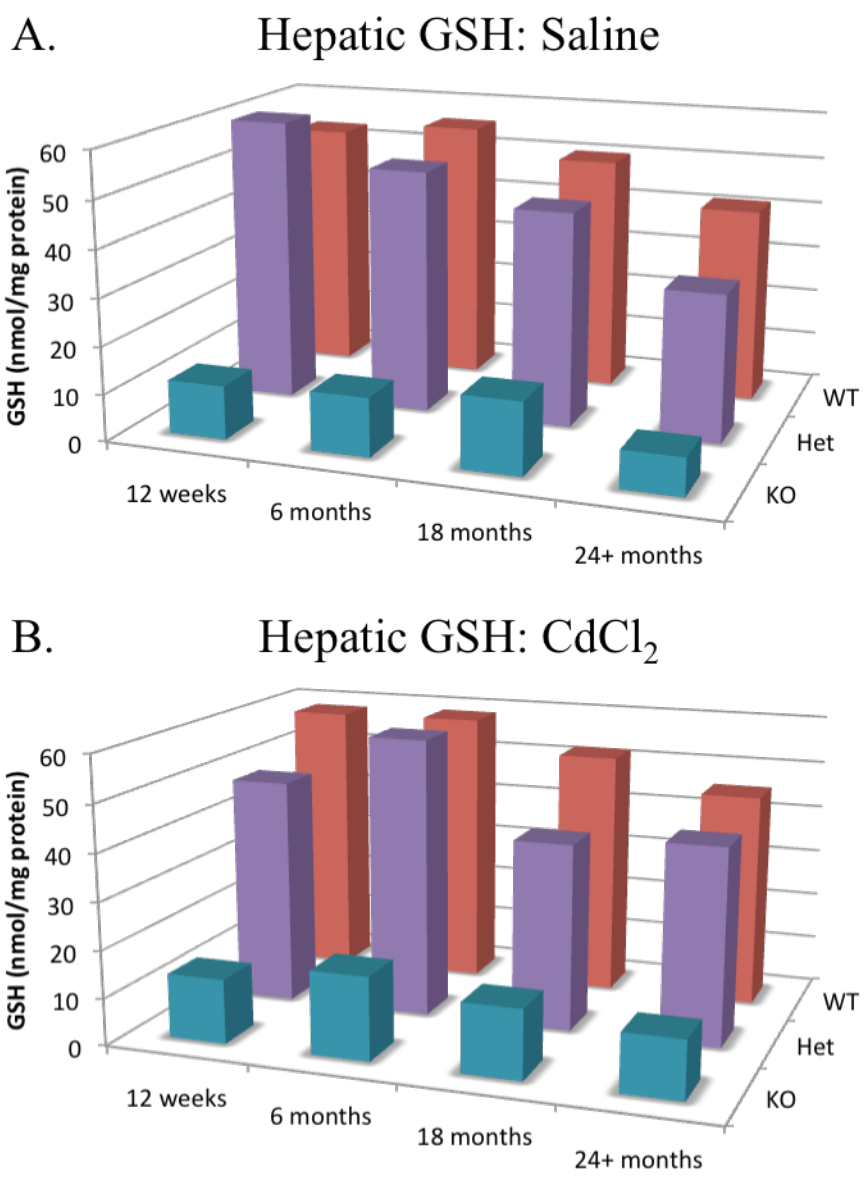

Figure 2.5. Hepatic GSH in (A) saline and (B) cadmium treated *Gclm* WT, Het, and null mice at 12 weeks, and at 6, 18, and 24+ months (n=6 mice/group).

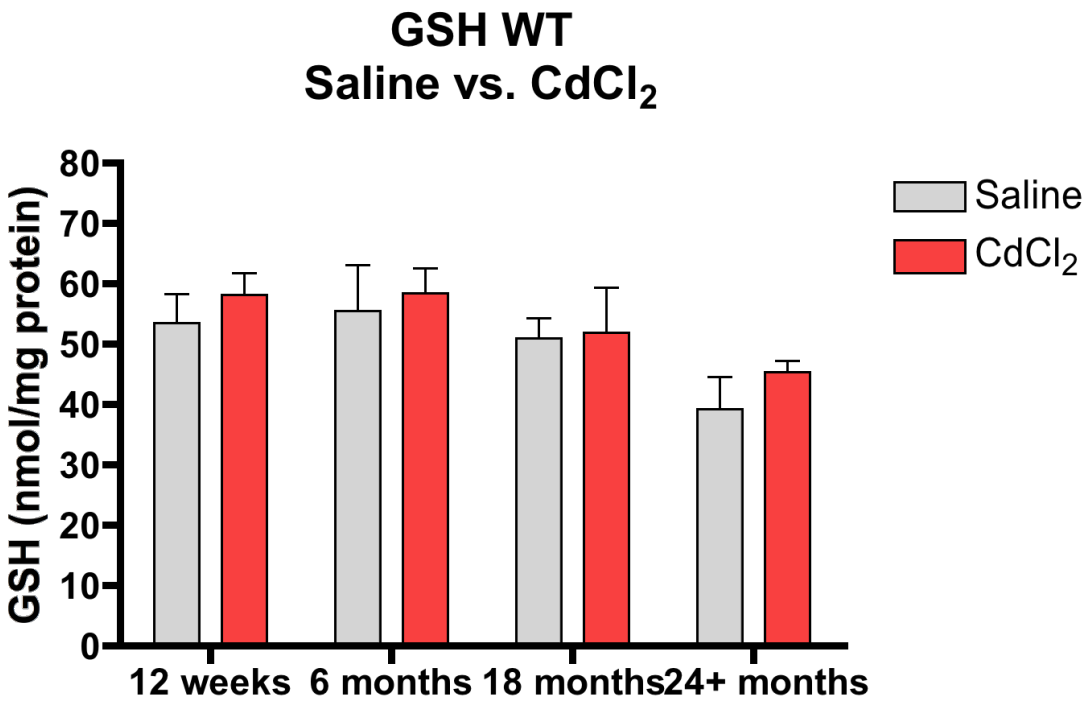

Figure 2.6. Hepatic total GSH in saline and cadmium treated *Gclm* WT mice at 12 weeks, and at 6, 18, and 24+ months (n=6 mice/group). Data analyzed using One- and Two-Way ANOVA. # = Dunnett's for saline by age: $^{\#}p<0.05$, $^{\#\#}p<0.01$, $^{\#\#\#}p<0.001$; ^ = Dunnett's for $CdCl_2$ by age: $^{\wedge}p<0.05$, $^{\wedge\wedge}p<0.01$, $^{\wedge\wedge\wedge}p<0.001$; * = Two-Way ANOVA for age and treatment (with Bonferroni correction): $^{*}p<0.05$, $^{**}p<0.01$, $^{***}p<0.001$.

<u>One-Way ANOVA</u>
Saline: p=0.1933
$CdCl_2$: p=0.1465
<u>Two-Way ANOVA</u>
Interaction: p=0.9618
Treatment: p=0.2918
Age: p=0.0210

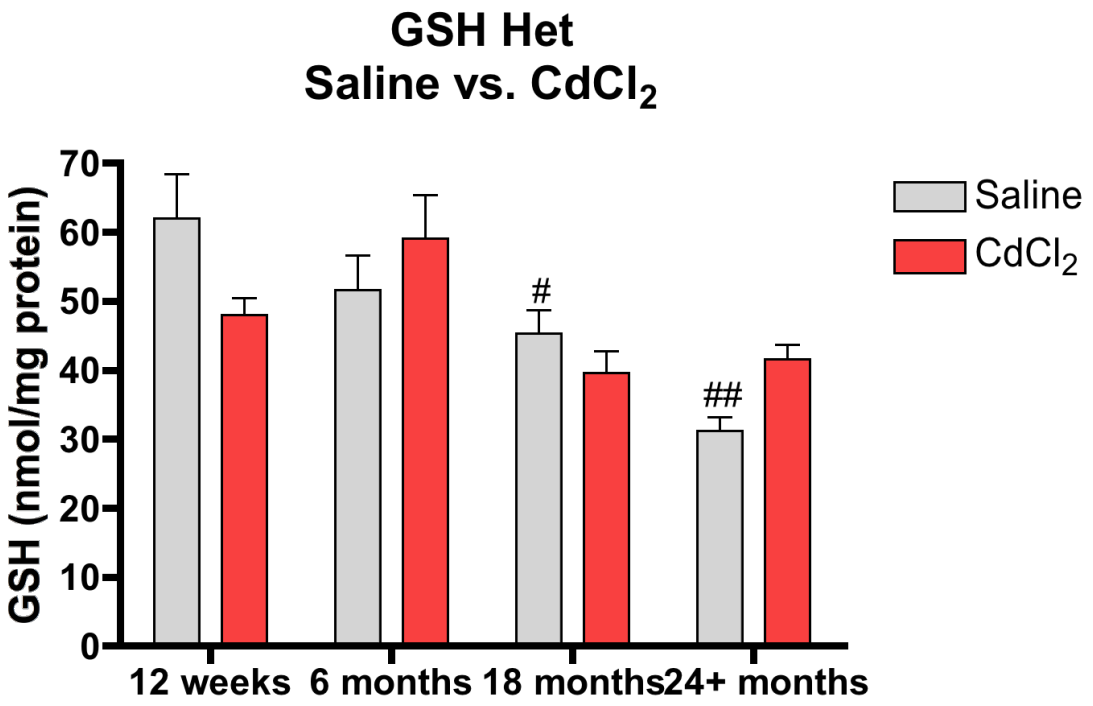

Figure 2.7. Hepatic total GSH in saline and cadmium treated *Gclm* Het mice at 12 weeks, and at 6, 18, and 24+ months (n=6 mice/group). Data analyzed using One- and Two-Way ANOVA. # = Dunnett's for saline by age: $^{\#}p<0.05$, $^{\#\#}p<0.01$, $^{\#\#\#}p<0.001$; ^ = Dunnett's for $CdCl_2$ by age: $^{\wedge}p<0.05$, $^{\wedge\wedge}p<0.01$, $^{\wedge\wedge\wedge}p<0.001$; * = Two-Way ANOVA for age and treatment (with Bonferroni correction): $^{*}p<0.05$, $^{**}p<0.01$, $^{***}p<0.001$.

<u>One-Way ANOVA</u>
Saline: p=0.0013
$CdCl_2$: p=0.0113
<u>Two-Way ANOVA</u>
Interaction: p=0.0267
Treatment: p=0.8878
Age: p=0.0001

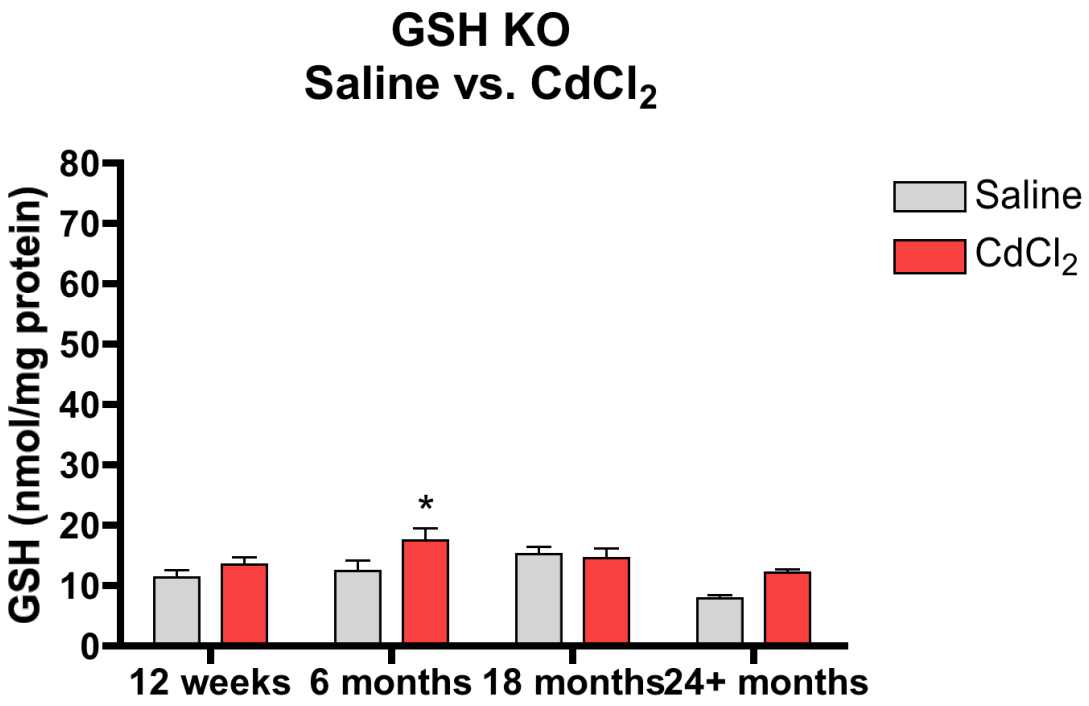

Figure 2.8. Hepatic total GSH in saline and cadmium treated *Gclm* null mice at 12 weeks, and at 6, 18, and 24+ months (n=6 mice/group). Data analyzed using One- and Two-Way ANOVA. # = Dunnett's for saline by age: $^{\#}p<0.05$, $^{\#\#}p<0.01$, $^{\#\#\#}p<0.001$; ^ = Dunnett's for $CdCl_2$ by age: $^{\wedge}p<0.05$, $^{\wedge\wedge}p<0.01$, $^{\wedge\wedge\wedge}p<0.001$; * = Two-Way ANOVA for age and treatment (with Bonferroni correction): $^{*}p<0.05$, $^{**}p<0.01$, $^{***}p<0.001$.

<u>One-Way ANOVA</u>
Saline: p=0.0055
$CdCl_2$: p=0.0898
<u>Two-Way ANOVA</u>
Interaction: p=0.1780
Treatment: p=0.0074
Age: p=0.0025

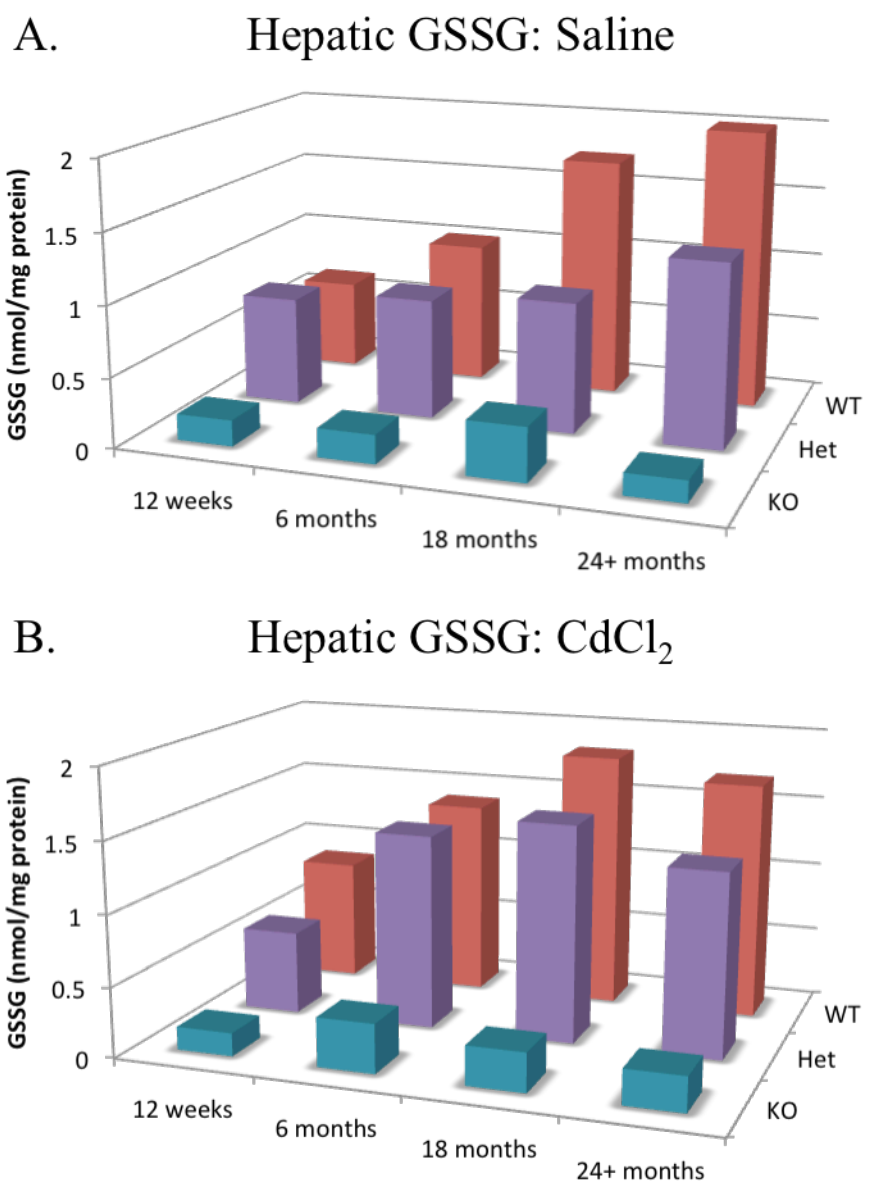

Figure 2.9. Hepatic GSSG in (A) saline and (B) cadmium treated *Gclm* WT, Het, and null mice at 12 weeks, and at 6, 18, and 24+ months (n=6 mice/group).

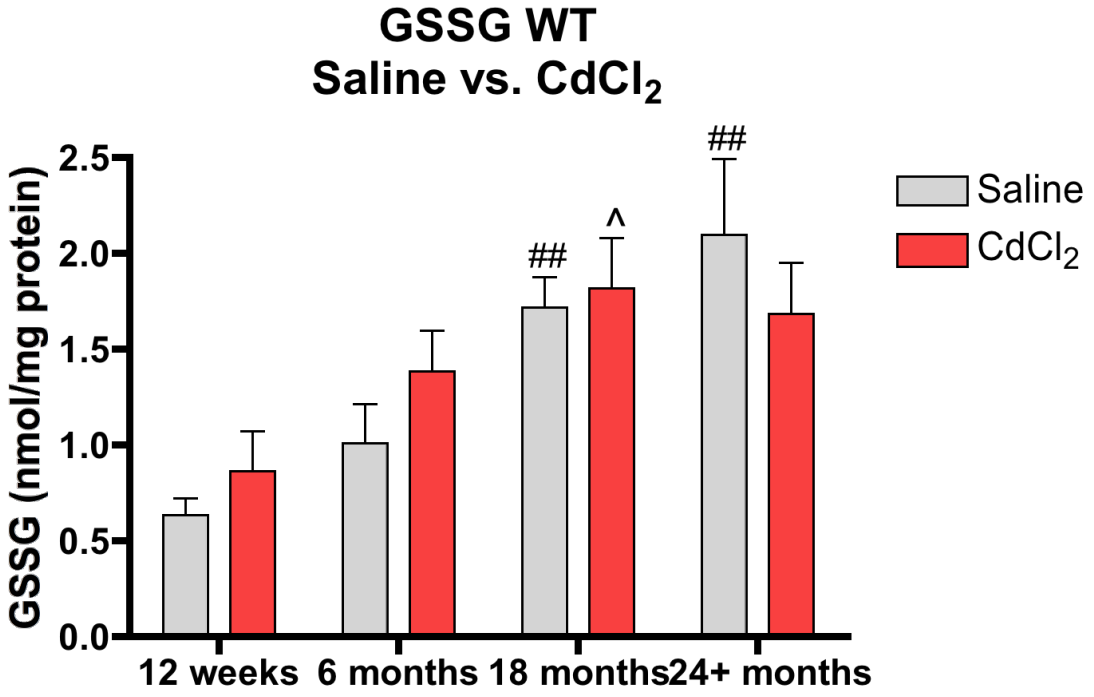

Figure 2.10. Hepatic oxidized glutathione in saline and cadmium treated *Gclm* WT mice at 12 weeks, and at 6, 18, and 24+ months (n=6 mice/group). Data analyzed using One- and Two-Way ANOVA. # = Dunnett's for saline by age: $^{\#}p<0.05$, $^{\#\#}p<0.01$, $^{\#\#\#}p<0.001$; ^ = Dunnett's for $CdCl_2$ by age: $^{\wedge}p<0.05$, $^{\wedge\wedge}p<0.01$, $^{\wedge\wedge\wedge}p<0.001$; * = Two-Way ANOVA for age and treatment (with Bonferroni correction): $^{*}p<0.05$, $^{**}p<0.01$, $^{***}p<0.001$.

<u>One-Way ANOVA</u>
Saline: p=0.0009
$CdCl_2$: p=0.0479
<u>Two-Way ANOVA</u>
Interaction: p=0.3908
Treatment: p=0.6580
Age: p<0.0001

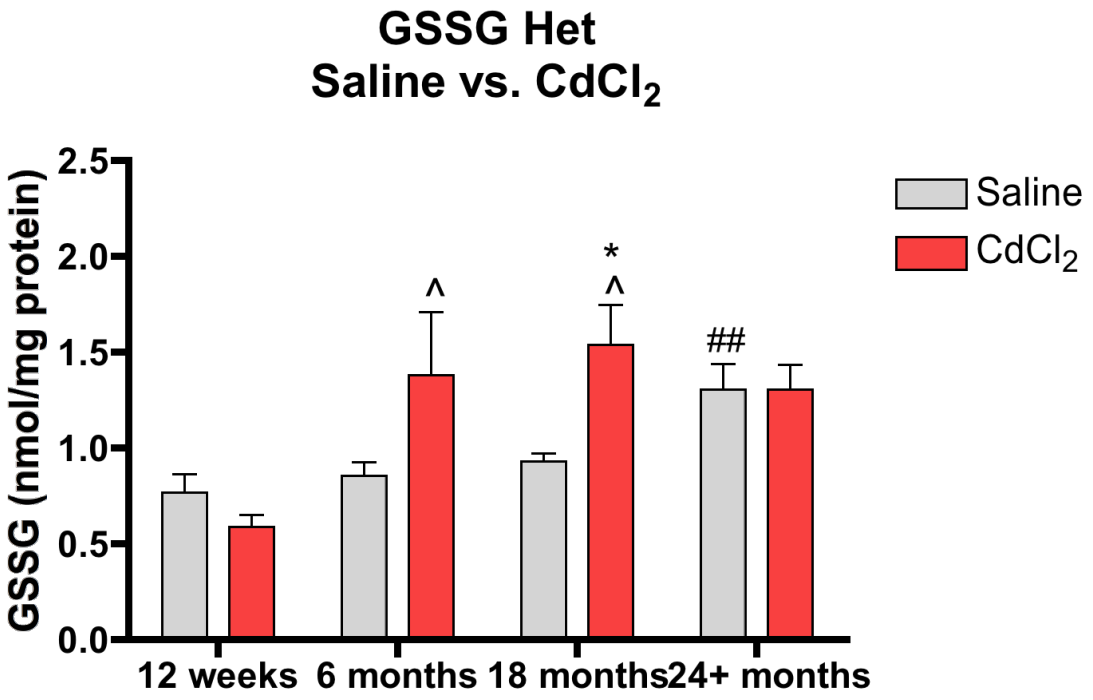

Figure 2.11. Hepatic oxidized glutathione in saline and cadmium treated *Gclm* Het mice at 12 weeks, and at 6, 18, and 24+ months (n=6 mice/group). Data analyzed using One- and Two-Way ANOVA. # = Dunnett's for saline by age: $^{\#}p<0.05$, $^{\#\#}p<0.01$, $^{\#\#\#}p<0.001$; ^ = Dunnett's for $CdCl_2$ by age: $^{\wedge}p<0.05$, $^{\wedge\wedge}p<0.01$, $^{\wedge\wedge\wedge}p<0.001$; * = Two-Way ANOVA for age and treatment (with Bonferroni correction): $^{*}p<0.05$, $^{**}p<0.01$, $^{***}p<0.001$.

<u>One-Way ANOVA</u>
Saline: p=0.0022
$CdCl_2$: p=0.0218
<u>Two-Way ANOVA</u>
Interaction: p=0.0409
Treatment: p=0.0393
Age: p=0.0015

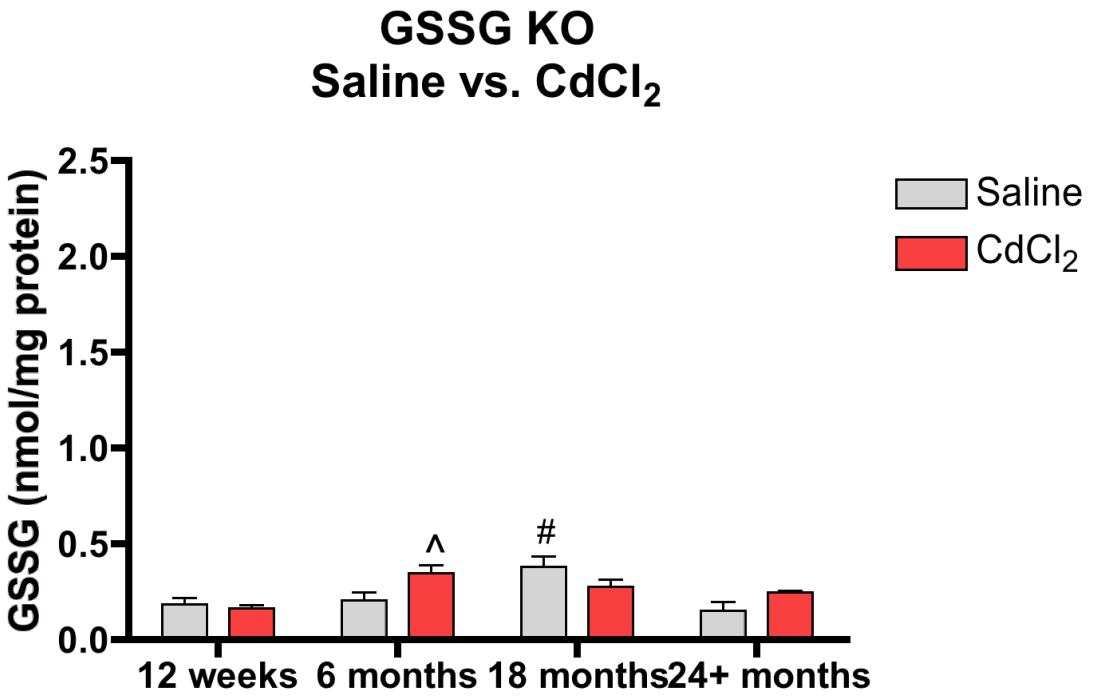

Figure 2.12. Hepatic oxidized glutathione in saline and cadmium treated *Gclm* null mice at 12 weeks, and at 6, 18, and 24+ months (n=6 mice/group). Data analyzed using One- and Two-Way ANOVA. # = Dunnett's for saline by age: $^{\#}p<0.05$, $^{\#\#}p<0.01$, $^{\#\#\#}p<0.001$; ^ = Dunnett's for $CdCl_2$ by age: $^{\wedge}p<0.05$, $^{\wedge\wedge}p<0.01$, $^{\wedge\wedge\wedge}p<0.001$; * = Two-Way ANOVA for age and treatment (with Bonferroni correction): $^{*}p<0.05$, $^{**}p<0.01$, $^{***}p<0.001$.

<u>One-Way ANOVA</u>
Saline: p=0.0069
$CdCl_2$: p=0.0018
<u>Two-Way ANOVA</u>
Interaction: p=0.0076
Treatment: p=0.3084
Age: p=0.0005

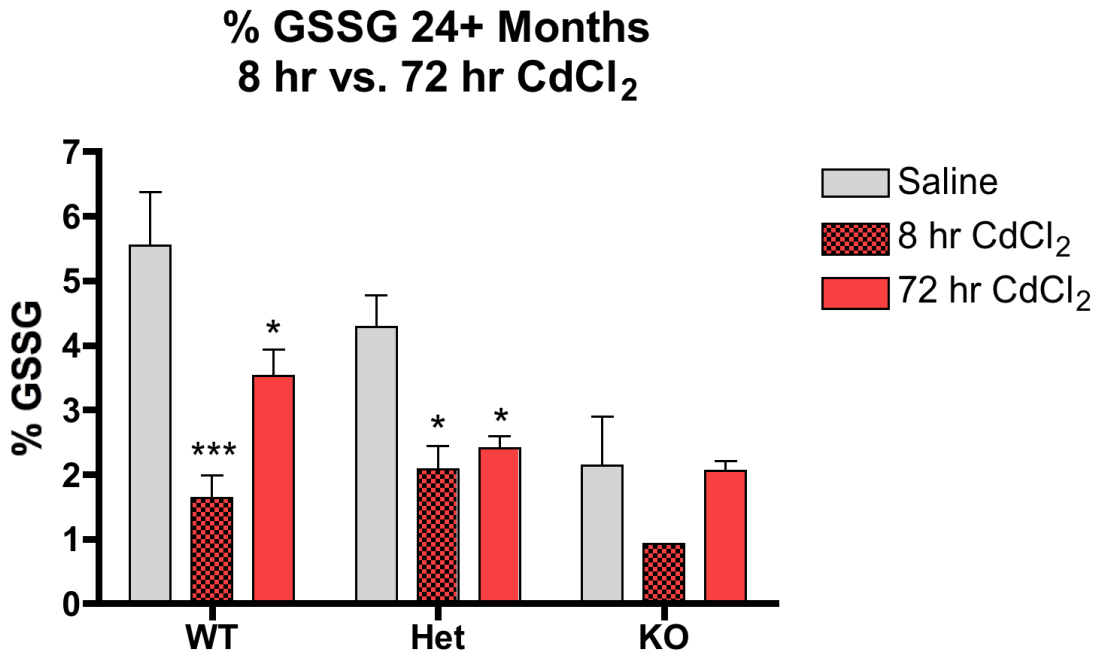

Figure 2.13. Hepatic % GSSG in saline and cadmium treated 24+ month *Gclm* WT, Het, and null mice at 8 and 72 hours post-dosing (n=6 mice for saline and 72 hr $CdCl_2$ groups for all genotypes; n=4 mice for WT and Het and n=2 mice for null for 8 hr $CdCl_2$ groups).

Two-Way ANOVA
Interaction: p=0.1205
Treatment: p=0.0002
Genotype: p=0.0079
* = Two-Way ANOVA for genotype and treatment: $^{*}p<0.05$, $^{**}p<0.01$, $^{***}p<0.001$

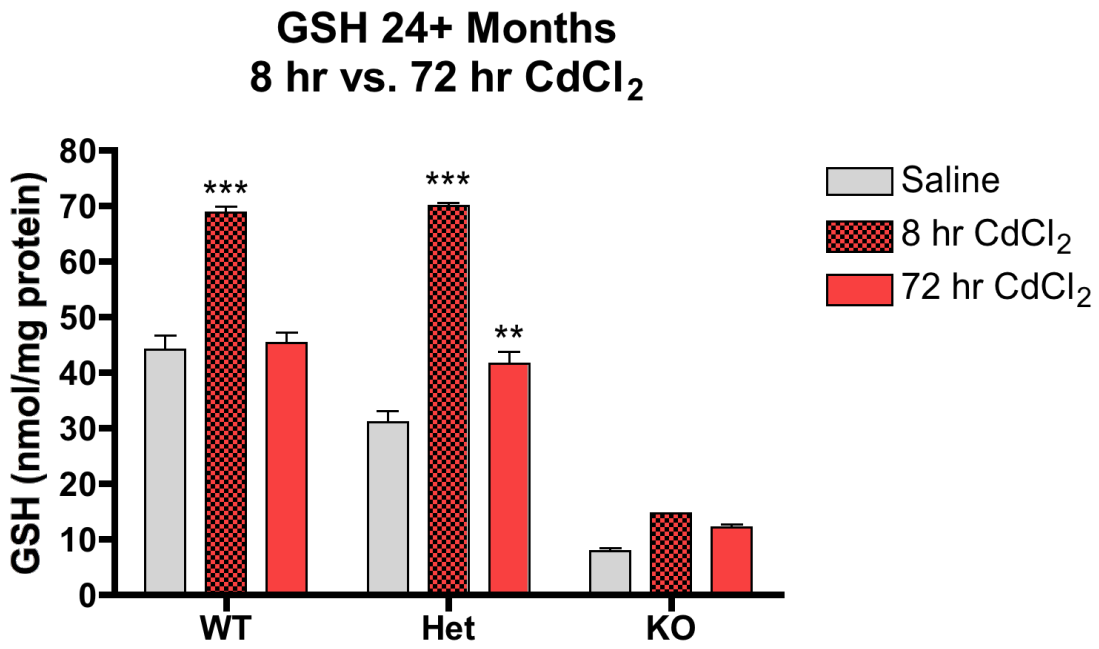

Figure 2.14. Hepatic total GSH in saline and cadmium treated 24+ month *Gclm* WT, Het, and null mice at 8 and 72 hours post-dosing (n=6 mice for saline and 72 hr $CdCl_2$ groups for all genotypes; n=4 mice for WT and Het and n=2 mice for null for 8 hr $CdCl_2$ groups).

Two-Way ANOVA
Interaction: $p<0.0001$
Treatment: $p<0.0001$
Genotype: $p<0.0001$
* = Two-Way ANOVA for genotype and treatment: $^{*}p<0.05$, $^{**}p<0.01$, $^{***}p<0.001$

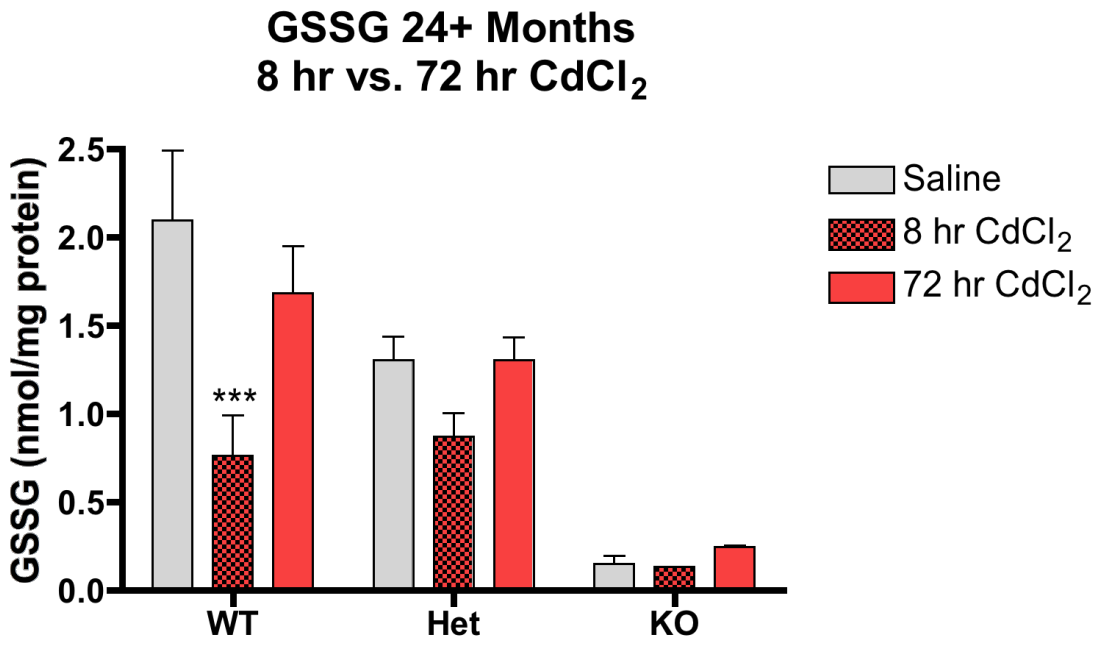

Figure 2.15. Hepatic glutathione disulfide (GSSG) in saline and cadmium treated 24+ month *Gclm* WT, Het, and null mice at 8 and 72 hours post-dosing (n=6 mice for saline and 72 hr $CdCl_2$ groups for all genotypes; n=4 mice for WT and Het and n=2 mice for null for 8 hr $CdCl_2$ groups).

Two-Way ANOVA
Interaction: p=0.1261
Treatment: p=0.0245
Genotype: p<0.0001
* = Two-Way ANOVA for genotype and treatment: $^{*}p<0.05$, $^{**}p<0.01$, $^{***}p<0.001$

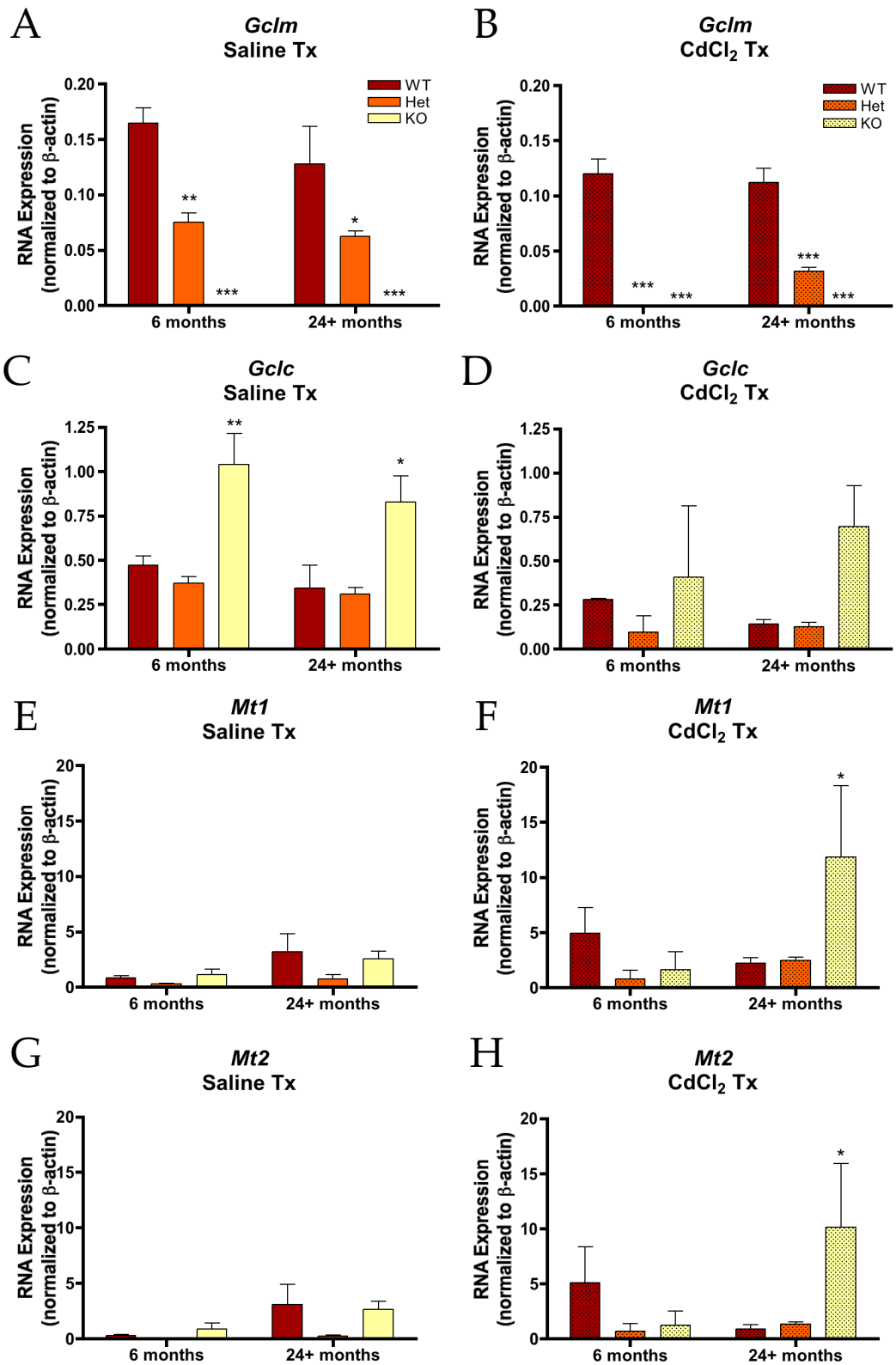
A
Gclm
Saline Tx
B
Gclm
CdCl2 Tx
WT
Het
KO
RNA Expression
(normalized to β-actin)
6 months
24+ months
C
Gclc
Saline Tx
D
Gclc
CdCl2 Tx
E
Mt1
Saline Tx
F
Mt1
CdCl2 Tx
G
Mt2
Saline Tx
H
Mt2
CdCl2 Tx

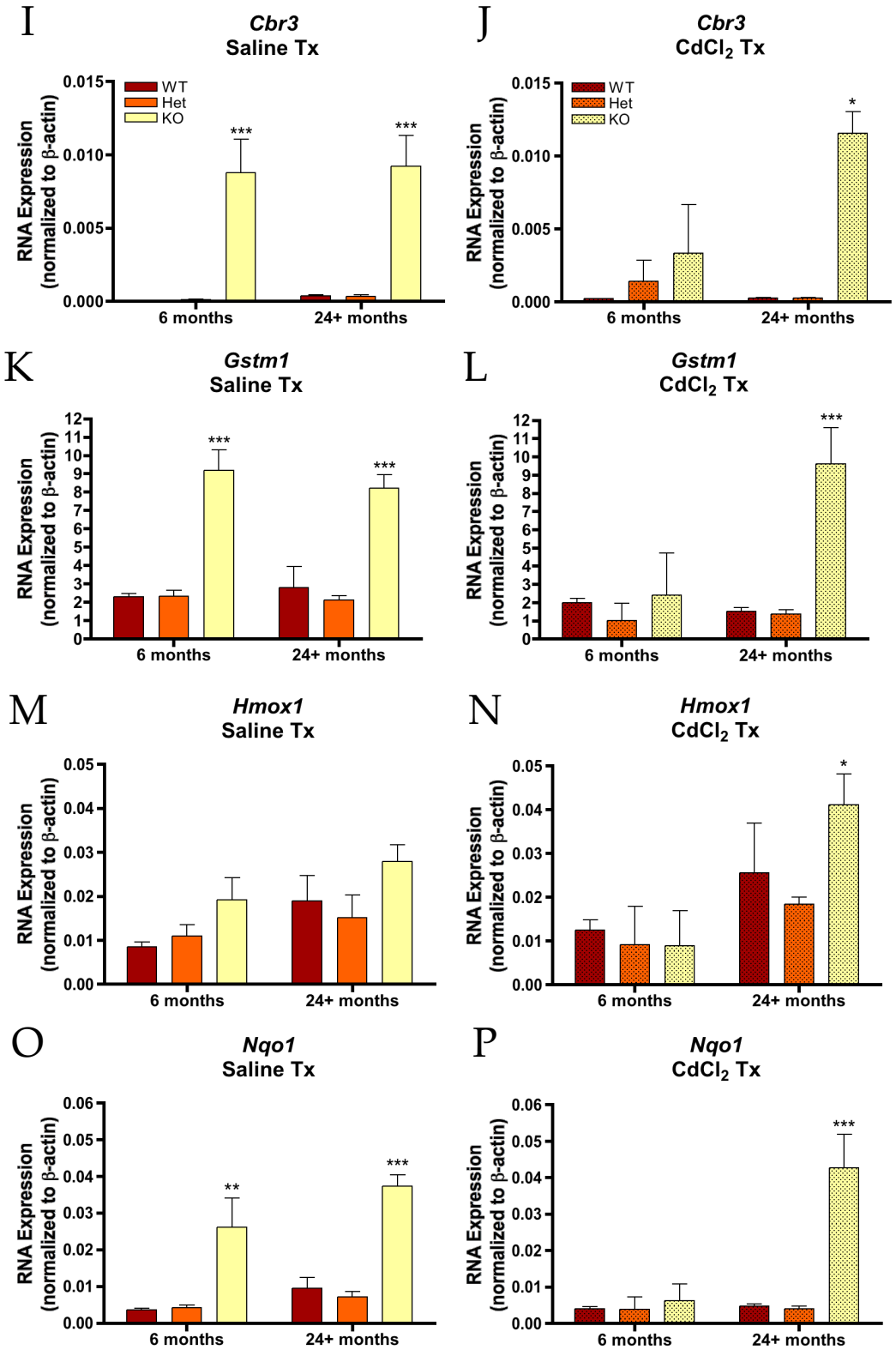

Figure 2.16. Hepatic mRNA expression of select Nrf2-regulated genes *Gclm* (A, B), *Gclc* (C, D), *Mt1* (E, F), *Mt2* (G, H), *Cbr3* (I, J), *Gstm1* (K, L), *Hmox1* (M, N), and *Nqo1*

(O, P) using qRT-PCR in the livers of 6 and 24+ month old saline and $CdCl_2$ treated *Gclm* mice. Expression values are reported as means and SEM (n=4 for all cohorts, except for the 6 month WT, Het, and null $CdCl_2$ groups, which had an n=3), normalized to β-actin mRNA expression. Data analyzed by Two-Way ANOVA for genotype and treatment (using 6 month WT saline as 'control' group), with Bonferroni corrections. $^{*}p<0.05$, $^{**}p<0.01$, $^{***}p<0.001$.

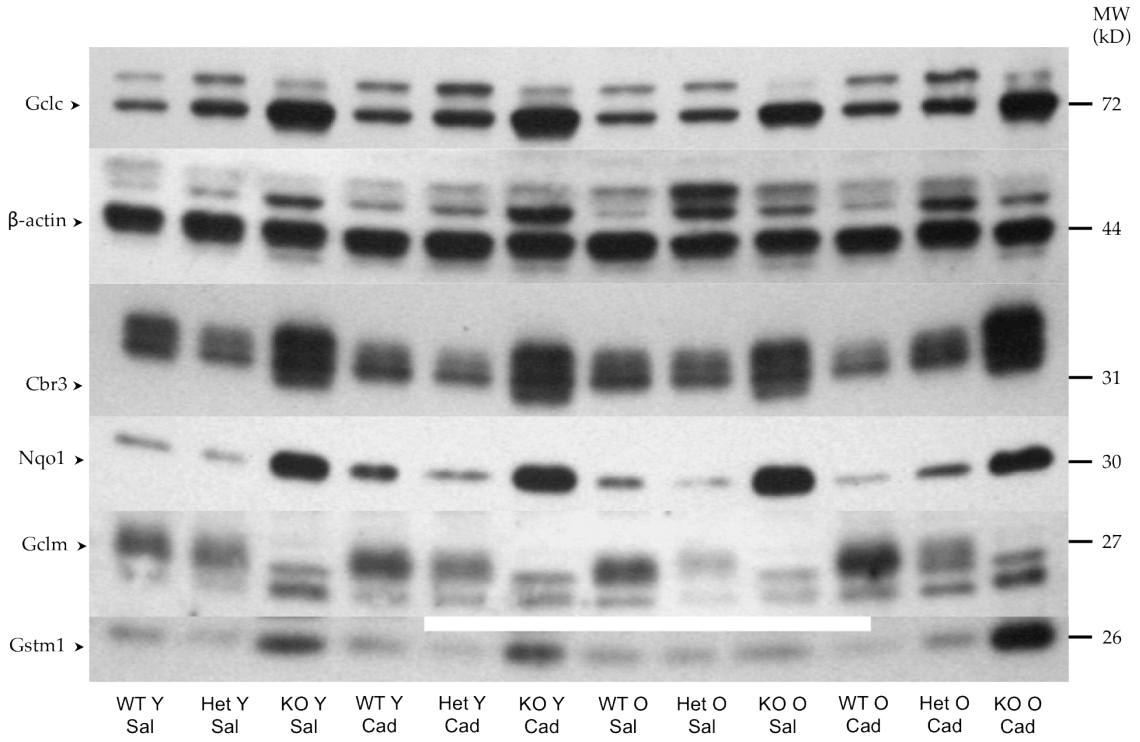

Figure 2.17. Representative immunoblots of Nrf2-regulated proteins in the livers of *Gclm* WT, Het, and null mice. "Y," young (6 months); "O," old (24+ months); "Sal," saline treated; "Cad," cadmium treated. β-actin was used as loading control. Blots were from the same membranes, which were stripped and re-probed.

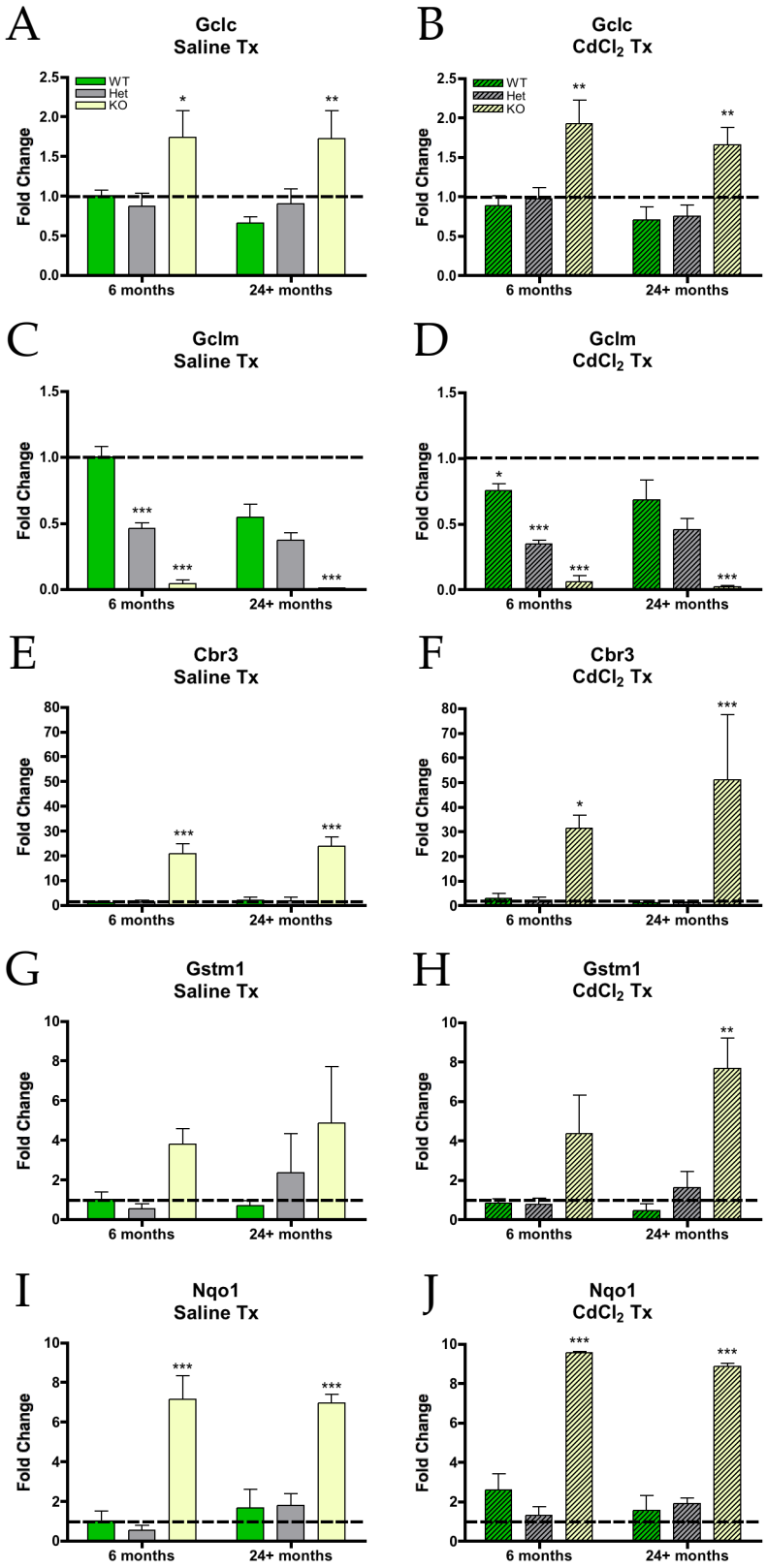
A
Gclc
Saline Tx
WT
Het
KO
Fold Change
6 months
24+ months
B
Gclc
CdCl2 Tx
C
Gclm
Saline Tx
D
Gclm
CdCl2 Tx
E
Cbr3
Saline Tx
F
Cbr3
CdCl2 Tx
G
Gstm1
Saline Tx
H
Gstm1
CdCl2 Tx
I
Nqo1
Saline Tx
J
Nqo1
CdCl2 Tx

Figure 2.18. Densitometric analysis of Western blots for expression of Nrf2-regulated proteins Gclc (A, B), Gclm (C, D), Cbr3 (E, F), Gstm1 (G, H), and Nqo1 (I, J) in liver homogenates from male *Gclm* WT, Het, and null mice, following treatment with saline or $CdCl_2$. Homogenates used for Westerns were derived from the same animals as those used for RNA expression. The results are expressed as means and SEM (n=3 mice/group), adjusted to the loading control, β-actin, and calculated as the fold-change relative to the mean of the control group (6 months WT saline) for each protein. * = Two-Way ANOVA: $^{*}p<0.05$, $^{**}p<0.01$, $^{***}p<0.001$.

Chapter 3

Persistence of improved glucose homeostasis in *Gclm* null mice with age and cadmium treatment.

3.1. Introduction

Data from colleagues at the University of Cincinnati, who have also developed *Gclm* null mice that closely mirror the phenotypes of our *Gclm* null mice, show that young (~10 weeks) *Gclm* null mice exhibit improved measures of glucose homeostasis relative to *Gclm* wild-type mice, as well as a lean phenotype which is resistant to HFD-induced obesity and development of T2DM (Dalton et al., 2004; Kendig et al., 2011; Yang et al., 2002). Another study examining *Gclm* null mice found they display reduced hepatic glycogen storage (Lavoie et al., 2016)—this finding stands in contrast to mice with hepatocyte-specific *Txnrd1*-knockdown (another model of chronic thiol insufficiency), which display increased hepatic glycogen storage (Iverson et al., 2013). Furthermore, both our lab's and the Cincinnati group's *Gclm* null models display increased Nrf2 activity and subsequently, increased expression of Nrf2-regulated genes (Kendig et al., 2011; McConnachie et al., 2007). *Gclm* null mice are also resistant to methionine and choline deficient (MCD) diet- and 2,3,7,8-Tetrachlorodibenzo-p-dioxin (TCDD)-induced steatosis, lending further evidence to the idea that adaptive responses in chronically GSH-deficient mice are protective (Chen et al., 2012; Haque et al., 2010).

The lean phenotype observed in *Gclm* null mice likely results from a switch in hepatic energy utilization in response to GSH deficiency. In the liver, *Gclm* null mice display decreased expression of genes involved in lipogenesis and gluconeogenesis, and

increased expression of genes involved in glycogenesis and lipid catabolism (unpublished data). The dysregulation of these pathways relative to WT mice may be central to the T2DM and obesity resistant phenotype observed in young *Gclm* null mice. Notably, Nrf2, the most highly upregulated pathway in *Gclm* null mice, is believed to have a protective effect in delaying T2DM and metabolic dysfunction (including impaired glucose homeostasis).

Therefore, we surmise that compensatory hepatic Nrf2 upregulation contributes significantly to the improved metabolic state observed in *Gclm* null mice. We expect young *Gclm* null mice (≤ 6 months) to display improved parameters of glucose homeostasis relative to wild-type mice. If cytoprotective pathway activities decline with age, as has been previously reported (Zhang et al., 2012a), we hypothesize that *Gclm* null mice will show signs of metabolic dysfunction (i.e. increased fasting blood glucose levels, impaired glucose tolerance, and decreased insulin sensitivity) relative to wild-type mice by 24+ months of age, especially following treatment with the toxicant and 'diabetogen' cadmium.

The aim of this section was to determine if improved parameters of glucose and metabolic homeostasis observed in young *Gclm* null mice relative to wild-type mice (i.e. insulin sensitivity, glucose tolerance, lean phenotype) are maintained through old age and in response to cadmium treatment. We hypothesize that *Gclm* null mice will be unable to maintain a favorable metabolic phenotype into old age compared to wild-type and heterozygotes, owing to an age-related decline in Nrf2 activity.

3.2. Materials and Methods

For *Reagents, Establishment of an Aging* Gclm *Mouse Colony, Experimental Design, Treatments, Necropsies,* and *Statistical Analyses*, see Chapter 2.2.

In Vitro *Assessment of Glucose Homeostasis*

Plasma was collected from 6 and 24+ month wild-type and null mice by saphenous vein puncture and centrifuged in heparin-coated tubes, then stored at -20°C. Fasted plasma insulin levels were measured using the Mouse Ultrasensitive Insulin ELISA kit, following the manufacturer's instructions (ALPCO Diagnostics, Salem, NH).

In Vivo *Functional Assessment of Glucose Homeostasis*

For each cohort, baseline data for functional measures of glucose homeostasis—glucose tolerance test (GTT) and insulin sensitivity (ITT)—were assessed. Prior to GTT, mice were fasted for 8 hours, from 6 a.m. to 2 p.m. At the time of testing, baseline blood glucose levels were taken, immediately followed by i.p. injection of 1.5 g glucose/kg body weight (D-(+)-Glucose, Sigma G8270, solubilized and sterile filtered in 0.9% sodium chloride injection, USP) after which blood glucose was measured at 15, 30, 45, 60, and 120 min post-injection (Figure 3.1). We used a glucometer and glucose strips purchased from a retail pharmacy (Walgreen's, Inc., Seattle, WA).

For 6 and 24+ month *Gclm* wild-type and null mice, blood was collected at the time of baseline measurement for fasting plasma insulin analysis. The following day, mice were fasted for 4-6 hours in preparation for an ITT (8-10 a.m. to 2 p.m.). Baseline

blood glucose levels were measured, followed by IP injection of 1 U human insulin/kg body weight (Humulin R, Eli-Lilly, solubilized in 0.9% sodium chloride injection, USP). Blood glucose was monitored at 15, 30, 45, 60, and 120 minutes post-insulin administration (Figure 3.1).

Following baseline measurements of glucose homeostasis, mice were allowed to recover for a week, then treated with either saline or cadmium chloride (Cadmium chloride, Sigma 202908, in 0.9% sodium chloride injection, USP) one to two weeks after baseline data was recorded. Mice were subjected to the same GTT and ITT on subsequent days beginning 24 hours post $CdCl_2$ (or saline) treatment (Figure 3.1).

3.3. Results

The first parameter of metabolic health we examined was body weight in *Gclm* mice. Our data shows that *Gclm* null mice display a leaner phenotype throughout old age compared to WT and Het mice (Figure 3.2). At 18 and 24+ months, this difference was statistically significant by Two-Way ANOVA , and the data also suggest that null mice display less variability in weight at 18 and 24+ months compared to WT and Het mice (Figure 3.2). This suggests that the downregulation of fatty acid synthesis observed previously in young *Gclm* null mice (Kendig et al., 2011) is likely maintained through 24+ months.

Next, we examined functional parameters of glucose homeostasis—glucose tolerance and insulin sensitivity. At baseline, *Gclm* null mice were more glucose tolerant

and insulin sensitive than WT and Het mice at all ages (Figures 3.3, 3.4, 3.7, 3.8). Saline did not have much of an effect on this general trend (Figures 3.3, 3.5, 3.7, 3.9), the only exception being ITT at 24+ months, where there was no observable difference in insulin sensitivity between any *Gclm* genotype (Figure 3.9). Surprisingly, cadmium treatment had no effect on the baseline GTT trend (Figures 3.3 and 3.6). Overall, ITT was also unaffected by cadmium administration, except at 18 months, where *Gclm* null mice were not more insulin sensitive than WT or Het mice (Figure 3.10). However, at 24+ months, cadmium-treated *Gclm* null mice were back to being more insulin-sensitive than *Gclm* WT and Het mice (Figure 3.10).

To complement GT and IT testing, we measured fasting plasma insulin levels in *Gclm* WT and null mice at 6 and 24+ months of age, following saline or cadmium treatment (Figure 3.11). At 24+ months, WT mice displayed a statistically significant increase in fasted insulin levels by two-way ANOVA ($p<0.05$ for saline; $p<0.0001$ for cadmium) (Figure 3.11). In contrast, *Gclm* null mice displayed a statistically significant *decrease* in fasted plasma insulin by 24+ months (Figure 3.12B, F). Cadmium treatment did not enhance this effect in nulls, but it did enhance the trend seen in WTs (Figure 3.12C, D).

3.4. Discussion

We settled on two functional parameters to examine general glucose homeostasis in *Gclm* mice of differing genotypes: glucose tolerance and insulin sensitivity tests.

During these tests, mice are challenged with a bolus of either glucose (GTT) or insulin (ITT), and blood glucose is periodically measured to see how mice respond to each challenge (i.e. how quickly blood glucose levels return to baseline). Impaired glucose tolerance and insulin sensitivity are associated with a T2DM phenotype and general metabolic dysfunction. Previous work (Kendig et al., 2011) demonstrated that young *Gclm* mice are more insulin sensitive (as indicated by the calculation of the homeostasis model assessment of insulin resistance; HOMA-IR), and glucose tolerant than WT mice, a trend we replicated here. However, this is the first study to examine how these findings are affected in Gclm Het mice, and with age and in response to a toxicant challenge.

Unexpectedly, our results contradict the hypothesis that age would have a significant effect on the ability of *Gclm* null mice to maintain improved insulin sensitivity and glucose tolerance relative to WT mice (Figures 3.3 to 3.10). Because recent evidence points to an important role for Nrf2/Keap1 in maintaining metabolic homeostasis and preventing T2DM-like phenotypes, the data presented here are consistent with Nrf2 activity not declining with age. The idea that *Gclm* null mice are protected from metabolic dysfunction with age is further supported by the finding that WT mice have increased fasted plasma insulin at old age, while null mice actually decrease fasting insulin with age (Figures 3.11, 3.12). High circulating insulin in a fasted state is indicative of insulin resistance, as it suggests that beta-cells within pancreatic islets need to produce and export more insulin to the periphery in order to maintain normal blood glucose.

A possible explanation for the improved glucose homeostasis observed in *Gclm* null mice is through Nrf2 acting as an effector of the AMPK axis. AMPK is an energy

sensor that maintains energy homeostasis and interacts with several cellular metabolic pathways, including Nrf2. AMPK activation results in suppressed hepatic lipogenesis and gluconeogenesis (Xu et al., 2013)—changes known to occur in the livers of *Gclm* null mice. Importantly, the improved metabolic phenotype observed in *Gclm* null cannot be attributed exclusively to differences in gluconeogenesis and lipogenesis in the liver. Tissues such as muscle, adipose, and pancreas also likely contribute to the increased glucose tolerance, insulin sensitivity, and increased basal metabolic rate *Gclm* null mice display. The role(s) of these tissues in glucose signaling warrant future investigation.

Our data go against the prevailing literature regarding glucose homeostasis changes with age in laboratory mice. Numerous studies have reported increasing insulin resistance and declining glucose tolerance concurrent with altered insulin secretion as characteristics of aging (Oh et al., 2016). However, notable exceptions have been documented in both humans and experimental animals (Bourey et al., 1993; Broughton et al., 1991; Chakraborty et al., 2009; Pacini et al., 1988). A study from 1988 which examined glucose homeostasis in male C57BL/6J mice (the same background strain as *Gclm* mice), came to the following conclusion: "the findings that glucose tolerance [does] not deteriorate with age, coupled with the lack of evidence for impaired beta cell responsiveness to glucose in old males, suggest that deterioration in glucose homeostasis is not an inevitable consequence of aging in the mouse" (Leiter et al., 1988). The results of a more recent study went further, showing glucose tolerance *improving* with age in this strain (Oh et al., 2016). In contrast, in the same study, Oh and colleagues found that insulin sensitivity declined with age (Oh et al., 2016).

It remains unresolved as to why insulin sensitivity improves with age in *Gclm* mice. These mice were derived from a C57BL/6J background many years ago, and even with backcrossing, it is quite possible that unknown factors, genetic, epigenetic, or otherwise, may have become fixed over time. Another potential explanation may be environmental differences that could alter gut microbiota in mice housed at UW compared to other institutions.

3.5. Figures

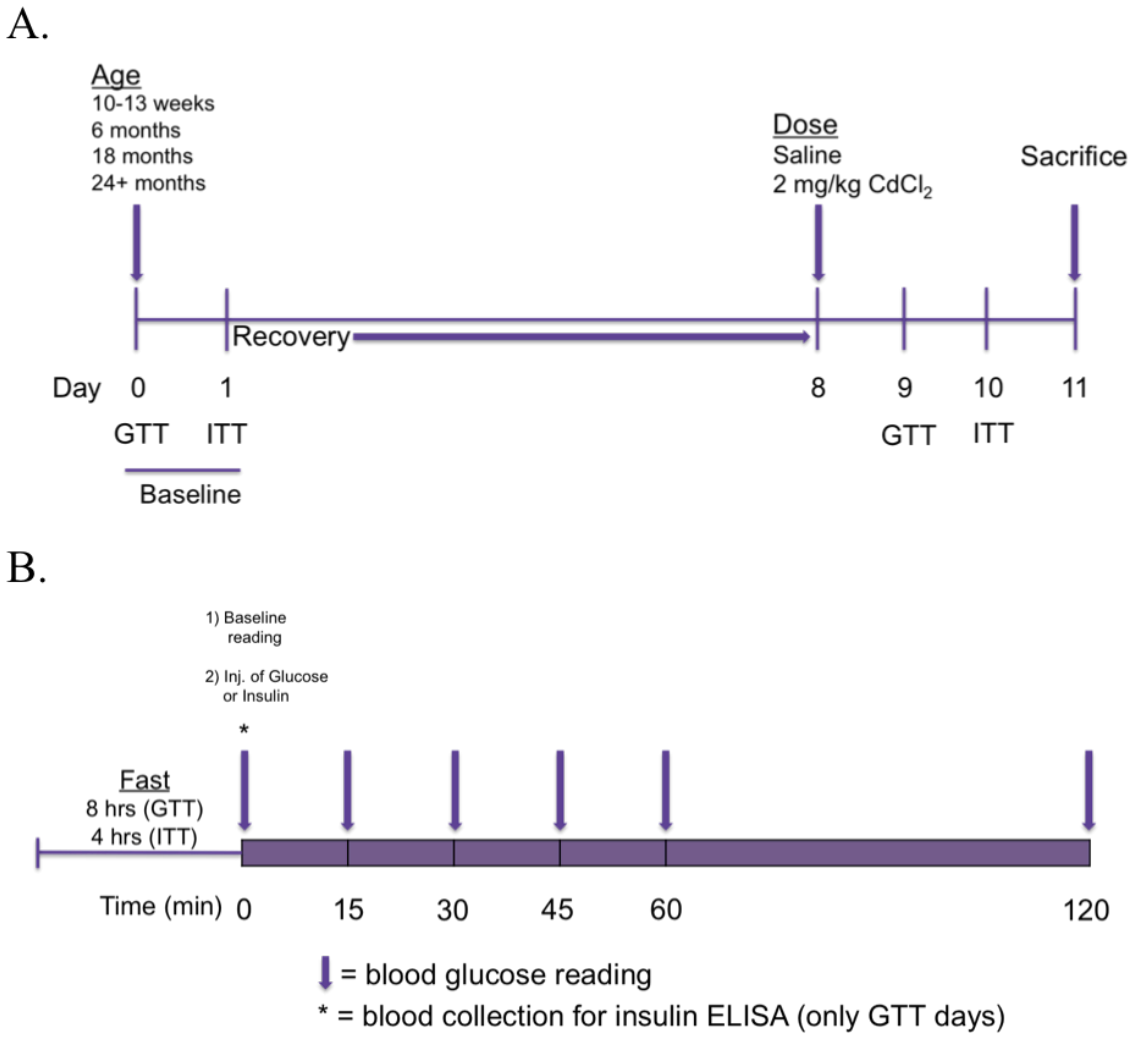

Figure 3.1. (A) Overall design schematic for functional tests of glucose homeostasis, and (B) daily experimental schematic for blood glucose reading and plasma collection.

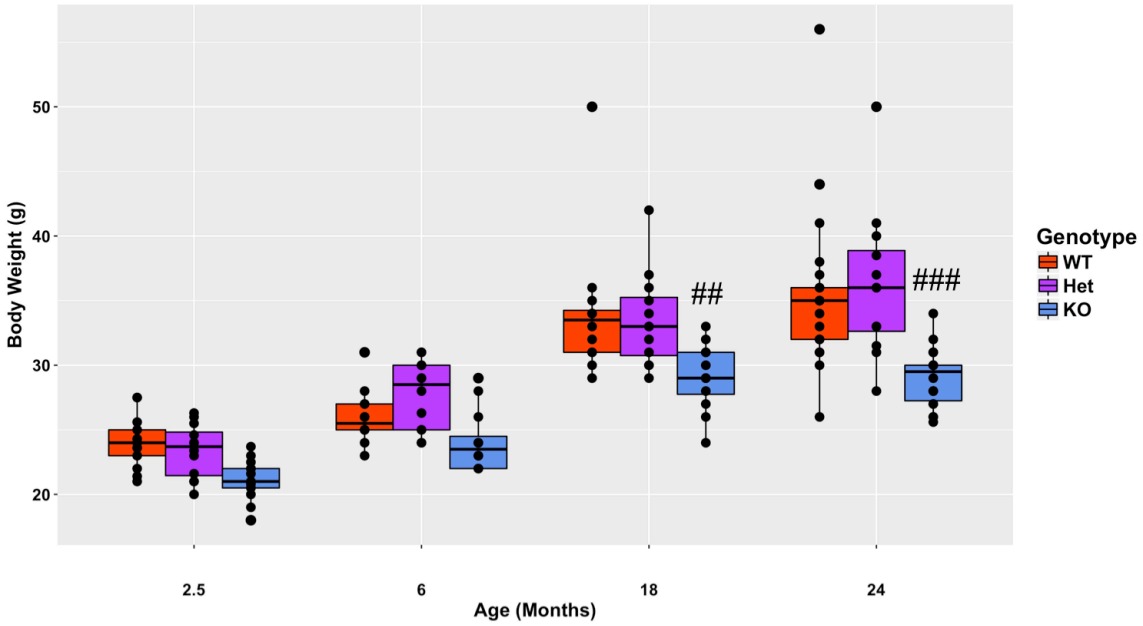

Figure 3.2. Body weights of *Gclm* WT, Het, and null mice at 12 weeks, and at 6, 18, and 24+ months (n=12-24 mice/group). Data analyzed using two-way ANOVA with Bonferroni corrections; #, $p<0.05$; ##, $p<0.001$; ###, $p<0.0001$.

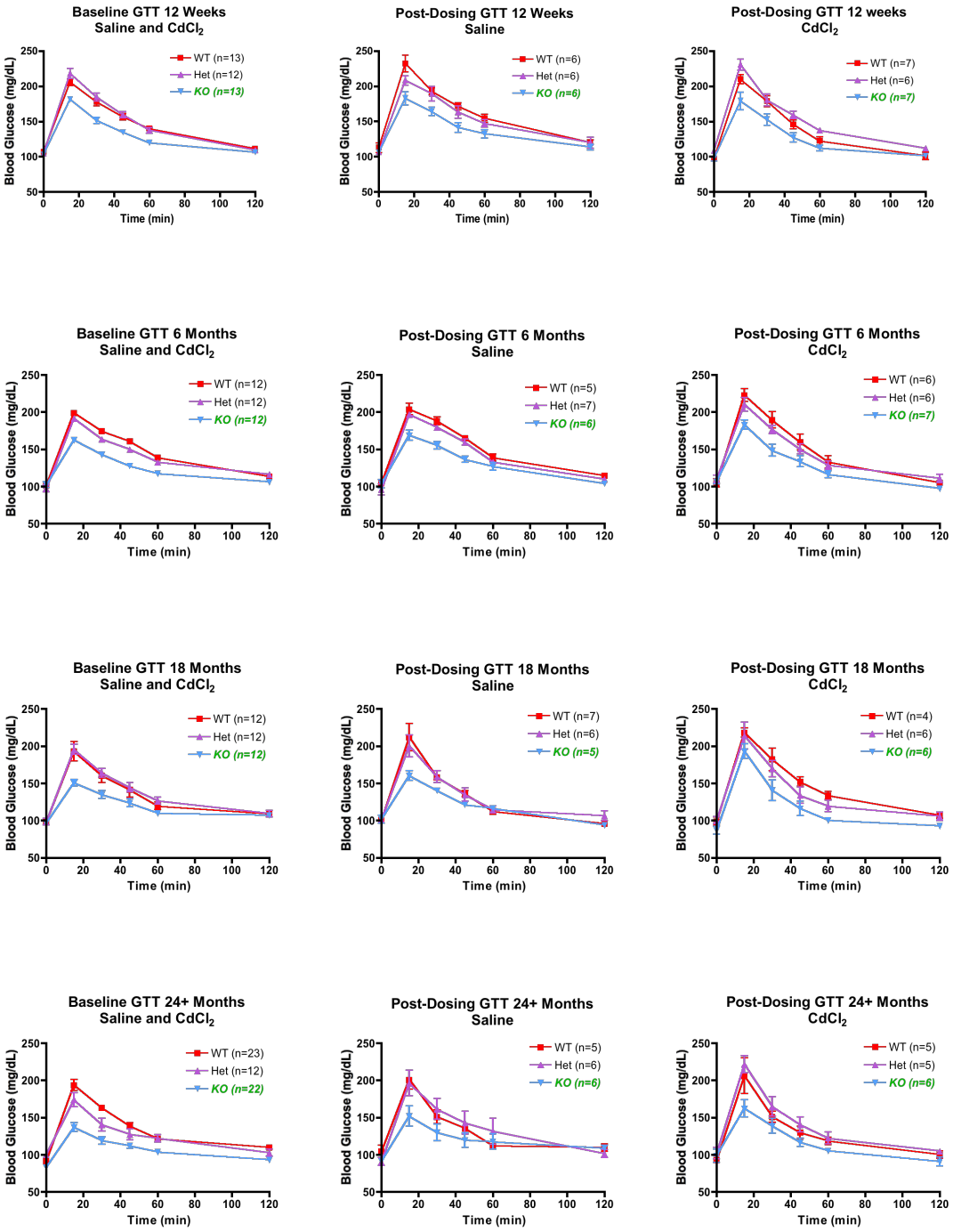

Figure 3.3. Measurements of glucose tolerance in *Gclm* WT, Het, and null mice at 12 weeks, 6, 18, and 24+ months at baseline or following saline/cadmium treatment. Errors bars represent the standard error of the mean. Green and italicized lettering indicates AUC significantly different from WT AUC by one-way ANOVA.

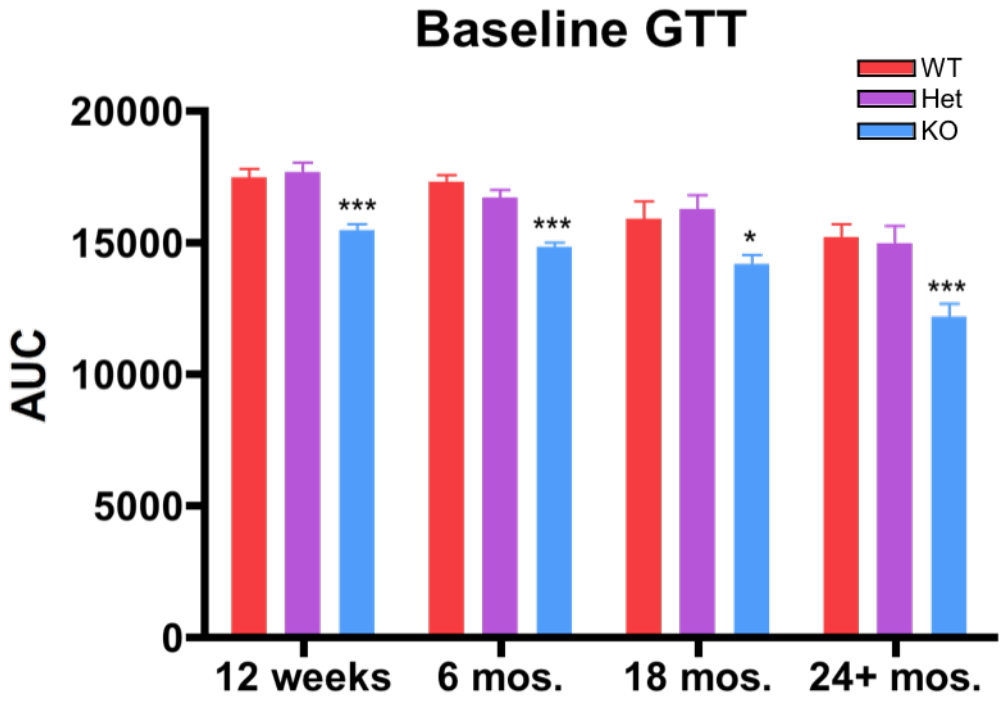

Figure 3.4. Measurements of baseline glucose tolerance in *Gclm* WT, Het, and null mice at 12 weeks, 6, 18, and 24+ months (n=12-24 mice/group). Data analyzed by one-way ANOVA (Dunnett's): *, $p<0.05$; **, $p<0.001$; ***, $p<0.0001$. Errors bars represent the standard error of the mean.

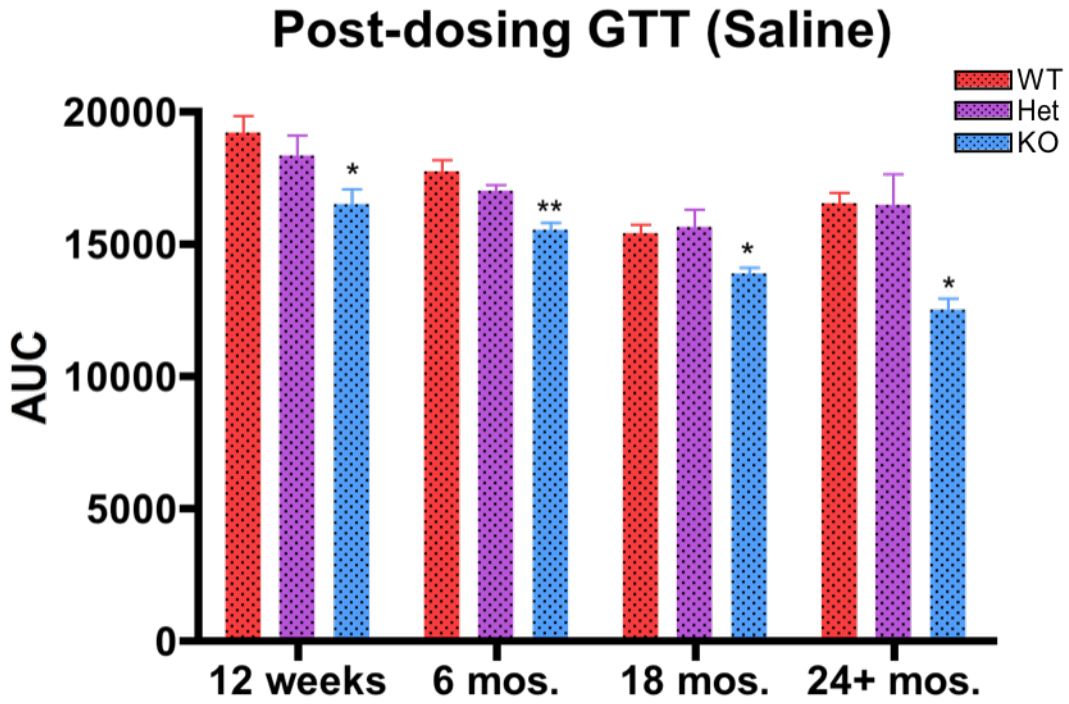

Figure 3.5. Measurements of glucose tolerance following saline dosing in *Gclm* WT, Het, and null mice at 12 weeks, 6, 18, and 24+ months (n=4-8 mice/group). Data analyzed by one-way ANOVA (Dunnett's): *, $p<0.05$; **, $p<0.001$; ***, $p<0.0001$. Errors bars represent the standard error of the mean.

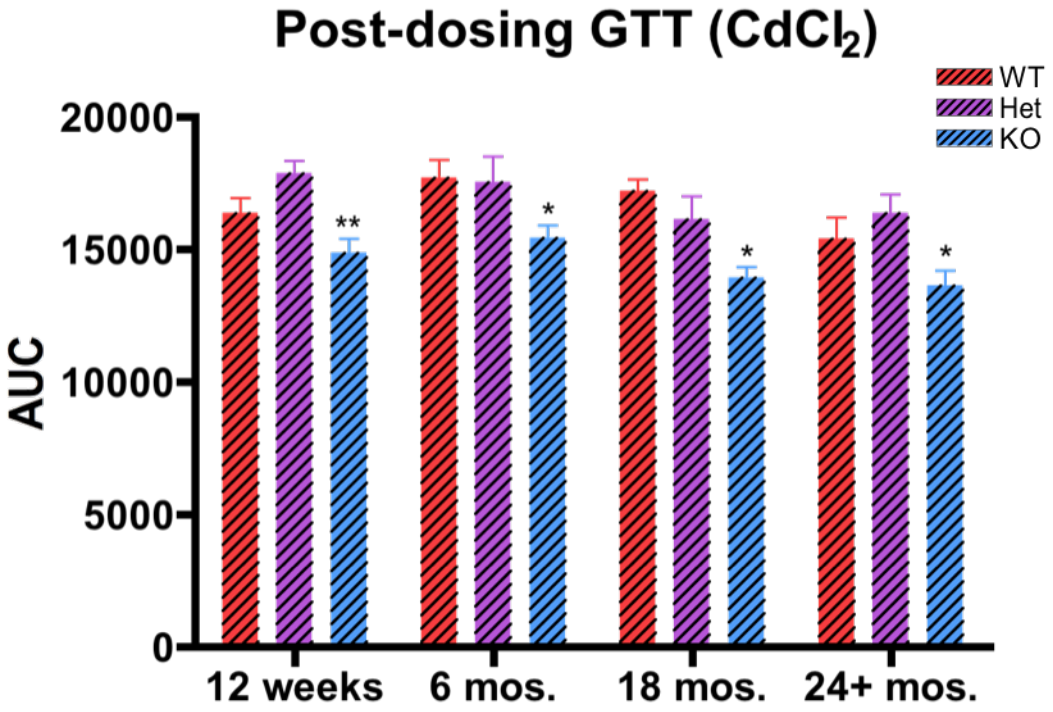

Figure 3.6. Measurements of glucose tolerance following cadmium dosing in *Gclm* WT, Het, and null mice at 12 weeks, 6, 18, and 24+ months (n=4-8 mice/group). Data analyzed by one-way ANOVA (Dunnett's): *, $p<0.05$; **, $p<0.001$; ***, $p<0.0001$. Errors bars represent the standard error of the mean.

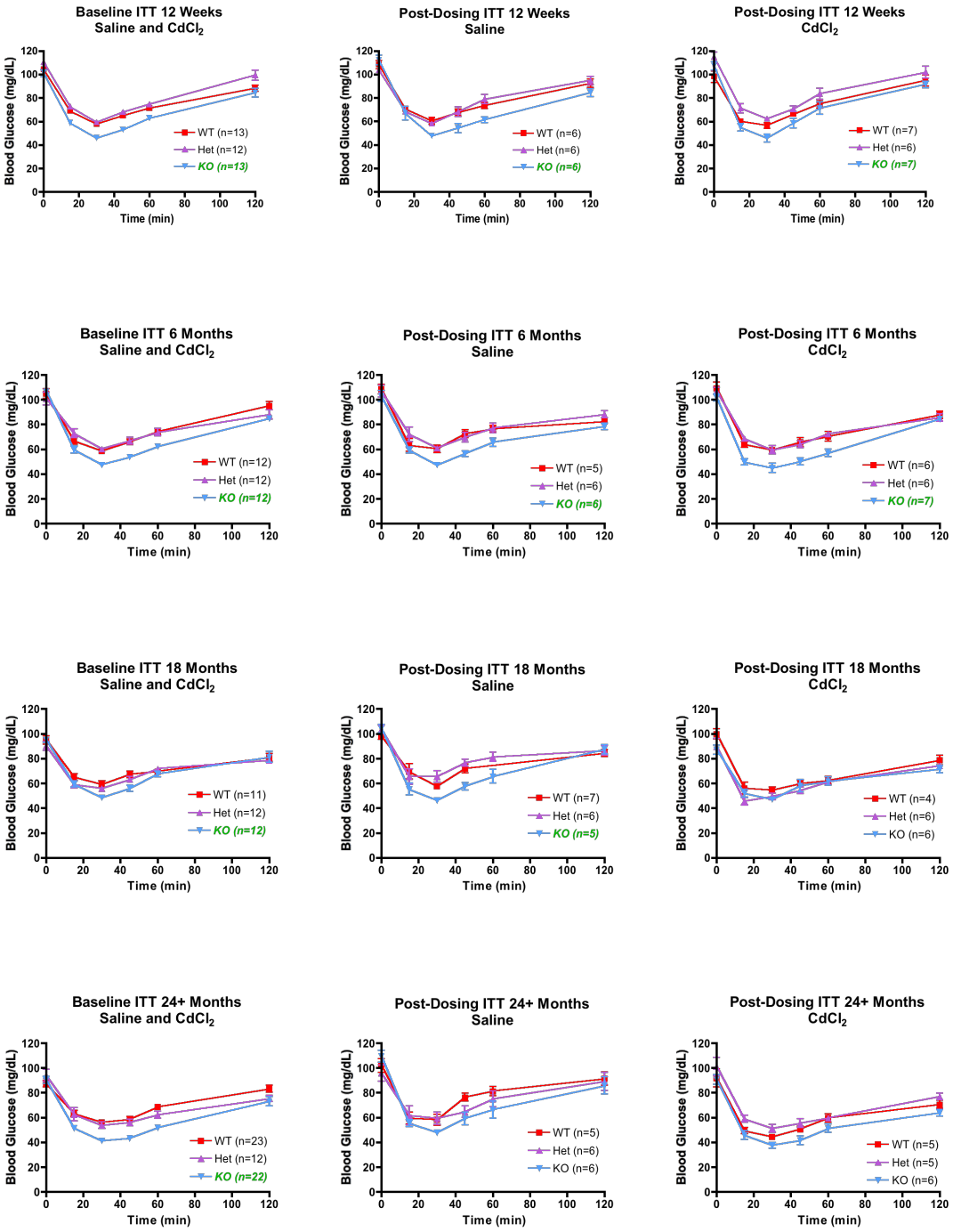

Figure 3.7. Measurements of insulin sensitivity in *Gclm* WT, Het, and null mice at 12 weeks, 6, 18, and 24+ months at baseline or following saline/cadmium treatment. Errors bars represent the standard error of the mean. Green and italicized lettering indicates AUC significantly different from WT AUC by one-way ANOVA.

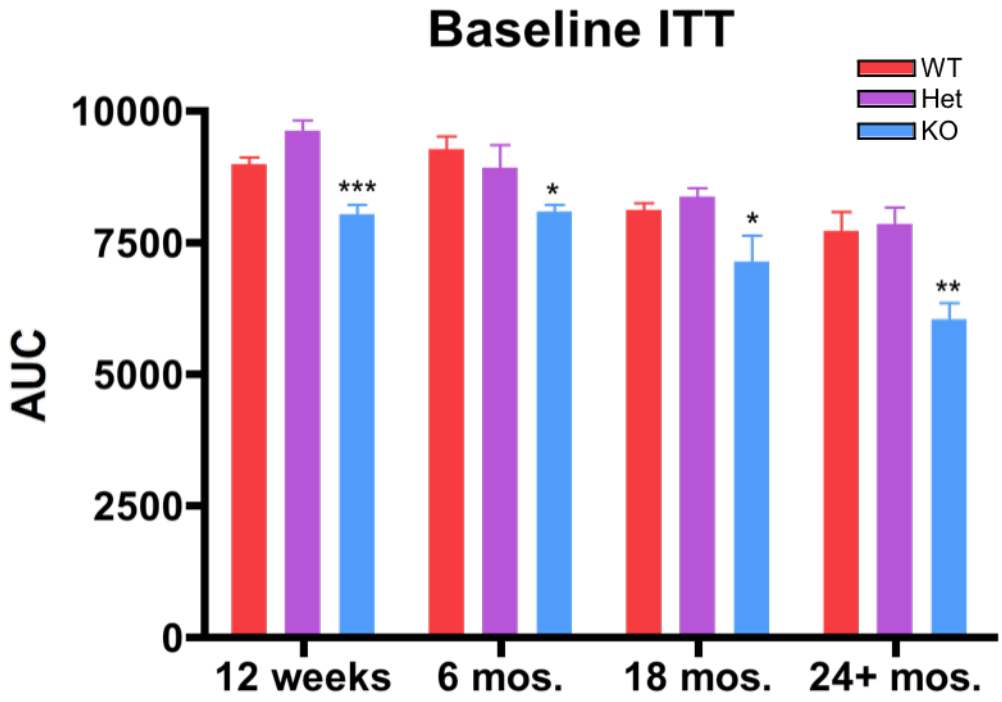

Figure 3.8. Measurements of baseline insulin sensitivity in *Gclm* WT, Het, and null mice at 12 weeks, 6, 18, and 24+ months (n=12-24 mice/group). Data analyzed by one-way ANOVA (Dunnett's): *, $p<0.05$; **, $p<0.001$; ***, $p<0.0001$. Errors bars represent the standard error of the mean.

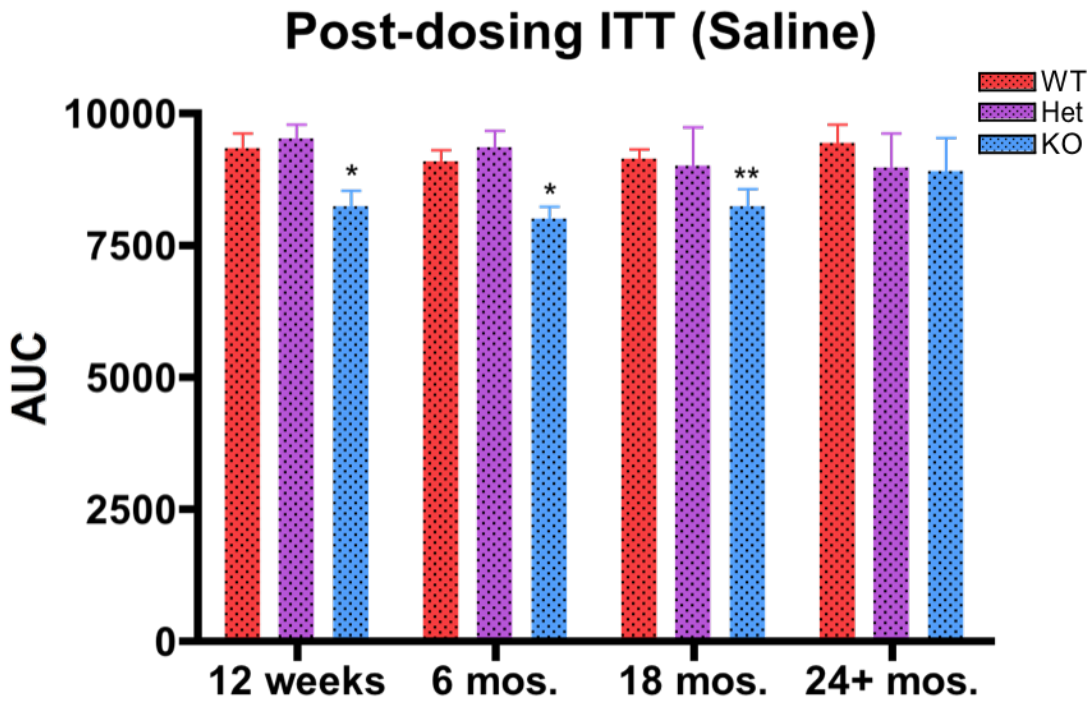

Figure 3.9. Measurements of insulin sensitivity following saline dosing in *Gclm* WT, Het, and null mice at 12 weeks, 6, 18, and 24+ months (n=4-8 mice/group). Data analyzed by one-way ANOVA (Dunnett's): *, $p<0.05$; **, $p<0.001$; ***, $p<0.0001$. Errors bars represent the standard error of the mean.

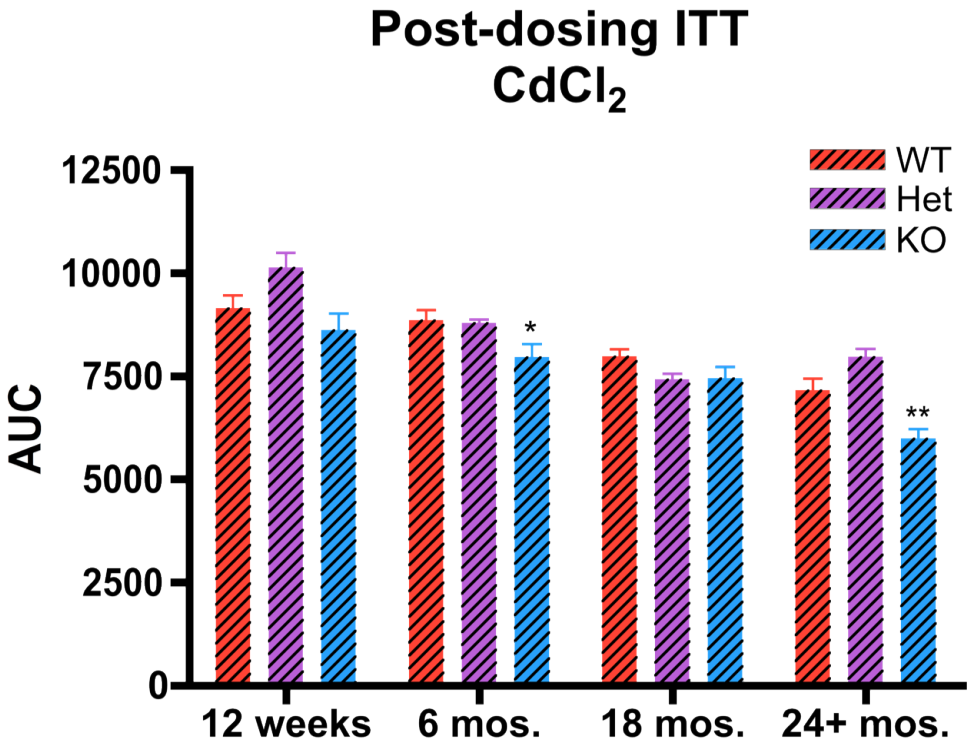

Figure 3.10. Measurements of insulin sensitivity following cadmium dosing in *Gclm* WT, Het, and null mice at 12 weeks, 6, 18, and 24+ months (n=4-8 mice/group). Data analyzed by one-way ANOVA (Dunnett's): *, $p<0.05$; **, $p<0.001$; ***, $p<0.0001$. Errors bars represent the standard error of the mean.

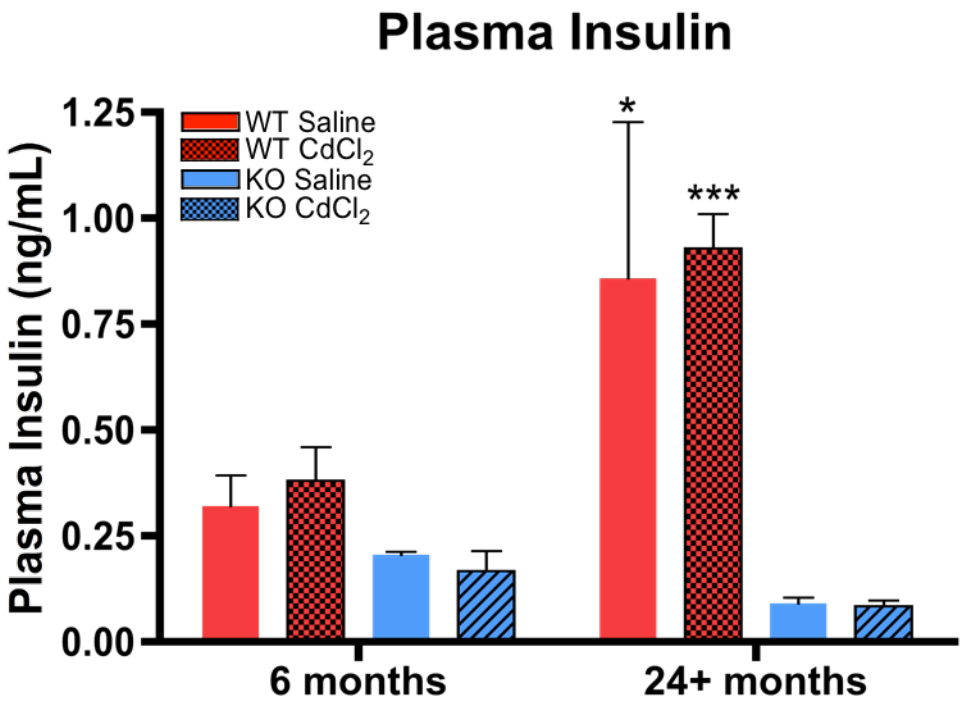

Figure 3.11. Measurements of plasma insulin levels in selected cohorts of mice (n=6 mice/group). * = Two-Way ANOVA for genotype and treatment (Bonferroni): $^{*}p<0.05$, $^{**}p<0.001$, $^{***}p<0.0001$.

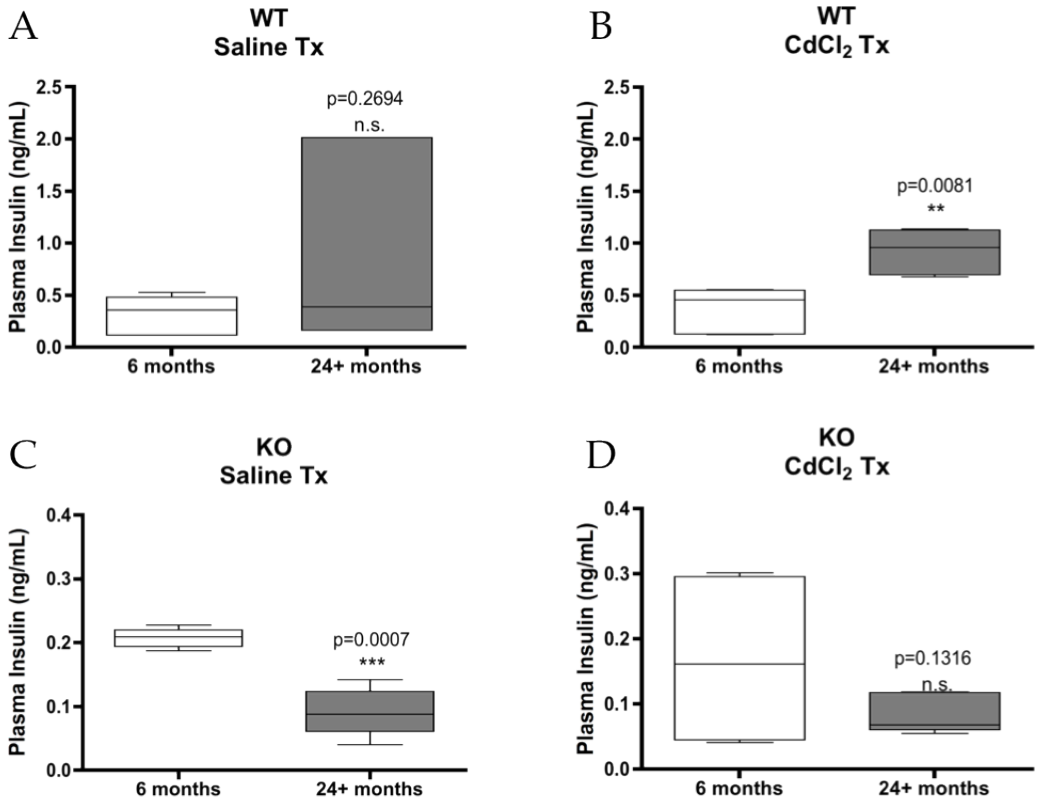

Figure 3.12. Comparisons of plasma insulin levels in selected cohorts of mice (n=6 mice/group). * = Student's t-test: $^{*}p<0.05$, $^{**}p<0.001$, $^{***}p<0.0001$.

Chapter 4

Hepatic and renal cadmium burden in *Gclm*$^{+/+}$, *Gclm*$^{+/-}$, and *Gclm*$^{-/-}$ mice.

4.1. Introduction

Glutathione is known to be an important line of defense against cadmium toxicity. *In vitro* studies consistently show that low glutathione levels leave cells susceptible to cadmium-induced oxidative damage (Gaubin et al., 2000; Ochi et al., 1988). Metallothioneins (MTs), low-molecular weight, heavy metal-binding proteins, are induced following cadmium exposure (Kennette et al., 2005). MT-I and II (the main MTs expressed in liver) null mice are sensitive to acute Cd-induced hepatotoxicity and chronic Cd-induced nephrotoxicity, highlighting the importance of these proteins in mediating cadmium toxicity (Klaassen and Liu, 1998). However, MT induction requires transcriptional activation by Nrf2/Keap1 to accumulate in protective amounts, meaning that sufficient MT expression is not achieved until hours after exposure. Thus, glutathione and metallothioneins act as complementary defense mechanisms against cadmium toxicity; GSH acts as an initial defense, and MTs acts as a second-stage defense (Klaassen and Liu, 1998; Ochi et al., 1988).

In this study, we wanted to examine the effect that chronic glutathione depletion has on hepatic and renal cadmium accumulation, and how age might modify this effect. We hypothesized that young *Gclm* WT and null mice would not display a significant difference in hepatic and renal cadmium burden at a relatively young age (6 months) following acute Cd exposure, because even though WT mice have ~10 times higher basal GSH, null mice have increased Nrf2 activity (which regulates MT expression) to make up

for decreased GSH. However, given that GSH and MTs share cooperative roles in defending against Cd-induced toxicity, we hypothesized that old *Gclm* null mice would be at a disadvantage in clearing cadmium from the liver and kidney compared to WT mice, owing to the fact that both GSH levels and Nrf2 activity have been shown to decline with age (Bruns et al., 2015; Giustarini et al., 2006; Liu et al., 2004; Maher, 2005; Rebrin and Sohal, 2008; Zhang et al., 2015; Zhang et al., 2012a).

4.2. Materials and Methods

For *Reagents, Establishment of an Aging* Gclm *Mouse Colony, Experimental Design, Treatments, Necropsies,* and *Statistical Analyses*, see Chapter 2.2.

ICP-MS analysis for hepatic and renal metal content

Inductively coupled plasma mass spectrometry (ICP-MS) was performed using a modified version of the EPA protocol 6020a Rev.1 2007 to analyze tissue for cadmium, selenium, and zinc, as previously described (Scoville et al., 2015).

4.3. Results

Following saline treatment, background hepatic cadmium and zinc levels, and Cd/Zn ratio were higher at 6 months in *Gclm* null mice compared to WT (Figures 4.1-4.3). At 24+ months of age, cadmium and Cd/Zn ratio remained higher in null mice

(Figures 4.1- 4.3). In the kidney, old *Gclm* null mice displayed much higher background cadmium levels and Cd/Zn ratio than WT mice.

Interestingly, cadmium treatment reversed the trend observed in saline-treated mice. After Cd exposure at 24+ months of age, *Gclm* null mice had *lower* cadmium and Cd/Zn burden in both liver and kidney tissues (Figures 4.1, 4.3). No statistical difference in Zn burden was seen following cadmium treatment at any age, genotype, or tissue (Figure 4.2).

4.4. Discussion

It seems curious that the trends in cadmium burden would reverse following cadmium treatment. However, an easy explanation for this is that when exposed to higher than background levels of cadmium (which likely result from the diet in this study), *Gclm* null mice are able to more effectively induce MTs (which are Nrf2 regulated) as a consequence of higher Nrf2/Keap1 activity. Indeed, we observed a statistically significant increase in *Mt1* and *Mt2* mRNA expression in 24+ month old Gclm null mice (Figure 2.16), which correlates quite well with hepatic cadmium burden (Figures 4.1, 4.3).

Because cadmium levels and Cd/Zn ratio are statistically lower in 24+ month *Gclm* null mice relative to WT mice of the same age, and *Mt1* and *Mt2* expression is increased in these animals, these data provide further evidence that Nrf2 remains responsive into old age in *Gclm* null mice. This is particularly important in the liver, as it is the primary location for MT transcription. However, other endpoints would also be

useful to fully elucidate importance of MT expression/induction in these mice, such as data on MT expression at the protein level, and investigation of differences in Cd-MT complexes between *Gclm* genotypes. It would also be interesting to examine the effect of other metals on inducing MT expression in young and aged *Gclm* mice, as well as different exposure levels, pathways, and time courses.

MTs are increased in some long-lived nematodes and mice, and have been shown to be important in age-related changes to immune plasticity and cardiac function, but the role of MTs in aging remains understudied (Mocchegiani et al., 2007; Swindell, 2011). It is also well known that metal homeostasis and transport is altered with age. However, changes in MT expression are usually observed in the context of altered Nrf2 and/or metal transcription factor-1 (MTF-1) expression and activity (Wang et al., 2004). Current data make it difficult to parse out a mechanistic role for MTs in aging, which are likely context-dependent and vary depending on tissue type. Regardless, the importance of MTs in protecting against oxidative stress, modulating intracellular metal content, and detoxifying exogenous heavy metal stressors, suggests an important function for them in aging.

4.5. Figures

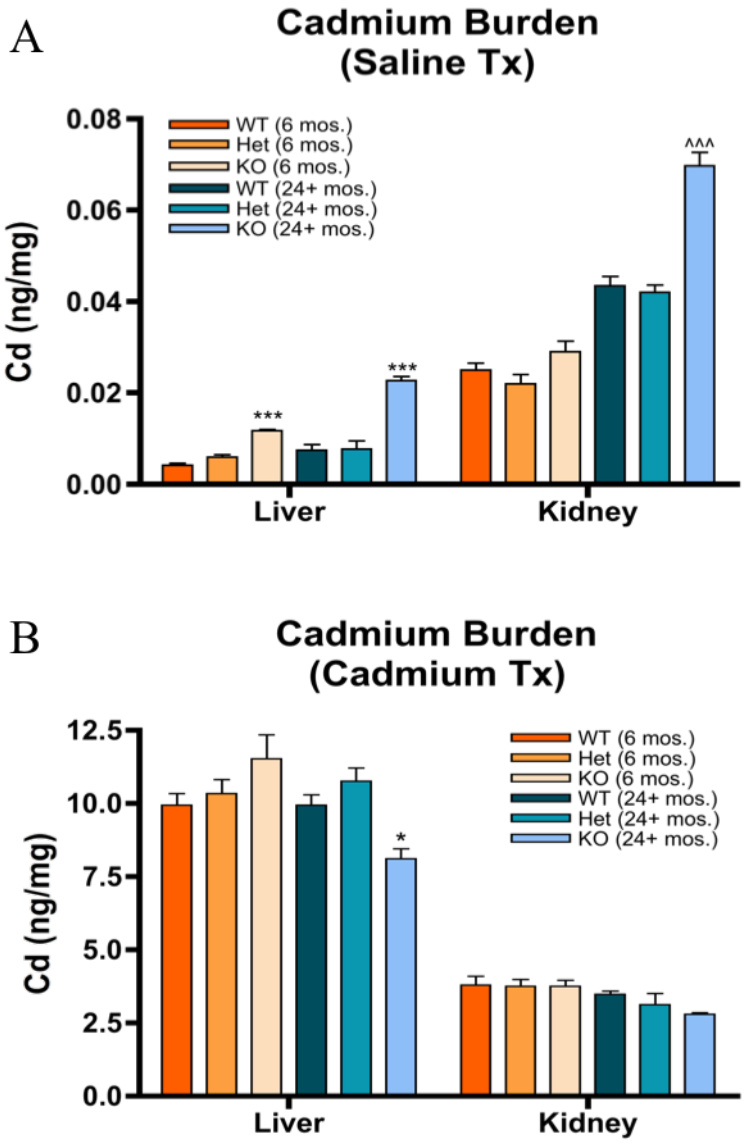

Figure 4.1. Cadmium burden in the livers and kidneys of 6 and 24+ month *Gclm*$^{+/+}$, *Gclm*$^{+/-}$, and *Gclm*$^{-/-}$ mice, following (A) saline and (B) cadmium treatment. Data analyzed by Two-Way ANOVA within tissue type; for liver, *p<0.05, **p<0.01, ***p<0.0001; for kidney, ^p<0.05, ^^p<0.01, ^^^p<0.0001.

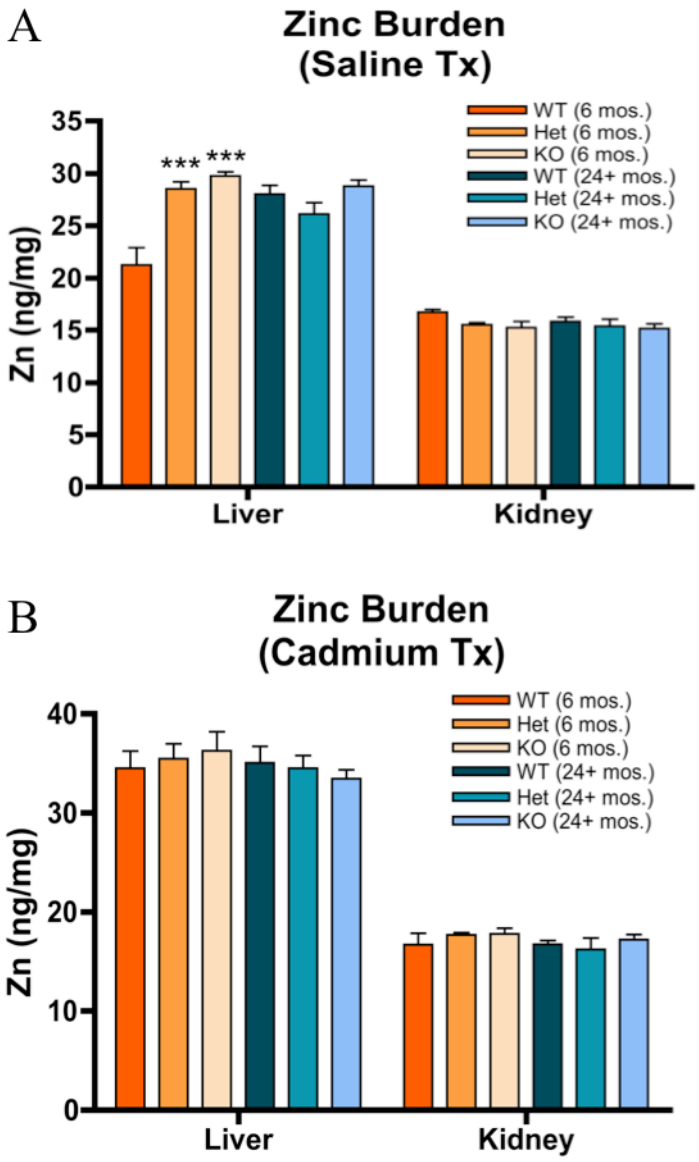

Figure 4.2. Zinc burden in the livers and kidneys of 6 and 24+ month *Gclm*$^{+/+}$, *Gclm*$^{+/-}$, and *Gclm*$^{-/-}$ mice, following (A) saline and (B) cadmium treatment. Data analyzed by Two-Way ANOVA within tissue type; for liver, *p<0.05, **p<0.01, ***p<0.0001; for kidney, ^p<0.05, ^^p<0.01, ^^^p<0.0001.

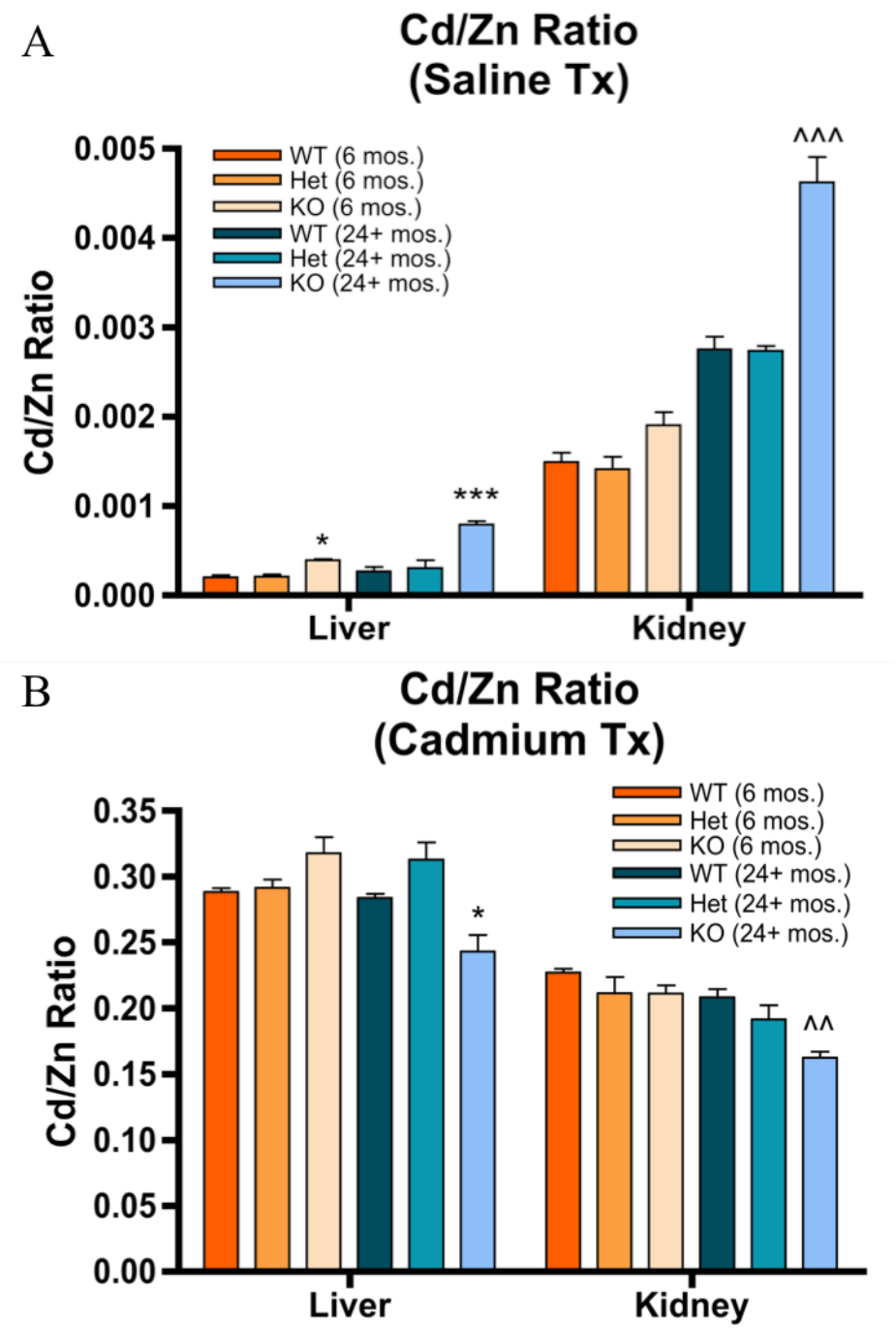

Figure 4.3. Ratio of Cd/Zn burden in the livers and kidneys of 6 and 24+ month *Gclm*$^{+/+}$, *Gclm*$^{+/-}$, and *Gclm*$^{-/-}$ mice, following (A) saline and (B) cadmium treatment. Data analyzed by Two-Way ANOVA within tissue type; for liver, *p<0.05, **p<0.01, ***p<0.0001; for kidney, ^p<0.05, ^^p<0.01, ^^^p<0.0001.

Chapter 5

Conclusions and future directions

Functional cellular antioxidant mechanisms are essential for organismal defense against the deleterious effects of endogenous (e.g., oxidative byproducts of aerobic metabolism) and exogenous (e.g., drugs, pathogens) stresses. Regulation of antioxidant capacity includes the maintenance of adequate levels of antioxidants and the localization of antioxidant compounds and enzymes (Sies, 1993). At the core of redox homeostasis are the thiol disulfide-based glutathione and thioredoxin systems. These complementary systems buffer against perturbations in redox homeostasis by acting as electron donors for reducing enzymes, scavenging oxidants directly, and signaling to other molecules. Despite the common perception that oxidants are damaging, they are not intrinsically harmful—the roles of oxidants and electrophiles are more nuanced. In fact, low-level oxidants and electrophiles are necessary for signaling and defense within the cell. Pro-oxidant enzymes, such as NADPH oxidase, complexes within the mitochondrial electron chain, and NO synthases are critical for maintaining healthy mammalian physiology, but can produce deleterious effects if overstimulated, or in the context of decreased antioxidant capacity. On the other hand, it is clear that oxidative stress contributes significantly to disease and aging. Thus, redox homeostasis can be conceptualized as a "rheostatic" mechanism, rather than an on/off switch, through which the cells maintain a proper balance of pro- and anti-oxidant molecules (Ursini et al., 2016).

Given the myriad roles glutathione plays in the cell, including detoxification of electrophiles, free radical scavenging, maintenance of the essential thiol status of proteins, providing a cysteine reservoir modulating critical cellular processes such as

DNA synthesis, and post-translational protein modification, all of which contribute to preservation of redox homeostasis, we sought to examine long-term adaptation(s) to decreased GSH in mice. One might expect that severe GSH deficiency, as is seen in *Gclm* null mice, would be highly detrimental to an organism. In some contexts, such as exposure to acetaminophen, which specifically requires GSH for detoxification, this holds true. In general, however, *Gclm* null mice are surprisingly resilient and resistant to endogenous and exogenous stress, owing to a compensatory upregulation of cytoprotective genes, particularly those in the Nrf2/Keap1 pathway (Dalton et al., 2000; Kendig et al., 2011; McConnachie et al., 2007). In addition to increased antioxidant defense, ablation of the *Gclm* gene results in improved metabolic fitness, as measured by glucose homeostasis. This favorable phenotype stems from a switch in energy production, including decreased fatty acid synthesis, leading to decreased body fat, improved glucose tolerance and insulin sensitivity, and increased basal metabolism and mitochondrial oxygen consumption.

A central figure in the *Gclm* null mouse's adaptation to chronically diminished GSH is Nrf2, a master regulator of cellular defense and metabolism. *Gclm* null mice rely on increased Nrf2 activity and expression of Nrf2-regulated genes to maintain normal cellular physiology and redox homeostasis. Impaired Nrf2 function is associated not only with sensitivity to oxidative stress, but also metabolic dysfunction, which can lead to T2DM-like changes in endogenous glucose homeostasis. As mentioned previously, *Gclm* null mice have shown resistance to these states of cellular distress.

Aging is known to compromise cellular redox status, defense mechanisms, and energy homeostasis. Given the public health impact that an ever increasing aged populace

presents, it is important to more fully understand how the aging process affects the ability of organisms to respond and adapt to stress. Here, we examined how aging affects the *Gclm* null phenotype. Importantly, we also exposed these mice to a stressor, cadmium, in order to assess the function of exogenous defense pathways with age. Because *Gclm* null mice rely so heavily on compensatory changes in cytoprotective pathways (especially Nrf2) which previous studies suggested exhibit functional decrements with age, our overarching hypothesis held that *Gclm* null mice would be sensitive to cadmium-induced toxicity.

The principal findings presented here do not support such a hypothesis. In the first aspect of this study, old (24+ months) *Gclm* null mice maintained normal glutathione redox homeostasis, under basal conditions and in response to acute cadmium treatment. In contrast, *Gclm* wild-type mice displayed detrimental age-related changes in GSH redox homeostasis. Increased basal Nrf2 target gene and protein expression observed in young *Gclm* null mice persisted into old age. Furthermore, Cbr3 and Gstm1, two important Nrf2-regulated genes, increased with cadmium treatment at 24+ months, suggesting Nrf2 inducibility is also maintained into old age in *Gclm* null mice.

In the second part of this work, we examined whether the favorable metabolic phenotype and resistance to diabetes observed in young *Gclm* null mice endured with age and in response to cadmium, a toxicant believed to hasten development of T2DM. Unexpectedly, compared to old *Gclm* wild-type mice, old *Gclm* null mice retained elevated insulin sensitivity and glucose tolerance. In addition, whereas wild-type mice showed increased plasma insulin at 24+ months relative to 6 months, under basal conditions, *Gclm* null mice actually had lower fasted insulin levels from 6 to 24+ months.

Together with the glucose and insulin tolerance tests, this suggests glucose homeostasis is perturbed with age in wild-type mice, but not *Gclm* null mice. Cadmium administration did not have much of an overall effect on these phenotypes.

Finally, we assessed the ability of *Gclm* wild-type, heterozygous, and null mice to detoxify and clear cadmium from the liver and kidney. Both young and old *Gclm* null mice showed higher background cadmium (presumably from trace amounts in their diet) retention in the liver, and higher renal retention at 24+ months, relative to wild-type and heterozygous mice. This finding was reversed following cadmium treatment at 24+ months, with *Gclm* null displaying lower hepatic and renal cadmium retention when normalized to zinc levels. As GSH and MT comprise the principal lines of defense against heavy metal toxicity, aged *Gclm* null mice express higher levels of metallothionein than wild-type mice, because they certainly are at a disadvantage in regards to GSH levels.

There are a few important caveats to consider for this work. First, a chronic dosing protocol would have been more relevant to 'real-world' human exposure. However, as noted previously, this was not feasible, given the age of some of these mice at the beginning of the study. Second, more time points for tissue collection and subsequent HPLC, RNA, and Western analysis would have been ideal. By electing to use what is essentially a 72 hr time point (and limited 8 hr data at 24+ months), we miss some of the temporal nuances in antioxidant response in these mice. The main 72 hr time point allowed us to collect functional data (see chapter 3) and maximize the data collected from each mouse within budget and manpower constraints. The results observed here may not hold in the contexts of alternative dosing regimens.

It is also necessary to point out that male *Gclm* null mice display reduced epididymal sperm abundance and motility, and lack of maternal *Gclm* decreases oocyte GSH concentrations and disrupts preimplantation development (Nakamura et al., 2011; Nakamura et al., 2012). Especially in the biology of aging field, these findings bring to mind the idea of antagonistic pleiotropy, i.e. that multiple effects of a gene have opposing effects on organismal fitness. Though we observe a favorable redox and metabolic phenotype in *Gclm* null mice that is maintained with age, there is a trade-off in reproductive fitness; this is a common finding in states of increased lifespan, and is a way to explain why some genetic changes that appear to be beneficial in one context (e.g., aging) are in fact selected against in another (e.g., reproduction).

Nonetheless, the results of this work suggest that compensatory changes to antioxidant defense and cytoprotective mechanisms are potentially less susceptible to age-related decline than previously suggested (Lewis et al., 2010; Suh et al., 2004; Zhang et al., 2012a). Moreover, in the context of life-long adaptation to altered GSH status, our findings directly challenge the notion presented by others that *inducibility* of defense pathways predictably degrades with age.

References

Al-Sawaf, O., T. Clarner, A. Fragoulis, Y. Wai Kan, T. Pufe, K. Streetz, and C. Jan Wruck, 2015, Nrf2 in health and disease: current and future clinical implications: Clinical Science, v. 129, p. 989-999.

ATSDR, 2011, Cadmium, Atlanta, GA, U.S., U.S. Department of Health and Human Services, Public Health Serivce, Agency for Toxic Substances and Disease Registry.

Bai, Y., W. Cui, Y. Xin, X. Miao, M. T. Barati, C. Zhang, Q. Chen, Y. Tan, T. Cui, Y. Zheng, and L. Cai, 2013, Prevention by sulforaphane of diabetic cardiomyopathy is associated with up-regulation of Nrf2 expression and transcription activation: J Mol Cell Cardiol, v. 57, p. 82-95.

Basinger, M. A., M. M. Jones, M. A. Holscher, and W. K. Vaughn, 1988, Antagonists for acute oral cadmium chloride intoxication: J Toxicol Environ Health, v. 23, p. 77-89.

Baum, L., X. Chen, W. S. Cheung, C. K. A. Cheung, L. W. Cheung, K. F. P. Chiu, H. M. Wen, P. Poon, K. S. Woo, H. K. Ng, and K. S. Wong, 2007, Polymorphisms and vascular cognitive impairment after ischemic stroke: Journal of Geriatric Psychiatry and Neurology, v. 20, p. 93-99.

Bekris, L. M., C. Shephard, M. Peterson, J. Hoehna, B. Van Yserloo, E. Rutledge, F. Farin, T. J. Kavanagh, and A. Lernmark, 2005, Glutathione-s-transferase M1 and T1 polymorphisms and associations with type 1 diabetes age-at-onset: Autoimmunity, v. 38, p. 567-75.

Bendavit, G., T. Aboulkassim, K. Hilmi, S. Shah, and G. Batist, 2016, Nrf2 transcription factor can directly regulate mTOR; linking cytoprotective gene expression to a major metabolic regulator that generates redox activity: Journal of Biological Chemistry, v. 291, p. 25476-25488.

Berlett, B. S., and E. R. Stadtman, 1997, Protein oxidation in aging, disease, and oxidative stress: J Biol Chem, v. 272, p. 20313-6.

Betteridge, D. J., 2000, What is oxidative stress?: Metabolism, v. 49, p. 3-8.

Beutler, E., R. Moroose, L. Kramer, T. Gelbrat, and L. Forman, 1990, Gamma-glutamylcysteine synthetase deficiency and hemolytic anemia: Blood, v. 75, p. 271-273.

Bhatti, J. S., G. K. Bhatti, and P. H. Reddy, 2017, Mitochondrial dysfunction and oxidative stress in metabolic disorders - A step towards mitochondria based therapeutic strategies: Biochim Biophys Acta, v. 1863, p. 1066-1077.

Bitar, M. S., and F. Al-Mulla, 2011, A defect in Nrf2 signaling constitutes a mechanism for cellular stress hypersensitivity in a genetic rat model of type 2 diabetes: Am J Physiol Endocrinol Metab, v. 301, p. E1119-29.

Bondareva, A. A., M. R. Capecchi, S. V. Iverson, Y. Li, N. I. Lopez, O. Lucas, G. F. Merrill, J. R. Prigge, A. M. Siders, M. Wakamiya, S. L. Wallin, and E. E. Schmidt, 2007, Effects of thioredoxin reductase-1 deletion on embryogenesis and transcriptome: Free Radic Biol Med, v. 43, p. 911-23.

Bourey, R. E., W. M. Kohrt, J. P. Kirwan, M. A. Staten, D. S. King, and J. O. Holloszy, 1993, Relationship between glucose tolerance and glucose-stimulated insulin response in 65-year-olds: J Gerontol, v. 48, p. M122-7.

Bradford, M. M., 1976, A rapid and sensitive method for the quantitation of microgram quantities of protein utilizing the principle of protein-dye binding: Anal Biochem, v. 72, p. 248-54.
Brandes, N., H. Tienson, A. Lindemann, V. Vitvitsky, D. Reichmann, R. Banerjee, and U. Jakob, 2013, Time line of redox events in aging postmitotic cells: Elife, v. 2, p. e00306.
Broughton, D. L., O. W. James, K. G. Alberti, and R. Taylor, 1991, Peripheral and hepatic insulin sensitivity in healthy elderly human subjects: Eur J Clin Invest, v. 21, p. 13-21.
Bruns, D. R., J. C. Drake, L. M. Biela, F. F. Peelor, 3rd, B. F. Miller, and K. L. Hamilton, 2015, Nrf2 Signaling and the Slowed Aging Phenotype: Evidence from Long-Lived Models: Oxid Med Cell Longev, v. 2015, p. 732596.
Calabrese, V., C. Cornelius, C. Mancuso, R. Lentile, A. M. Stella, and D. A. Butterfield, 2010, Redox homeostasis and cellular stress response in aging and neurodegeneration: Methods Mol Biol, v. 610, p. 285-308.
Cartwright, M. M., S. C. Schmuck, C. Corredor, B. Wang, D. K. Scoville, C. R. Chisholm, H.-W. Wilkerson, Z. Afsharinejad, T. K. Bammler, J. D. Posner, V. Shutthanandan, D. R. Baer, S. Mitra, W. A. Altemeier, and T. J. Kavanagh, 2016, The pulmonary inflammatory response to multiwalled carbon nanotubes is influenced by gender and glutathione synthesis: Redox Biology, v. 9, p. 264-275.
Chakraborty, G., S. Thumpayil, D. E. Lafontant, W. Woubneh, and J. H. Toney, 2009, Age dependence of glucose tolerance in adult KK-Ay mice, a model of non-insulin dependent diabetes mellitus: Lab Anim (NY), v. 38, p. 364-8.
Chang, K. C., C. C. Hsu, S. H. Liu, C. C. Su, C. C. Yen, M. J. Lee, K. L. Chen, T. J. Ho, D. Z. Hung, C. C. Wu, T. H. Lu, Y. C. Su, Y. W. Chen, and C. F. Huang, 2013, Cadmium induces apoptosis in pancreatic beta-cells through a mitochondria-dependent pathway: the role of oxidative stress-mediated c-Jun N-terminal kinase activation: PLoS One, v. 8, p. e54374.
Chartoumpekis, D. V., and T. W. Kensler, 2013, New player on an old field; the keap1/Nrf2 pathway as a target for treatment of type 2 diabetes and metabolic syndrome: Curr Diabetes Rev, v. 9, p. 137-45.
Chen, Y., M. Krishan, D. W. Nebert, and H. G. Shertzer, 2012, Glutathione-deficient mice are susceptible to TCDD-Induced hepatocellular toxicity but resistant to steatosis: Chemical Research in Toxicology, v. 25, p. 94-100.
Chen, Y. W., C. Y. Yang, C. F. Huang, D. Z. Hung, Y. M. Leung, and S. H. Liu, 2009, Heavy metals, islet function and diabetes development: Islets, v. 1, p. 169-76.
Cheresh, P., S.-J. Kim, S. Yulasiram, and D. W. Kamp, 2013, Oxidative stress and pulmonary fibrosis: Biochimica et Biophysica Acta (BBA) - Molecular Basis of Disease, v. 1832, p. 1028-1040.
Cho, H.-Y., W. Gladwell, X. Wang, B. Chorley, D. Bell, S. P. Reddy, and S. R. Kleeberger, 2010, Nrf2-regulated PPAR{gamma} expression is critical to protection against acute lung injury in mice: American Journal of Respiratory and Critical Care Medicine, v. 182, p. 170-182.
Cole, T. B., J. Coburn, K. Dao, P. Roqué, Y.-C. Chang, V. Kalia, T. R. Guilarte, J. Dziedzic, and L. G. Costa, 2016, Sex and genetic differences in the effects of

acute diesel exhaust exposure on inflammation and oxidative stress in mouse brain: Toxicology, v. 374, p. 1-9.
Coughlan, M. T., D. R. Thorburn, S. A. Penfold, A. Laskowski, B. E. Harcourt, K. C. Sourris, A. L. Tan, K. Fukami, V. Thallas-Bonke, P. P. Nawroth, M. Brownlee, A. Bierhaus, M. E. Cooper, and J. M. Forbes, 2009, RAGE-induced cytosolic ROS promote mitochondrial superoxide generation in diabetes: J Am Soc Nephrol, v. 20, p. 742-52.
Coyle, J. T., and P. Puttfarcken, 1993, Oxidative stress, glutamate, and neurodegenerative disorders: Science, v. 262, p. 689-95.
Custodio, H. M., R. Harari, L. Gerhardsson, S. Skerfving, and K. Broberg, 2005, Genetic influences on the retention of inorganic mercury: Archives of Environmental & Occupational Health, v. 60, p. 17-23.
Cuypers, A., M. Plusquin, T. Remans, M. Jozefczak, E. Keunen, H. Gielen, K. Opdenakker, A. R. Nair, E. Munters, T. J. Artois, T. Nawrot, J. Vangronsveld, and K. Smeets, 2010, Cadmium stress: an oxidative challenge: Biometals, v. 23, p. 927-40.
D'Autréaux, B., and M. B. Toledano, 2007, ROS as signalling molecules: mechanisms that generate specificity in ROS homeostasis: Nature Reviews Molecular Cell Biology, v. 8, p. 813-824.
Dai, D. F., Y. A. Chiao, G. M. Martin, D. J. Marcinek, N. Basisty, E. K. Quarles, and P. S. Rabinovitch, 2017, Mitochondrial-Targeted Catalase: Extended Longevity and the Roles in Various Disease Models: Prog Mol Biol Transl Sci, v. 146, p. 203-241.
Dalton, T. P., Y. Chen, S. N. Schneider, D. W. Nebert, and H. G. Shertzer, 2004, Genetically altered mice to evaluate glutathione homeostasis in health and disease: Free Radic Biol Med, v. 37, p. 1511-26.
Dalton, T. P., M. Z. Dieter, Y. Yang, H. G. Shertzer, and D. W. Nebert, 2000, Knockout of the mouse glutamate cysteine ligase catalytic subunit (Gclc) gene: embryonic lethal when homozygous, and proposed model for moderate glutathione deficiency when heterozygous: Biochemical and Biophysical Research Communications, v. 279, p. 324-329.
de Haan, J. B., 2011, Nrf2 activators as attractive therapeutics for diabetic nephropathy: Diabetes, v. 60, p. 2683-4.
de Nadal, E., G. Ammerer, and F. Posas, 2011, Controlling gene expression in response to stress: Nat Rev Genet, v. 12, p. 833-45.
de Zeeuw, D., T. Akizawa, P. Audhya, G. L. Bakris, M. Chin, H. Christ-Schmidt, A. Goldsberry, M. Houser, M. Krauth, H. J. Lambers Heerspink, J. J. McMurray, C. J. Meyer, H. H. Parving, G. Remuzzi, R. D. Toto, N. D. Vaziri, C. Wanner, J. Wittes, D. Wrolstad, and G. M. Chertow, 2013, Bardoxolone methyl in type 2 diabetes and stage 4 chronic kidney disease: N Engl J Med, v. 369, p. 2492-503.
Delalande, O., H. Desvaux, E. Godat, A. Valleix, C. Junot, J. Labarre, and Y. Boulard, 2010, Cadmium-glutathione solution structures provide new insights into heavy metal detoxification: Febs j, v. 277, p. 5086-96.
Dhakshinamoorthy, S., A. K. Jain, D. A. Bloom, and A. K. Jaiswal, 2005, Bach1 competes with Nrf2 leading to negative regulation of the antioxidant response element (ARE)-mediated NAD(P)H:quinone oxidoreductase 1 gene expression

and induction in response to antioxidants: Journal of Biological Chemistry, v. 280, p. 16891-16900.
Dhalla, N. S., R. M. Temsah, and T. Netticadan, 2000, Role of oxidative stress in cardiovascular diseases: J Hypertens, v. 18, p. 655-73.
Dieter, B. P., 2015, Dysregulation of Nrf2 signaling in diabetes: an opportunity for a multitarget approach: Journal of Diabetes and Metabolism, v. 6.
Dinkova-Kostova, A. T., K. T. Liby, K. K. Stephenson, W. D. Holtzclaw, X. Gao, N. Suh, C. Williams, R. Risingsong, T. Honda, G. W. Gribble, M. B. Sporn, and P. Talalay, 2005, Extremely potent triterpenoid inducers of the phase 2 response: correlations of protection against oxidant and inflammatory stress: Proc Natl Acad Sci U S A, v. 102, p. 4584-9.
Du, Y., H. Zhang, J. Lu, and A. Holmgren, 2012, Glutathione and glutaredoxin act as a backup of human thioredoxin reductase 1 to reduce thioredoxin 1 preventing cell death by aurothioglucose: Journal of Biological Chemistry, v. 287, p. 38210-38219.
Edwards, J., and C. Ackerman, 2016, A Review of Diabetes Mellitus and Exposure to the Environmental Toxicant Cadmium with an Emphasis on Likely Mechanisms of Action: Curr Diabetes Rev, v. 12, p. 252-8.
Edwards, J. R., and W. C. Prozialeck, 2009, Cadmium, diabetes and chronic kidney disease: Toxicol Appl Pharmacol, v. 238, p. 289-93.
El Muayed, M., M. R. Raja, X. Zhang, K. W. MacRenaris, S. Bhatt, X. Chen, M. Urbanek, T. V. O'Halloran, and W. L. Lowe, Jr., 2012, Accumulation of cadmium in insulin-producing beta cells: Islets, v. 4, p. 405-16.
Ellrichmann, G., E. Petrasch-Parwez, D.-H. Lee, C. Reick, L. Arning, C. Saft, R. Gold, and R. A. Linker, 2011, Efficacy of fumaric acid esters in the R6/2 and YAC128 models of Huntington's disease: PLoS One, v. 6.
Feleciano, D. R., and J. Kirstein, 2016, Collapse of redox homeostasis during aging and stress: Mol Cell Oncol, v. 3, p. e1091060.
Fontana, L., and L. Partridge, 2015, Promoting health and longevity through diet: from model organisms to humans: Cell, v. 161, p. 106-18.
Franklin, C. C., D. S. Backos, I. Mohar, C. C. White, H. J. Forman, and T. J. Kavanagh, 2009, Structure, function, and post-translational regulation of the catalytic and modifier subunits of glutamate cysteine ligase: Molecular Aspects of Medicine, v. 30, p. 86-98.
Friedman, E. A., 1999, Advanced glycosylated end products and hyperglycemia in the pathogenesis of diabetic complications: Diabetes Care, v. 22 Suppl 2, p. B65-71.
Fuhr, B. J., and D. L. Rabenstein, 1973, Nuclear magnetic resonance studies of the solution chemistry of metal complexes. IX. The binding of cadmium, zinc, lead, and mercury by glutathione: J Am Chem Soc, v. 95, p. 6944-50.
Gaubin, Y., F. Vaissade, F. Croute, B. Beau, J. Soleilhavoup, and J. Murat, 2000, Implication of free radicals and glutathione in the mechanism of cadmium-induced expression of stress proteins in the A549 human lung cell-line: Biochim Biophys Acta, v. 1495, p. 4-13.
Gavazzo, P., E. Morelli, and C. Marchetti, 2005, Susceptibility of insulinoma cells to cadmium and modulation by L-type calcium channels: Biometals, v. 18, p. 131-42.

Giustarini, D., I. Dalle-Donne, S. Lorenzini, A. Milzani, and R. Rossi, 2006, Age-related influence on thiol, disulfide, and protein-mixed disulfide levels in human plasma: J Gerontol A Biol Sci Med Sci, v. 61, p. 1030-8.

Guimaraes, E. L., C. Empsen, A. Geerts, and L. A. van Grunsven, 2010, Advanced glycation end products induce production of reactive oxygen species via the activation of NADPH oxidase in murine hepatic stellate cells: J Hepatol, v. 52, p. 389-97.

Hamilton, R. T., M. E. Walsh, and H. Van Remmen, 2014, Mouse models of oxidative stress indicate a role for modulating healthy aging: Journal of Clinical and Experimental Pathology, v. S4, p. 005.

Han, J. C., S. Y. Park, B. G. Hah, G. H. Choi, Y. K. Kim, T. H. Kwon, E. K. Kim, M. Lachaal, C. Y. Jung, and W. Lee, 2003, Cadmium induces impaired glucose tolerance in rat by down-regulating GLUT4 expression in adipocytes: Arch Biochem Biophys, v. 413, p. 213-20.

Haque, J. A., R. S. McMahan, J. S. Campbell, M. Shimizu-Albergine, A. M. Wilson, D. Botta, T. K. Bammler, R. P. Beyer, T. J. Montine, M. M. Yeh, T. J. Kavanagh, and N. Fausto, 2010, Attenuated progression of diet-induced steatohepatitis in glutathione-deficient mice: Laboratory Investigation, v. 90, p. 1704-1717.

Harder, B., T. Jiang, T. Wu, S. Tao, M. Rojo de la Vega, W. Tian, E. Chapman, and D. D. Zhang, 2015, Molecular mechanisms of Nrf2 regulation and how these influence chemical modulation for disease intervention: Biochemical Society Transactions, v. 43, p. 680-686.

Harman, D., 1957, Aging: a theory based on free radical and radiation chemistry: Journal of Gerontology, v. 2, p. 298-300.

Hassoun, E. A., and S. J. Stohs, 1996, Cadmium-induced production of superoxide anion and nitric oxide, DNA single strand breaks and lactate dehydrogenase leakage in J774A.1 cell cultures: Toxicology, v. 112, p. 219-26.

Hayflick, L., 1998, How and why we age: Exp Gerontol, v. 33, p. 639-53.

He, H. J., G. Y. Wang, Y. Gao, W. H. Ling, Z. W. Yu, and T. R. Jin, 2012, Curcumin attenuates Nrf2 signaling defect, oxidative stress in muscle and glucose intolerance in high fat diet-fed mice: World J Diabetes, v. 3, p. 94-104.

He, X., and Q. Ma, 2009, NRF2 cysteine residues are critical for oxidant/electrophile-sensing, Kelch-like ECH-associated protein-1-dependent ubiquitination-proteasomal degradation, and transcription activation: Molecular Pharmacology, v. 76, p. 1265-1278.

Imai, S. I., 2016, The NAD World 2.0: the importance of the inter-tissue communication mediated by NAMPT/NAD+/SIRT1 in mammalian aging and longevity control: NPJ Syst Biol Appl, v. 2, p. 16018.

Itoh, K., N. Wakabayashi, Y. Katoh, T. Ishii, T. O'Connor, and M. Yamamoto, 2003, Keap1 regulates both cytoplasmic-nuclear shuttling and degradation of Nrf2 in response to electrophiles: Genes to Cells, v. 8, p. 379-391.

Iverson, S. V., S. Eriksson, J. Xu, J. R. Prigge, E. A. Talago, T. A. Meade, E. S. Meade, M. R. Capecchi, E. S. Arner, and E. E. Schmidt, 2013, A Txnrd1-dependent metabolic switch alters hepatic lipogenesis, glycogen storage, and detoxification: Free Radic Biol Med, v. 63, p. 369-80.

Jadeja, R. N., R. V. Devkar, and S. Nammi, 2017, Oxidative Stress in Liver Diseases: Pathogenesis, Prevention, and Therapeutics: Oxid Med Cell Longev, v. 2017, p. 8341286.
Jarup, L., and A. Akesson, 2009, Current status of cadmium as an environmental health problem: Toxicol Appl Pharmacol, v. 238, p. 201-8.
Jiang, T., B. Harder, M. Rojo de la Vega, P. K. Wong, E. Chapman, and D. D. Zhang, 2015, p62 links autophagy and Nrf2 signaling: Free Radical Biology and Medicine, v. 88, p. 199-204.
Jin, K., 2010, Modern Biological Theories of Aging: Aging Dis, v. 1, p. 72-74.
Johansson, E., S. C. Wesselkamper, H. G. Shertzer, G. D. Leikauf, T. P. Dalton, and Y. Chen, 2010, Glutathione deficient C57BL/6J mice are not sensitized to ozone-induced lung injury: Biochemical and Biophysical Research Communications, v. 396, p. 407-412.
Jones, D. P., 2015, Redox theory of aging: Redox Biology, v. 5, p. 71-79.
Joo, M. S., W. D. Kim, K. Y. Lee, J. H. Kim, J. H. Koo, and S. G. Kim, 2016, AMPK facilitates nuclear accumulation of Nrf2 by phosphorylating at serine 550: Molecular and Cellular Biology, v. 36, p. 1931-1942.
Kaspar, J. W., and A. K. Jaiswal, 2011, Tyrosine phosphorylation controls nuclear export of Fyn, allowing Nrf2 activation of cytoprotective gene expression: Faseb j, v. 25, p. 1076-87.
Kawai, Y., L. Garduno, M. Theodore, J. Yang, and I. J. Arinze, 2011, Acetylation-deacetylation of the transcription factor Nrf2 (nuclear factor erythroid 2-related factor 2) regulates its transcriptional activity and nucleocytoplasmic localization: J Biol Chem, v. 286, p. 7629-40.
Kendig, E. L., Y. Chen, M. Krishan, E. Johansson, S. N. Schneider, M. B. Genter, D. W. Nebert, and H. G. Shertzer, 2011, Lipid metabolism and body composition in Gclm(-/-) mice: Toxicol Appl Pharmacol, v. 257, p. 338-48.
Kennette, W., O. M. Collins, R. K. Zalups, and J. Koropatnick, 2005, Basal and zinc-induced metallothionein in resistance to cadmium, cisplatin, zinc, and tertbutyl hydroperoxide: studies using MT knockout and antisense-downregulated MT in mammalian cells: Toxicol Sci, v. 88, p. 602-13.
Kensler, T. W., N. Wakabayashi, and S. Biswal, 2007, Cell survival responses to environmental stresses via the Keap1-Nrf2-ARE pathway: Annual Review of Pharmacology and Toxicology, v. 47, p. 89-116.
Klaassen, C. D., L. J. Casarett, and J. Doull, 2008, Casarett and Doull's toxicology : the basic science of poisons: New York, New York, U.S., McGraw-Hill Medical.
Klaassen, C. D., and J. Liu, 1998, Metallothionein transgenic and knock-out mouse models in the study of cadmium toxicity: J Toxicol Sci, v. 23 Suppl 2, p. 97-102.
Klaassen, C. D., J. Liu, and B. A. Diwan, 2009, Metallothionein protection of cadmium toxicity: Toxicol Appl Pharmacol, v. 238, p. 215-20.
Kubben, N., W. Zhang, L. Wang, T. C. Voss, J. Yang, J. Qu, G. H. Liu, and T. Misteli, 2016, Repression of the Antioxidant NRF2 Pathway in Premature Aging: Cell, v. 165, p. 1361-1374.
Kulkarni, S. R., L. E. Armstrong, and A. L. Slitt, 2013, Caloric restriction-mediated induction of lipid metabolism gene expression in liver is enhanced by Keap1-knockdown: Pharm Res, v. 30, p. 2221-31.

Kurata, Y., O. Katsuta, T. Doi, T. Kawasuso, H. Hiratsuka, M. Tsuchitani, and T. Umemura, 2003, Chronic cadmium treatment induces islet B cell injury in ovariectomized cynomolgus monkeys: Jpn J Vet Res, v. 50, p. 175-83.

Lau, A., X. J. Wang, F. Zhao, N. F. Villeneuve, T. Wu, T. Jiang, Z. Sun, E. White, and D. D. Zhang, 2010, A noncanonical mechanism of Nrf2 activation by autophagy deficiency: direct interaction between Keap1 and p62: Mol Cell Biol, v. 30, p. 3275-85.

Lavoie, S., P. Steullet, A. Kulak, F. Preitner, K. Q. Do, and P. J. Magistretti, 2016, Glutamate cysteine ligase-modulatory subunit knockout mouse shows normal insulin sensitivity but reduced liver glycogen storage: Frontiers in Physiology, v. 7, p. 142.

Lee, B. K., and Y. Kim, 2013, Blood cadmium, mercury, and lead and metabolic syndrome in South Korea: 2005-2010 Korean National Health and Nutrition Examination Survey: Am J Ind Med, v. 56, p. 682-92.

Lei, L. J., L. Chen, T. Y. Jin, M. Nordberg, and X. L. Chang, 2007, Estimation of benchmark dose for pancreatic damage in cadmium-exposed smelters: Toxicol Sci, v. 97, p. 189-95.

Leiter, E. H., F. Premdas, D. E. Harrison, and L. G. Lipson, 1988, Aging and glucose homeostasis in C57BL/6J male mice: Faseb j, v. 2, p. 2807-11.

Levy, S., and H. J. Forman, 2011, C-Myc is a Nrf2-interacting protein that negatively regulates phase II genes through their electrophile responsive elements: International Union of Biochemistry and Molecular Biology Life, v. 62, p. 237-246.

Lewis, K. N., J. Mele, J. D. Hayes, and R. Buffenstein, 2010, Nrf2, a guardian of healthspan and gatekeeper of species longevity: Integr Comp Biol, v. 50, p. 829-43.

Lewis, K. N., E. Wason, Y. H. Edrey, D. M. Kristan, E. Nevo, and R. Buffenstein, 2015, Regulation of Nrf2 signaling and longevity in naturally long-lived rodents: Proc Natl Acad Sci U S A, v. 112, p. 3722-7.

Li, H., L. Zhang, F. Wang, Y. Shi, Y. Ren, Q. Liu, Y. Cao, and H. Duan, 2011, Attenuation of glomerular injury in diabetic mice with tert-butylhydroquinone through nuclear factor erythroid 2-related factor 2-dependent antioxidant gene activation: Am J Nephrol, v. 33, p. 289-97.

Li, J., M. S. Bonkowski, S. Moniot, D. Zhang, B. P. Hubbard, A. J. Ling, L. A. Rajman, B. Qin, Z. Lou, V. Gorbunova, L. Aravind, C. Steegborn, and D. A. Sinclair, 2017a, A conserved NAD+ binding pocket that regulates protein-protein interactions during aging: Science, v. 355, p. 1312-1317.

Li, Y., Y. Zhang, W. Wang, and Y. Wu, 2017b, Association of urinary cadmium with risk of diabetes: a meta-analysis: Environ Sci Pollut Res Int, v. 24, p. 10083-10090.

Liu, H., H. Wang, S. Shenvi, T. M. Hagen, and R. M. Liu, 2004, Glutathione metabolism during aging and in Alzheimer disease: Ann N Y Acad Sci, v. 1019, p. 346-9.

Liu, J., W. Qu, and M. B. Kadiiska, 2009, Role of oxidative stress in cadmium toxicity and carcinogenesis: Toxicol Appl Pharmacol, v. 238, p. 209-14.

Lu, J., and A. Holmgren, 2014, The thioredoxin antioxidant system: Free Radical Biology and Medicine, v. 66, p. 75-87.

López-Otín, C., M. A. Blasco, L. Partridge, M. Serrano, and G. Kroemer, 2013, The hallmarks of aging: Cell, v. 153, p. 1194–1217.
Ma, Q., 2013, Role of Nrf2 in Oxidative Stress and Toxicity: Annual Review of Pharmacology and Toxicology, v. 53, p. 401-426.
Maher, P., 2005, The effects of stress and aging on glutathione metabolism: Ageing Res Rev, v. 4, p. 288-314.
Malhotra, D., E. Portales-Casamar, A. Singh, S. Srivastava, D. Arenillas, C. Happel, C. Shyr, N. Wakabayashi, T. W. Kensler, W. W. Wasserman, and S. Biswal, 2010, Global mapping of binding sites for Nrf2 identifies novel targets in cell survival response through ChIP-Seq profiling and network analysis: Nucleic Acids Research, v. 38, p. 5718-5734.
McConnachie, L. A., D. Botta, C. C. White, C. S. Weldy, H.-W. Wilkerson, J. Yu, R. Dills, X. Yu, W. C. Griffith, E. M. Faustman, F. M. Farin, S. E. Gill, W. C. Parks, X. Hu, X. Gao, D. L. Eaton, and T. J. Kavanagh, 2013, The glutathione synthesis gene Gclm modulates amphiphilic polymer-coated CdSe/ZnS quantum dot-induced lung inflammation in mice: PLoS One, v. 8.
McConnachie, L. A., I. Mohar, F. N. Hudson, C. B. Ware, W. C. Ladiges, C. Fernandez, S. Chatteron-Kirchmeier, C. C. White, R. H. Pierce, and T. J. Kavanagh, 2007, Glutamate cysteine ligase modifier subunit deficiency and gender as determinants of acetaminophen-induced hepatotoxicity in mice: Toxicological Sciences, v. 99, p. 628-636.
McKone, E. F., J. Shao, D. D. Frangolias, C. L. Keener, C. A. Shephard, F. M. Farin, M. R. Tonelli, P. D. Pare, A. J. Sandford, M. L. Aitken, and T. J. Kavanagh, 2006, Variants in the glutamate-cysteine-ligase gene are associated with cystic fibrosis lung disease: Am J Respir Crit Care Med, v. 174, p. 415-9.
Meister, A., and M. E. Anderson, 1983, Glutathione: Annual Review of Biochemistry, v. 52, p. 711-760.
Menke, A., E. Guallar, and C. C. Cowie, 2016, Metals in Urine and Diabetes in U.S. Adults: Diabetes, v. 65, p. 164-71.
Merali, Z., and R. L. Singhal, 1975, Protective effect of selenium on certain hepatotoxic and pancreotoxic manifestations of subacute cadmium administration: J Pharmacol Exp Ther, v. 195, p. 58-66.
Merali, Z., and R. L. Singhal, 1980, Diabetogenic effects of chronic oral cadmium adminstration to neonatal rats: Br J Pharmacol, v. 69, p. 151-7.
Mitsui, A., J. Hamuro, H. Nakamura, N. Kondo, Y. Hirabayashi, S. Ishizaki-Koizumi, T. Hirakawa, T. Inoue, and J. Yodoi, 2002, Overexpression of human thioredoxin in transgenic mice controls oxidative stress and life span: Antioxid Redox Signal, v. 4, p. 693-6.
Mocchegiani, E., R. Giacconi, E. Muti, C. Cipriano, L. Costarelli, S. Tesei, N. Gasparini, and M. Malavolta, 2007, Zinc-bound metallothioneins and immune plasticity: lessons from very old mice and humans: Immun Ageing, v. 4, p. 7.
Nakamura, B. N., T. J. Fielder, Y. D. Hoang, J. Lim, L. A. McConnachie, T. J. Kavanagh, and U. Luderer, 2011, Lack of maternal glutamate cysteine ligase modifier subunit (Gclm) decreases oocyte glutathione concentrations and disrupts preimplantation development in mice: Endocrinology, v. 152, p. 2806-15.

Nakamura, B. N., I. Mohar, G. W. Lawson, M. M. Cortes, Y. D. Hoang, L. Ortiz, R. Patel, B. A. Rau, L. A. McConnachie, T. J. Kavanagh, and U. Luderer, 2012, Increased sensitivity to testicular toxicity of transplacental benzo[a]pyrene exposure in male glutamate cysteine ligase modifier subunit knockout (Gclm-/-) mice: Toxicol Sci, v. 126, p. 227-41.

Nie, X., N. Wang, Y. Chen, C. Chen, B. Han, C. Zhu, F. Xia, Z. Cang, M. Lu, Y. Meng, B. Jiang, D. J. M, and Y. Lu, 2016, Blood cadmium in Chinese adults and its relationships with diabetes and obesity: Environ Sci Pollut Res Int, v. 23, p. 18714-23.

Nilsson, T., F. Rorsman, P. O. Berggren, and B. Hellman, 1986, Accumulation of cadmium in pancreatic beta cells is similar to that of calcium in being stimulated by both glucose and high potassium: Biochim Biophys Acta, v. 888, p. 270-7.

Nobrega-Pereira, S., P. J. Fernandez-Marcos, T. Brioche, M. C. Gomez-Cabrera, A. Salvador-Pascual, J. M. Flores, J. Vina, and M. Serrano, 2016, G6PD protects from oxidative damage and improves healthspan in mice: Nat Commun, v. 7, p. 10894.

NRC, 2011, Guide for the Care and Use of Laboratory Animals. National Academies Press, Washington, D.C.

O'Connell, M. A., and J. D. Hayes, 2015, The Keap1/Nrf2 pathway in health and disease: from the bench to the clinic: Biochem Soc Trans, v. 43, p. 687-9.

Ochi, T., F. Otsuka, K. Takahashi, and M. Ohsawa, 1988, Glutathione and metallothioneins as cellular defense against cadmium toxicity in cultured Chinese hamster cells: Chem Biol Interact, v. 65, p. 1-14.

Oh, S. H., and S. C. Lim, 2006, A rapid and transient ROS generation by cadmium triggers apoptosis via caspase-dependent pathway in HepG2 cells and this is inhibited through N-acetylcysteine-mediated catalase upregulation: Toxicol Appl Pharmacol, v. 212, p. 212-23.

Oh, Y. S., E. H. Seo, Y. S. Lee, S. C. Cho, H. S. Jung, S. C. Park, and H. S. Jun, 2016, Increase of Calcium Sensing Receptor Expression Is Related to Compensatory Insulin Secretion during Aging in Mice: PLoS One, v. 11, p. e0159689.

Pacini, G., A. Valerio, F. Beccaro, R. Nosadini, C. Cobelli, and G. Crepaldi, 1988, Insulin sensitivity and beta-cell responsivity are not decreased in elderly subjects with normal OGTT: J Am Geriatr Soc, v. 36, p. 317-23.

Park, S. S., D. A. Skaar, R. L. Jirtle, and C. Hoyo, 2017, Epigenetics, obesity and early-life cadmium or lead exposure: Epigenomics, v. 9, p. 57-75.

Patlolla, J. M., and C. V. Rao, 2012, Triterpenoids for cancer prevention and treatment: current status and future prospects: Curr Pharm Biotechnol, v. 13, p. 147-55.

Perez, V. I., A. Bokov, H. Van Remmen, J. Mele, Q. Ran, Y. Ikeno, and A. Richardson, 2009, Is the oxidative stress theory of aging dead?: Biochim Biophys Acta, v. 1790, p. 1005-14.

Petersen, M. C., D. F. Vatner, and G. I. Shulman, 2017, Regulation of hepatic glucose metabolism in health and disease: Nat Rev Endocrinol.

Pizzino, G., A. Bitto, M. Interdonato, F. Galfo, N. Irrera, A. Mecchio, G. Pallio, V. Ramistella, F. De Luca, L. Minutoli, F. Squadrito, and D. Altavilla, 2014, Oxidative stress and DNA repair and detoxification gene expression in

adolescents exposed to heavy metals living in the Milazzo-Valle del Mela area (Sicily, Italy): Redox Biol, v. 2, p. 686-93.
Polonikov, A. V., V. P. Ivanov, M. A. Solodilova, I. V. Khoroshaya, M. A. Kozhuhov, and V. I. Panfilov, 2007, The relationship between polymorphisms in the glutamate cysteine ligase gene and asthma susceptibility: Respiratory Medicine, v. 101, p. 2422–2424.
Rahman, M. M., G. P. Sykiotis, M. Nishimura, R. Bodmer, and D. Bohmann, 2013, Declining signal dependence of Nrf2-MafS-regulated gene expression correlates with aging phenotypes: Aging Cell, v. 12, p. 554-62.
Rajanna, B., M. Hobson, J. Reese, E. Sample, and K. D. Chapatwala, 1984, Chronic hepatic and renal toxicity by cadmium in rats: Drug Chem Toxicol, v. 7, p. 229-41.
Ramprasath, T., and G. S. Selvam, 2013, Potential impact of genetic variants in Nrf2 regulated antioxidant genes and risk prediction of diabetes and associated cardiac complications: Curr Med Chem, v. 20, p. 4680-93.
Ray, P. D., B.-W. Huang, and Y. Tsuji, 2012, Reactive oxygen species (ROS) homeostasis and redox regulation in cellular signaling: Cellular Signaling, v. 24, p. 981-990.
Rebrin, I., and R. S. Sohal, 2008, Pro-oxidant shift in glutathione redox state during aging: Adv Drug Deliv Rev, v. 60, p. 1545-52.
Ristoff, E., and A. Larsson, 2007, Inborn errors in the metabolism of glutathione: Orphanet Journal of Rare Diseases, v. 2.
Roberts, C. K., and K. K. Sindhu, 2009, Oxidative stress and metabolic syndrome: Life Sci, v. 84, p. 705-12.
Ruetenik, A., and A. Barrientos, 2015, Dietary restriction, mitochondrial function and aging: from yeast to humans: Biochim Biophys Acta, v. 1847, p. 1434-47.
Salmon, A. B., A. Richardson, and V. I. Perez, 2010, Update on the oxidative stress theory of aging: does oxidative stress play a role in aging or healthy aging?: Free Radic Biol Med, v. 48, p. 642-55.
Sanz, A., and R. K. Stefanatos, 2008, The mitochondrial free radical theory of aging: a critical view: Curr Aging Sci, v. 1, p. 10-21.
Sato, H., R. C. Siow, S. Bartlett, S. Taketani, T. Ishii, S. Bannai, and G. E. Mann, 1997, Expression of stress proteins heme oxygenase-1 and -2 in acute pancreatitis and pancreatic islet betaTC3 and acinar AR42J cells: FEBS Lett, v. 405, p. 219-23.
Schaupp, C. M., C. C. White, G. F. Merrill, and T. J. Kavanagh, 2015, Metabolism of doxorubicin to the cardiotoxic metabolite doxorubicinol is increased in a mouse model of chronic glutathione deficiency: A potential role for carbonyl reductase 3: Chem Biol Interact, v. 234, p. 154-61.
Schriner, S. E., N. J. Linford, G. M. Martin, P. Treuting, C. E. Ogburn, M. Emond, P. E. Coskun, W. Ladiges, N. Wolf, H. Van Remmen, D. C. Wallace, and P. S. Rabinovitch, 2005, Extension of murine life span by overexpression of catalase targeted to mitochondria: Science, v. 308, p. 1909-11.
Schulze, P. C., J. Yoshioka, T. Takahashi, Z. He, G. L. King, and R. T. Lee, 2004, Hyperglycemia promotes oxidative stress through inhibition of thioredoxin function by thioredoxin-interacting protein: J Biol Chem, v. 279, p. 30369-74.

Schwartz, G. G., D. Il'yasova, and A. Ivanova, 2003, Urinary cadmium, impaired fasting glucose, and diabetes in the NHANES III: Diabetes Care, v. 26, p. 468-70.
Scoville, D. K., C. C. White, D. Botta, L. A. McConnachie, M. E. Zadworny, S. C. Schmuck, X. Hu, X. Gao, J. Yu, R. L. Dills, L. Sheppard, M. A. Delaney, W. C. Griffith, R. P. Beyer, R. C. Zangar, J. G. Pounds, E. M. Faustman, and T. J. Kavanagh, 2015, Susceptibility to quantum dot induced lung inflammation differs widely among the Collaborative Cross founder mouse strains: Toxicol Appl Pharmacol, v. 289, p. 240-50.
Shih, P. H., and G. C. Yen, 2007, Differential expressions of antioxidant status in aging rats: the role of transcriptional factor Nrf2 and MAPK signaling pathway: Biogerontology, v. 8, p. 71-80.
Siegel, M. P., S. E. Kruse, J. M. Percival, J. Goh, C. C. White, H. C. Hopkins, T. J. Kavanagh, H. H. Szeto, P. S. Rabinovitch, and D. J. Marcinek, 2013, Mitochondrial-targeted peptide rapidly improves mitochondrial energetics and skeletal muscle performance in aged mice: Aging Cell, v. 12, p. 763-71.
Sies, H., 1993, Strategies of antioxidant defense: Eur J Biochem, v. 215, p. 213-9.
Siewert, S., I. González, L. Santillán, R. Lucero, M. S. Ojeda, and M. S. Gimenez, 2013, Downregulation of Nrf2 and HO-1 expression contributes to oxidative stress in type 2 diabetes mellitus: A study in Juana Koslay City, San Luis, Argentina Journal of Diabetes Mellitus, v. 3, p. 71-78.
Singhal, R. K., M. E. Anderson, and A. Meister, 1987, Glutathione, a first line of defense against cadmium toxicity: Faseb j, v. 1, p. 220-3.
Slocum, S. L., J. J. Skoko, N. Wakabayashi, S. Aja, M. Yamamoto, T. W. Kensler, and D. V. Chartoumpekis, 2016, Keap1/Nrf2 pathway activation leads to a repressed hepatic gluconeogenic and lipogenic program in mice on a high-fat diet: Arch Biochem Biophys, v. 591, p. 57-65.
Sohal, R. S., and R. Weindruch, 1996, Oxidative stress, caloric restriction, and aging: Science, v. 273, p. 59-63.
Stillman, M. J., W. Cai, and A. J. Zelazowski, 1987, Cadmium binding to metallothioneins. Domain specificity in reactions of alpha and beta fragments, apometallothionein, and zinc metallothionein with Cd2+: J Biol Chem, v. 262, p. 4538-48.
Suh, J. H., S. V. Shenvi, B. M. Dixon, H. Liu, A. K. Jaiswal, R. M. Liu, and T. M. Hagen, 2004, Decline in transcriptional activity of Nrf2 causes age-related loss of glutathione synthesis, which is reversible with lipoic acid: Proc Natl Acad Sci U S A, v. 101, p. 3381-6.
Sun, J., M. Brand, Y. Zenke, S. Tashiro, M. Groudine, and K. Igarashi, 2004, Heme regulates the dynamic exchange of Bach1 and NF-E2-related factors in the Maf transcription factor network: Proceedings of the National Academy of Sciences, v. 101, p. 1461–1466.
Sun, Z., Z. Huang, and D. D. Zhang, 2009, Phosphorylation of Nrf2 at multiple sites by MAP kinases has a limited contribution in modulating the Nrf2-dependent antioxidant response: PLoS One, v. 4.
Suvorova, E. S., O. Lucas, C. M. Weisend, M. F. Rollins, G. F. Merrill, M. R. Capecchi, and E. E. Schmidt, 2009, Cytoprotective Nrf2 pathway is induced in chronically txnrd 1-deficient hepatocytes: PLoS One, v. 4, p. e6158.

Swindell, W. R., 2011, Metallothionein and the biology of aging: Ageing Res Rev, v. 10, p. 132-45.
Sykiotis, G. P., I. G. Habeos, A. V. Samuelson, and D. Bohmann, 2011, The role of the antioxidant and longevity-promoting Nrf2 pathway in metabolic regulation: Curr Opin Clin Nutr Metab Care, v. 14, p. 41-8.
Tan, A. L., J. M. Forbes, and M. E. Cooper, 2007, AGE, RAGE, and ROS in diabetic nephropathy: Semin Nephrol, v. 27, p. 130-43.
Tan, S.-X., D. Greetham, S. Raeth, C. M. Grant, I. W. Dawes, and G. G. Perrone, 2010, The thioredoxin-thioredoxin reductase system can function in vivo as an alternative system to reduce oxidized glutathione in Saccharomyces cerevisiae: Journal of Biological Chemistry, v. 285, p. 6118-6126.
Tan, S. M., and J. B. de Haan, 2014, Combating oxidative stress in diabetic complications with Nrf2 activators: how much is too much?: Redox Rep, v. 19, p. 107-17.
Tan, Y., T. Ichikawa, J. Li, Q. Si, H. Yang, X. Chen, C. S. Goldblatt, C. J. Meyer, X. Li, L. Cai, and T. Cui, 2011, Diabetic downregulation of Nrf2 activity via ERK contributes to oxidative stress-induced insulin resistance in cardiac cells in vitro and in vivo: Diabetes, v. 60, p. 625-33.
Tinkov, A. A., T. Filippini, O. P. Ajsuvakova, J. Aaseth, Y. G. Gluhcheva, J. M. Ivanova, G. Bjorklund, M. G. Skalnaya, E. R. Gatiatulina, E. V. Popova, O. N. Nemereshina, M. Vinceti, and A. V. Skalny, 2017, The role of cadmium in obesity and diabetes: Sci Total Environ, v. 601-602, p. 741-755.
Toroser, D., and R. S. Sohal, 2007, Age-associated perturbations in glutathione synthesis in mouse liver: Biochem J, v. 405, p. 583-9.
Tosic, M., J. Ott, S. Barral, P. Bovet, P. Deppen, F. Gheorghita, M.-L. Matthey, J. Parnas, M. Preisig, M. Saraga, A. Solida, S. Timm, A. G. Wang, T. Werge, M. Cuénod, and K. Q. Do, 2006, Schizophrenia and Oxidative Stress: Glutamate Cysteine Ligase Modifier as a Susceptibility Gene: American Journal of Human Genetics, v. 79, p. 586-592.
Trevino, S., M. P. Waalkes, J. A. Flores Hernandez, B. A. Leon-Chavez, P. Aguilar-Alonso, and E. Brambila, 2015, Chronic cadmium exposure in rats produces pancreatic impairment and insulin resistance in multiple peripheral tissues: Arch Biochem Biophys, v. 583, p. 27-35.
Ursini, F., M. Maiorino, and H. J. Forman, 2016, Redox homeostasis: The Golden Mean of healthy living: Redox Biol, v. 8, p. 205-15.
Uruno, A., Y. Furusawa, Y. Yagishita, T. Fukutomi, H. Muramatsu, T. Negishi, A. Sugawara, T. W. Kensler, and M. Yamamoto, 2013, The Keap1-Nrf2 system prevents onset of diabetes mellitus: Mol Cell Biol, v. 33, p. 2996-3010.
Uttara, B., A. V. Singh, P. Zamboni, and R. T. Mahajan, 2009, Oxidative stress and neurodegenerative diseases: a review of upstream and downstream antioxidant therapeutic options: Curr Neuropharmacol, v. 7, p. 65-74.
Veal, E., and A. Day, 2011, Hydrogen peroxide as a signaling molecule: Antioxidants & Redox Signaling, v. 15, p. 147-151.
Waalkes, M. P., 2003, Cadmium carcinogenesis: Mutat Res, v. 533, p. 107-20.
Waalkes, M. P., and P. L. Goering, 1990, Metallothionein and other cadmium-binding proteins: recent developments: Chem Res Toxicol, v. 3, p. 281-8.

Wakabayashi, N., D. Chartoumpekis, and T. W. Kensler, 2016, Crosstalk between Nrf2 and Notch signaling: Free Radical Biology and Medicine, v. 88, p. 158-167.
Wallia, A., N. B. Allen, S. Badon, and M. El Muayed, 2014, Association between urinary cadmium levels and prediabetes in the NHANES 2005-2010 population: Int J Hyg Environ Health, v. 217, p. 854-60.
Wang, Y., U. Wimmer, P. Lichtlen, D. Inderbitzin, B. Stieger, P. J. Meier, L. Hunziker, T. Stallmach, R. Forrer, T. Rulicke, O. Georgiev, and W. Schaffner, 2004, Metal-responsive transcription factor-1 (MTF-1) is essential for embryonic liver development and heavy metal detoxification in the adult liver: Faseb j, v. 18, p. 1071-9.
Wang, Y. Y., Y. X. Yang, H. Zhe, Z. X. He, and S. F. Zhou, 2014, Bardoxolone methyl (CDDO-Me) as a therapeutic agent: an update on its pharmacokinetic and pharmacodynamic properties: Drug Des Devel Ther, v. 8, p. 2075-88.
Wardyn, J. D., A. H. Ponsford, and C. M. Sanderson, 2015, Dissecting molecular cross-talk between Nrf2 and NF-κB response pathways: Biochemical Society Transactions, v. 43, p. 621-626.
Warner, H. R., R. L. Sprott, E. L. Schneider, and R. N. Butler, 1987, Modern biological theories of aging, v. 31: New York, New York, U.S., Raven Press.
Weinert, B. T., and P. S. Timiras, 2003, Invited review: theories of aging: Journal of Applied Physiology, v. 95, p. 1706-1716.
Weldy, C. S., I. P. Luttrell, C. C. White, V. Morgan-Stevenson, T. K. Bammler, R. P. Beyer, Z. Afsharinejad, F. Kim, K. Chitaley, and T. J. Kavanagh, 2012, Glutathione (GSH) and the GSH synthesis gene Gclm modulate vascular reactivity in mice: Free Radic Biol Med, v. 53, p. 1264-78.
Weldy, C. S., C. C. White, H.-W. Wilkerson, T. V. Larson, J. A. Stewart, S. E. Gill, W. C. Parks, and T. J. Kavanagh, 2011, Heterozygosity in the glutathione synthesis gene Gclm increases sensitivity to diesel exhaust particulate induced lung inflammation in mice: Inhalation Toxicology, v. 23, p. 724-735.
Winterbourn, C. C., and A. J. Kettle, 2013, Redox Reactions and Microbial Killing in the Neutrophil Phagosome: Antioxidants & Redox Signaling, v. 18, p. 642-660.
Wu, K. C., J. J. Liu, and C. D. Klaassen, 2012, Nrf2 activation prevents cadmium-induced acute liver injury: Toxicol Appl Pharmacol, v. 263, p. 14-20.
Xu, J., A. C. Donepudi, J. E. Moscovitz, and A. L. Slitt, 2013, Keap1-knockdown decreases fasting-induced fatty liver via altered lipid metabolism and decreased fatty acid mobilization from adipose tissue: PLoS One, v. 8, p. e79841.
Xu, J., S. R. Kulkarni, A. C. Donepudi, V. R. More, and A. L. Slitt, 2012, Enhanced Nrf2 activity worsens insulin resistance, impairs lipid accumulation in adipose tissue, and increases hepatic steatosis in leptin-deficient mice: Diabetes, v. 61, p. 3208-18.
Yan, S. F., R. Ramasamy, and A. M. Schmidt, 2008, Mechanisms of disease: advanced glycation end-products and their receptor in inflammation and diabetes complications: Nat Clin Pract Endocrinol Metab, v. 4, p. 285-93.
Yang, Y., M. Z. Dieter, Y. Chen, H. G. Shertzer, D. W. Nebert, and T. P. Dalton, 2002, Initial characterization of the glutamate-cysteine ligase modifier subunit Gclm(-/-) knockout mouse. Novel model system for a severely compromised oxidative stress response: Journal of Biological Chemistry, v. 277, p. 49446-49452.

Yao, D., and M. Brownlee, 2010, Hyperglycemia-induced reactive oxygen species increase expression of the receptor for advanced glycation end products (RAGE) and RAGE ligands: Diabetes, v. 59, p. 249-55.

Yates, M. S., M. Tauchi, F. Katsuoka, K. C. Flanders, K. T. Liby, T. Honda, G. W. Gribble, D. A. Johnson, J. A. Johnson, N. C. Burton, T. R. Guilarte, M. Yamamoto, M. B. Sporn, and T. W. Kensler, 2007, Pharmacodynamic characterization of chemopreventive triterpenoids as exceptionally potent inducers of Nrf2-regulated genes: Mol Cancer Ther, v. 6, p. 154-62.

Yore, M. M., A. N. Kettenbach, M. B. Sporn, S. A. Gerber, and K. T. Liby, 2011, Proteomic analysis shows synthetic oleanane triterpenoid binds to mTOR: PLoS One, v. 6, p. e22862.

Yu, T., J. L. Robotham, and Y. Yoon, 2006, Increased production of reactive oxygen species in hyperglycemic conditions requires dynamic change of mitochondrial morphology: Proc Natl Acad Sci U S A, v. 103, p. 2653-8.

Zhang, D. D., and M. Hannink, 2003, Distinct cysteine residues in Keap1 are required for Keap1-dependent ubiquitination of Nrf2 and for stabilization of Nrf2 by chemopreventive agents and oxidative stress: Molecular and Cellular Biology, v. 23, p. 8137-8151.

Zhang, H., K. J. Davies, and H. J. Forman, 2015, Oxidative stress response and Nrf2 signaling in aging: Free Radic Biol Med, v. 88, p. 314-36.

Zhang, H., H. Liu, K. J. A. Davies, C. Sioutas, C. E. Finch, T. E. Morgan, and H. J. Forman, 2012a, Nrf2-regulated phase II enzymes are induced by chronic ambient nanoparticle exposure in young mice with age-related impairments: Free Radical Biology and Medicine, v. 52, p. 2038-2046.

Zhang, Y. K., K. C. Wu, J. Liu, and C. D. Klaassen, 2012b, Nrf2 deficiency improves glucose tolerance in mice fed a high-fat diet: Toxicol Appl Pharmacol, v. 264, p. 305-14.

Zhao, Z., J. S. Hyun, H. Satsu, S. Kakuta, and M. Shimizu, 2006, Oral exposure to cadmium chloride triggers an acute inflammatory response in the intestines of mice, initiated by the over-expression of tissue macrophage inflammatory protein-2 mRNA: Toxicol Lett, v. 164, p. 144-54.

Appendix A: Abbreviations and acronyms

ANOVA – Analysis of Variance
AGE – Advanced glycation end product
AMPK – 5' adenosine monophosphate-activated protein kinase
ARE – Anti-oxidant Response Element
ATP – Adenosine triphosphate
BEACON – Bardoxolone Methyl Evaluation in Patients With Chronic Kidney Disease and Type 2 Diabetes: the Occurrence of Renal Events
BSO – L-Buthionine-[S,R]-Sulfoximine
CBP – CREB-binding protein
CBR3 – Carbonyl reductase 3
CDDO-Me – 1[2-Cyano-3,12-dioxooleana-1,9(11)-dien-28-oyl]imidazole-methyl; bardoxolone methyl
Cd – Cadmium
$CdCl_2$ – Cadmium chloride
CdSe – Cadmium selenide
CO_2 – Carbon dioxide
Cys – Cysteine
DNA – Deoxyribonucleic acid
ELISA – Enzyme-linked immunosorbent assay
EPA – Environmental Protection Agency
EpRE – Electrophilic response element
γ-GC – γ-glutamylcysteine
G6PD – Glucose-6-Phosphate Dehydrogenase
GCL – Glutamate Cysteine Ligase
GCLC – Glutamate Cysteine Ligase Catalytic Subunit
GCLM – Glutamate Cysteine Ligase Modifier Subunits
Glu – Glutamate
GPx – Glutathione peroxidase
GR – Glutathione reductase
Grx – Glutaredoxin
GS – Glutathione synthetase
GSH – Glutathione
GSK3β – Glycogen synthase kinase 3 beta
GSSG – Glutathione Disulfide
Gsr – Glutathione reductase (gene)
GST – Glutathione *S*-transferase
GTT – Glucose tolerance test
Het – Heterozygous
HPLC – High pressure liquid chromatography
i.p. – Intraperitoneal
ITT – Insulin tolerance/sensitivity test
Keap1 – Kelch-like erythroid cell-derived protein with CNC homology [ECH]-associated protein 1
K_i – Inhibitory constant

KO – Knockout
MAPK – Mitogen-activated protein kinase
MCAT – Mitochondrially-targeted catalase
MCD – Methionine and choline-deficient
mRNA – Messenger ribonucleic acid
MTF1 – Zinc-regulated metal transcription factor 1
mTOR – Mechanistic target of rapamycin
NAD^+ – Nicotinamide adenine dinucleotide, oxidized
NADH – Nicotinamide adenine dinucleotide, reduced
$NADP^+$ – Nicotinamide adenine dinucleotide phosphate, oxidized
NADPH – Nicotinamide adenine dinucleotide phosphate, reduced
NASH – Nonalcoholic steatohepatitis
NF-kB – Nuclear factor kappa-light-chain-enhancer of activated B cells
Nrf2 – Nuclear factor (erythroid-derived 2)-like 2
OCT – Optimal cutting temperature
PBS – Phosphate Buffered Saline
PGC1α – Peroxisome proliferator-activated receptor gamma coactivator 1-alpha
PPAR – Peroxisome proliferator-activated receptors
Prx – Peroxiredoxin
RNA – Ribonucleic acid
RNR – Ribonucleotide reductase
RNS – Reactive Nitrogen Species
ROS – Reactive oxygen species
RT-PCR – Reverse transcriptase Real Time Polymerase Chain Reaction
SEM – Standard Error of the Mean
sMAF – Small musculoaponeurotic fibrosarcoma protein
SNP – Single Nucleotide Polymorphism
SOD – Superoxide dismutase
SPF – Specific pathogen free
TCDD – 2,3,7,8-tetrachlorodibenzodioxin
T2DM – Type II diabetes mellitus
Trx – Thioredoxin
TrxR – Thioredoxin reductase
WT – Wild-type
XRE – Xenobiotic response element
Zn – Zinc
ZnS – Zinc sulfide

Appendix B: Cbr3 and Doxorubicin

Metabolism of Doxorubicin to the Cardiotoxic Metabolite Doxorubicinol Is Increased in a Mouse Model of Chronic Glutathione Deficiency: A Potential Role for Carbonyl Reductase 3

Christopher M. Schaupp*, Collin C. White*, Gary F. Merrill[†], and Terrance J. Kavanagh*

*Department of Environmental and Occupational Health Sciences, University of Washington, Seattle, WA 98105

[†]Department of Biochemistry and Biophysics, Oregon State University, Corvallis, OR 97331

Published in *Chem Biol Interact.* 2015 Jun 5; 234: 154–161.

Abstract

Doxorubicin is highly effective at inducing DNA double-strand breaks in rapidly dividing cells, which has led to it being a widely used cancer chemotherapeutic. However, clinical administration of doxorubicin is limited by off-target cardiotoxicity, which is thought to be mediated by doxorubicinol, the primary alcohol metabolite of doxorubicin. Carbonyl reductase 1 (CBR1), a well-characterized monomeric enzyme present at high basal levels in the liver, is known to exhibit activity toward doxorubicin. Little is known about a closely related enzyme, carbonyl reductase 3 (CBR3), which is present in the liver at low basal levels but is highly inducible by the transcription factor Nrf2. Genetic polymorphisms in *CBR3,* but not *CBR1*, are associated with differential cardiac outcomes in doxorubicin treated pediatric patients. *Cbr3* mRNA and CBR3 protein are highly expressed in the livers of *Gclm* −/− mice (a mouse model of glutathione deficiency) relative to wild type mice. In the present study, we first investigated the ability of CBR3 to metabolize doxorubicin. Incubations of doxorubicin and purified recombinant murine CBR3 (mCBR3) were analyzed for doxorubicinol

formation using HPLC, revealing for the first time that doxorubicin is a substrate of mCBR3. Moreover, hepatocytes from *Gclm* −/− mice produced more doxorubicinol than *Gclm* +/+ hepatocytes. In addition, differentiated rat myoblasts (C2C12 cells) co-cultured with primary *Gclm* −/− murine hepatocytes were more sensitive to doxorubicin-induced cytostasis/cytotoxicity than incubations with *Gclm* +/+ hepatocytes. Our results indicate a potentially important role for CBR3 in doxorubicin-induced cardiotoxicity. Because there is likely to be variability in hepatic CBR3 activity in humans (due to either genetic or epigenetic influences on its expression), these data also suggest that inhibition of CBR3 may provide protection from doxorubicinol cardiotoxicity.

1.1. Introduction

The anthracycline doxorubicin (also known as Adriamycin) is indicated for a broad range of malignant neoplasms, including blood cancers, carcinomas, and sarcomas. Its central role in hematological cancer regimens also makes it one of the most widely prescribed chemotherapeutics in children [1,2]. Despite the general effectiveness of doxorubicin in destroying cancer cells, its use is dose-limited by off-target complications, namely cardiomyopathies [1,3]. A dose-dependent increase in cardiomyopathy risk is observed in patients; approximately 50-60% of patients given high doses of doxorubicin develop cardiomyopathies [1,4]. The risk of developing cardiomyopathy resulting from administration represents a major impediment to the continued use of doxorubicin in chemotherapy regimens. Elimination of doxorubicin-associated cardiotoxicity would thus represent a major advance in the clinical setting, especially in the context of chronic doxorubicin administration.

Doxorubicinol, an alcohol metabolite of doxorubicin, has been implicated in the cardiotoxicity observed in doxorubicin-treated patients, largely due to doxorubicinol targeting Na^+/K^+ channels present in cardiac sarcolemma [5,6]. The NADPH-dependent two-electron reduction of doxorubicin to doxorubicinol is shown in Figure 1. Carbonyl reductase 1 (CBR1) has been shown to catalyze the reduction of doxorubicin to doxorubicinol [7]. However, another carbonyl reductase, CBR3, has been less well characterized [8]. Interestingly, in childhood cancer patients treated with doxorubicin, a relatively common polymorphism in the *CBR3* gene (present in ~30% of Caucasians) encodes for a non-synonymous amino acid change (V244M), which is associated with decreased risk of developing cardiomyopathy, while a polymorphism in the gene encoding *CBR1* (1096 G>A) is not associated with differential cardiomyopathy risk [3]. Furthermore, another *CBR3* variant (11 G>A) has been shown to influence the relative expression of CBR3—and subsequent doxorubicinol formation—in a cohort of Southeast Asian breast cancer patients [9]. Though the importance of specific CBR3 variants remains controversial, currently available data taken as a whole suggest an important role for this protein in doxorubicin-induced cardiotoxicity [3,9,10,11]; factors such as tissue-specific expression, polymorphisms present in other genes, patient age, duration of treatment, dosage, and co-therapies, among others, likely influence the relative role of CBR3.

While CBR1 and CBR3 share high amino acid identity (~78%) and are both NADPH-dependent, the endogenous substrate(s) and function(s) of these enzyme appear distinct,

and the endogenous role of CBR3 remains unknown. We were initially drawn to CBR3 due to our lab's interest in the tripeptide glutathione (GSH), an abundant low-molecular weight antioxidant thiol within cells. GSH synthesis is rate-limited by the conjugation of glutamate to cysteine by glutamate cysteine ligase (GCL), which is composed of catalytic (GCLC) and modifier (GLCM) subunits. The level of GSH synthesized in the livers of mice lacking two copies of *Gclm* (*Gclm* -/-) is only ~10% relative to that of wild-type mice [12]. To compensate for low GSH levels, *Gclm* -/- mice have up-regulated a number of genes, especially those involved in antioxidant defense. *Cbr3* mRNA is the most highly up-regulated gene in the livers of *Gclm* -/- mice. On average, primary transcripts of *Cbr3* are increased approximately 10-fold relative to *Gclm* +/+ mice, a trend mirrored in another model of thiol insufficiency—conditional hepatic knockout of *Txnrd1* [13,14]. This is especially relevant in the context of doxorubicin metabolism, given the liver's critical role in xenobiotic biotransformation and detoxification.

While we are currently working to identify the endogenous substrate(s) of CBR3, which currently remain unknown, we present here evidence that doxorubicin is an exogenous substrate of mouse CBR3, a previously undocumented finding. We demonstrate a significantly higher rate of doxorubicinol formation in doxorubicin-treated *Gclm* -/- mouse hepatocytes relative to *Gclm* +/+ mouse hepatocytes, and also show that differentiated rat myoblasts (C2C12 cells) co-cultured with primary *Gclm* -/- mouse hepatocytes are more sensitive to doxorubicin-induced changes in cell growth and/or viability relative to those co-cultured with *Gclm* +/+mouse hepatocytes. Our findings are important for the ongoing elucidation of mechanisms of doxorubicin-induced

cardiotoxicity, and, given the central role of doxorubicin use in chemotherapy regimens, our results may prove clinically relevant upon further investigation.

2. Materials and Methods

2.1 Chemicals

All reagents for cell culture and biochemical analyses were purchased from Life Technologies (Carlsbad, CA) and/or Sigma-Aldrich (Saint Louis, MO), unless otherwise noted.

2.2 Purification of recombinant murine CBR3

The Cbr3 expression plasmid was made in two steps. First, the complete open reading frame (ORF) was amplified by polymerase chain reaction (PCR) using a RIKEN cDNA clone as template and primers that placed a Nde1 site overlapping the AUG start codon. The PCR product was blunt end-ligated into Sma1-cut pBluescipt II KS (Stratagene California, La Jolla, CA). The Nde1 site and a downstream *Hind3* site in the polylinker were then used to move the ORF into a similarly cleaved pET28a expression vector (EMD Millipore, Billerica, MA). The plasmid was shuttled to BL21, and a 500 ml culture was induced by addition of 1 mM isopropyl β-D-1-thiogalactopyranoside when it reached an A600 of 0.6. Six hours later, cells were collected by centrifugation, and disrupted by sonication (five one-minute bursts, on ice) in 20 ml of extraction buffer (300 mM NaCl, 50 mM Na_2HPO_4, pH 7), containing 20 mM imidazole and protease inhibitors (1 mM PMSF, 1μg/ml leupeptin, 1μg/ml pepstatin). Lysate was clarified by centrifugation (15 min at 15,000 rpm, SS-34 rotor) and mixed on a rotating wheel with a 1 ml slurry of Talon resin (Clontech Laboratories, Inc., Mountain View, CA). After collecting the resin by centrifugation and washing twice with 50 ml extraction buffer containing 20 mM imidazole, the resin was transferred in small volume of washing buffer to a nickel mini-column, and protein was eluted in extraction buffer containing 150 mM

imidazole. The first milliliter of eluate contained the highest concentration of recombinant protein and was used for gel and enzymatic analyses.

2.3 Animals

All procedures for animal use were in accordance with the National Institutes of Health Guide for the Use and Care of Laboratory Animals and were approved by the University of Washington Institutional Animal Care and Use Committee (IACUC). Female *Gclm* -/- mice were derived by homologous recombination techniques in mouse embryonic stem (ES) cells, as previously documented [12]. Mice were anesthetized with 0.02 ml/g of a mixture of ketamine and xylazine prior to liver perfusion and/or liver excision.

2.4 Liver excision and homogenization

Livers were excised from anesthetized mice and placed in TES/SB buffer (20 mM Tris, 1 mM ethylenediaminetetraacetic acid, 250 mM sucrose, 20 mM sodium borate, 2 mM serine) with protease inhibitor cocktail (Roche Molecular Biochemicals, Indianapolis, IN) on ice, and homogenized. Homogenates were then centrifuged at 9000 *x* g for 20 minutes at 4°C; the resulting supernatant was extracted and prepared for dialysis.

2.5 Primary murine hepatocyte isolation

Mouse livers were perfused and hepatocytes isolated by cannulating the hepatic portal vein and perfusing with Hanks' Balanced Salt Solution (HBSS) containing 0.5 mM ethylene glycol tetraacetic acid (EGTA) for 4 minutes, after which livers were perfused with 15 mg TH Research Grade Liberase (Roche, Madison, WI) per 100 ml perfusion medium (William's E medium supplemented with 2 mM L-glutamine, 10 mM HEPES

(pH 7.55), and 5 ug/ml ITS+ Premix (BD Biosciences, Bedford, MA)) for 6 minutes. Digested liver lobes were immediately placed in William's E Medium (supplemented with 2 mM L-glutamine, 5 ug/ml ITS+ Premix, 100 U penicillin and 100 ug/ml streptomycin, and 25 mM dexamethasone; WECM), on ice and then centrifuged at 130 x g for 5 minutes at 4 °C. Following centrifugation, enriched cell pellets were resuspended in Hepatozyme medium (Life Technologies) supplemented with 2 mM L-glutamine,100 U penicillin and 100 ug/ml streptomycin. Hepatocyte yields were assessed by trypan blue exclusion using a hemacytometer. A typical perfusion yielded approximately 20-30 million hepatocytes per liver.

2.6 Cell culture

All cells were cultured in 5% CO_2/95% air in a humidified incubator at 37 °C .

2.6.1 Primary hepatocytes.

Murine hepatocytes were seeded on collagen (25 ug/well)-coated six well plates (Corning Inc., Corning, NY) at a density of ~500,000 cells/well. After 4 hours incubation at 37 °C to allow for attachment, fresh WECM was added to each well.

2.6.2 C2C12 culture and differentiation.

Undifferentiated mouse C2C12 myoblasts were cultured in 75 cm^2 flasks at 37 °C for 24 hours using Dulbecco's Modified Eagle Medium (DMEM) supplemented with 10% fetal bovine serum and 100 IU penicillin plus 100 ug/ml streptomycin . C2C12 cells were then trypsinized and re-seeded onto 6-well Transwell Permeable Supports (0.4 μm polyester membrane; Corning Inc., Corning, NY), at a density of 75,000 cells/well, at which time medium was switched to DMEM supplemented with 2% horse serum and 100 U

penicillin plus 100 μg/ml streptomycin (differentiation medium) to allow for differentiation. Differentiation medium was replaced every 24 hours for 3 days.

2.7 Treatment and co-culture of primary mouse hepatocytes with C2C12 cells

After four hours incubation at 37 °C in Hepatozyme to allow for attachment, primary mouse hepatocytes were given 2 ml of fresh WECM, and treated with 0 (vehicle control), 2, 5, or 10 μM doxorubicin hydrochloride (dissolved in dimethyl sulfoxide (DMSO) vehicle; volume of DMSO did not exceed 0.2% for any treatment). Concomitantly, transwell inserts containing differentiated C2C12 cells were placed in wells containing hepatocytes cultured on the bottom of the wells. Medium within each insert was replaced with fresh differentiation medium (1.5 ml/insert). Underlying doxorubicin-treated hepatocytes and overlying C2C12 cells were co-cultured for 18 hours following treatment, after which time metabolic and toxicological endpoints were assessed.

2.8 High pressure liquid chromatography

HPLC analyses for hepatocyte lysates, culture media, and liver homogenate incubations were performed using a Shimadzu LC6A reverse-phase HPLC, with an RFIOAxI fluorescence detector and a C-R5A integrator (Kyoto, Japan). Samples were loaded in 50 mM monobasic potassium phosphate buffer (pH 2.5) and eluted under isocratic conditions, with the mobile phase containing 27% acetonitrile, 73% 50 mM monobasic potassium phosphate (pH 2.5) and a flow rate of 1 ml/minute through a 150-mm Synergi 5u Hydro – RP 80A column (Phenomenex, Torrance, CA). HPLC analysis of purified mCBR3 incubations was performed on a Waters 2690 Separations Module, with a Waters 474 Scanning Fluorescence Detector (Waters Corporation, Milford, MA). A slightly modified gradient to more effectively separate doxorubicin and doxorubicinol peaks was

employed—22% Acetonitrile, 78% in 50 mM monobasic potassium phosphate (pH 2.5) and a flow rate of 1 ml/minute through a 150-mm Synergi 5u Hydro – RP 80A column (Phenomenex, Torrance, CA). Excitation and emission wavelengths were 470 nm and 590 nm, respectively, and Waters Millenium Software V2.0 was used for data processing (Waters Corporation, Milford, MA).

2.8.1 Detection of doxorubicinol in media and primary mouse hepatocytes.

Following 18 hours doxorubicin treatment, 5% 5-sulfosalicylic acid (SSA) was added to culture media in microfuge tubes, on ice, for 10 min and then centrifuged at 14,000 x g for 2 minutes at room temperature. Resulting supernatants were analyzed by HPLC. For hepatocytes, cells were washed with phosphate-buffered saline and trypsinized for 15 min at 37 °C using 0.25% trypsin/2.21 mM EDTA in HBSS (Cellgro, Corning Inc., Corning, NY). They were then removed from the dishes by scraping, triturated 3-5 times and transferred to microfuge tubes. Next, hepatocytes were centrifuged for five minutes at 130 x g, 4°C, resuspended in TES/SB and sonicated on ice. Cell lysates were centrifuged for 2 minutes at 14,000 x g (4°C) and the resulting supernatant was added to 5% SSA, incubated on ice for 15 minutes, and centrifuged again at 14,000 x g (room temperature) for 2 minutes. Resulting supernatants (pH=2.5) were used for HPLC analyses.

2.8.2 Detection of doxorubicinol formation in liver homogenates.

Aliquots of liver cytosolic fractions prepared by centrifugation of liver homogenates at 9000 x g (S9 fraction) from female *Gclm* +/+ and *Gclm* -/- mice were placed in 3.0 mL dialysis cassettes (Thermo Scientific, Waltham, MA) overnight in a solution of 100 mM monobasic potassium phosphate, pH 7.4. The following day, 20 µl of the dialyzed liver S9 fraction (approximately 50-70 mg/ml concentration) were transferred to microfuge

tubes containing 15 µl of 10 mM nicotinamide adenine dinucleotide phosphate (NADPH) in 100 mM monobasic potassium phosphate (pH 7.4), 1.5 µl of 1 mg/ml doxorubicin hydrochloride (in DMSO), and 113.5 µl of 100 mM monobasic potassium phosphate buffer (pH 7.4). Samples were briefly vortexed, then placed on a rocker in the dark at 37 °C, and allowed to incubate for one hour. Next, 50 µl of 5% SSA was added to each sample, on ice, for 15 minutes, and samples were centrifuged at 14,000 x g for 2 minutes. Resulting supernatants were used for HPLC analysis.

2.8.3 Detection of doxorubicinol formation using purified recombinant murine CBR3.

Incubations with purified recombinant mouse CBR3 (mCBR3), followed the same protocol as incubations with liver homogenates. Briefly, 1 µl of 55 mM mCbr3, 1 µl of 1 mg/ml doxorubicin, 15 µl of 10 mM NADPH, and 133 µl 100 mM monobasic potassium phosphate buffer (pH 7.4) were briefly vortexed, then placed on a rocker in the dark at 37 °C, and allowed to incubate for one hour. Next, 50 µl of 5% SSA was added to each sample, on ice, for 15 min, and samples were centrifuged at 14,000 X g for 2 minutes. Resulting supernatants were used for HPLC analysis. For control experiments, the same protocol was followed, with the additional step of boiling mCBR3 for ten minutes prior to incubation with doxorubicin and NADPH.

2.9 Liquid Chromatography/Mass Spectrometry (LC/MS)

Gclm WT and null murine liver homogenates were incubated with 0.067 µg (1 µg/150 µl total incubation volume) doxorubicin for 60 minutes at 37 °C in the dark, as described in section 2.8.2 of Methods. Following incubation and derivitization, samples were analyzed using LC/MS to confirm the presence of the doxorubicinol metabolite. Samples were run

on an Agilent Technologies (Santa Clara, CA) MS QQQ Mass Spectrometer using a Poroshell SB-C18 (3.0mm x 50mm x 2.7 μ) column at 0.4 ml/minute flow rate (0.1% formic acid buffer). An internal standard of epirubicin (4'-epimer of doxorubicin) was used to differentiate between doxorubicinol and doxorubicin. The mass to charge (*m/z*) ratio for the precursor ions of doxorubicin and epirubicin were 544.2, and 546.1 for doxorubicinol (determined using standards of each compound). The *m/z* of the product ions were 361.1 and 397.1 for epirubicin and doxorubicin, respectively, and 363.1 and 399.2 for doxorubicinol. Analyses were performed in triplicate for each *Gclm* genotype.

2.10 Assessment of C2C12 cell viability

Cellular cytostasis and/or cytotoxicity of C2C12 cells following 18 hour co-culture with doxorubicin-treated primary mouse hepatocytes was determined spectrophotometrically by measuring the reduction of the tetrazolium salt 3-(4,5-dimethylthiazol-2-yl)-2,5-diphenyltetrazolium bromide (MTT) to formazan as previously described [15].

2.11 Protein isolation

Total protein concentration in cell lysates from primary mouse hepatocytes and S9 liver homogenate fractions was determined using the Bio-Rad Protein Assay Dye Reagent (Bio-Rad Laboratories Inc., Hercules, CA), in 96-well microtiter plates, following the manufacturer's protocol.

2.12 Western Blotting

Western blotting was performed using standard techniques. Briefly, ~15 ug protein per sample were separated by electrophoresis using 12% Tris-Glycine mini-gels in a Novex XCell *SureLock* Mini-Cell (Life Technologies, Carlsbad, CA). Following electrophoresis,

proteins were transferred to polyvinyldiene difluoride (PVDF) membranes (Immobilon-P, Millipore, Billerica, MA). Membranes were blocked with 5% milk in tris-buffered saline with Tween 20 (TBS-T) and incubated with primary antibodies raised against mouse Cbr3 (1:1000 dilution; rabbit polyclonal antisera; GFM, unpublished), β-actin (1:1000 dilution; Cell Signaling, Beverly, MA), and Gclm (1:50000; rabbit polyclonal antisera, as described previously [12]), followed by incubation with horseradish peroxidase-conjugated secondary rat anti-rabbit antibody (Millipore, Billerica, MA), diluted 1:10,000 in 5% milk TBS-T.

2.13 Statistical Analyses

Data are expressed as the mean and SEM, unless otherwise noted. Data were analyzed by one- or two-way ANOVA, followed by a Dunnett's post-hoc test (for cytotoxicity experiments), or a Student's *t*-test (for pair-wise comparisons) using a statistical software package (Prism, GraphPad, Inc., San Diego, CA). Differences yielding a *p* value of less than 0.05 were considered statistically significant.

3. Results

3.1 Carbonyl reductase 3 levels in the livers of Gclm -/- and Gclm +/+ mice

Western blotting of primary hepatocyte lysates and dialyzed liver homogenates (S9 fraction) confirmed that CBR3 protein is highly up-regulated in the livers of *Gclm -/-* mice relative to *Gclm +/+* mice (Figure 2).

3.2 Assessment of the ability of mCBR3 to metabolize doxorubicin to doxorubicinol

We report here that doxorubicin is a substrate of murine CBR3. Incubation of purified mCBR3 with doxorubicin and NADPH, revealed the formation of doxorubicinol with HPLC analysis, at the expected elution time of approximately 10 minutes (Figure 3).

3.3 Doxorubicinol formation in primary mouse hepatocytes and liver homogenates

Primary *Gclm -/-* mouse hepatocytes treated for 18 hours with 2, 5, or 10 uM doxorubicin had significantly higher levels (~2.5- to 3.5-fold) of both cellular and extracellular doxorubicinol than *Gclm +/+* mouse hepatocytes, as measured by HPLC (Figure 4; n=12, $p < 0.001$ for all doses). A graded dose-response of doxorubicinol formation was observed with increasing doxorubicin treatment (Figure 4). Additionally, dialyzed liver S9 homogenates (cytosolic + microsomal fraction) from *Gclm -/-* mice produced approximately 2.5-fold more doxorubicinol than S9 fractions from *Gclm +/+* homogenates (Figure 5; n=4, $p < 0.05$).

3.4 LC/MS Analysis of doxorubicinol formation in liver homogenates

Analysis of doxorubicinol formation using mass spectrometry confirmed the identity of the putative doxorubicinol peak observed in HPLC analyses. Additionally, following the trend observed in HPLC analyses, 2- to 3-fold more doxorubicinol was formed in

incubations containing *Gclm* -/- liver homogenate relative to *Gclm* +/+ liver homogenate (Figure 6).

3.5 Co-culture of differentiated mouse myoblasts with doxorubicin-treated primary murine hepatocytes

C2C12 cells differentiated on transwell inserts were placed on top of primary *Gclm* -/- or *Gclm* +/+ mouse hepatocytes and then treated with doxorubicin to assess the effect of hepatocyte genotype on the production of compound(s) affecting myocyte viability, an *in vitro* proxy of liver-mediated metabolism resulting in cardiotoxicity. Significantly decreased C2C12 cell viability and/or cell growth (as measured by the MTT assay) was observed in C2C12 cells co-cultured with primary *Gclm* -/- hepatocytes relative to those co-cultured with primary *Gclm* +/+ hepatocytes (Figure 7; n=6 per dose and genotype, $p < 0.001$ by two-way ANOVA and Dunnet's post-hoc analysis).

4. Discussion

In this study, we investigated the potential role of a poorly characterized enzyme, mouse CBR3, in doxorubicin metabolism. Preliminary epidemiological data implicate human CBR3 polymorphisms as being important in predicting doxorubicinol formation [3,9,16,17]. Because doxorubicinol is believed to contribute significantly to cardiotoxicity in cancer patients given doxorubicin as part of chemotherapy regimens, further investigation into the role of CBR3 in doxorubicin metabolism was warranted [6].

We first tested the ability of purified recombinant mCBR3 to metabolize doxorubicin. Our results indicate that murine CBR3 is indeed able to convert doxorubicin to doxorubicinol, a previously undocumented finding. The Nrf2-regulated CBR3 enzyme [18] is highly up-regulated in *Gclm* -/- mice (a model of glutathione deficiency) relative to *Gclm* +/+ mice. Accordingly, we evaluated the ability of primary mouse hepatocytes and liver homogenates from *Gclm* -/- and *Gclm* +/+ mice to produce doxorubicinol. *Gclm* -/- hepatocytes produced significantly higher levels of doxorubicinol following 18 hours of doxorubicin treatment in a dose-dependent fashion, relative to *Gclm* +/+ hepatocytes. Additionally, dialyzed liver homogenates from *Gclm* -/- mice produced significantly higher amounts of doxorubicinol following incubation with doxorubicin.

Following these observations, we expanded our focus to a physiologically-relevant *in vitro* system to model cardiotoxicity induced by doxorubicin treatment. We used differentiated C2C12 cells (a murine myoblast cell line) as a surrogate for cardiomyocytes, and co-cultured them with primary murine hepatocytes from *Gclm* -/-

and *Gclm* +/+ mice. As anticipated, a greater impact on C2C12 cell viability/numbers was observed in co-cultures with doxorubicin-treated *Gclm* -/- mouse hepatocytes relative to cultures with *Gclm* +/+ mouse hepatocytes. Moreover, there was an inverse relationship between doxorubicinol concentration and cell numbers and/or viability in these *in vitro* cell culture studies.

Because of their enhanced CBR3 expression, *Gclm -/-* mice are likely to exhibit increased sensitivity to doxorubicin-induced cardiomyopathy, relative to *Gclm* +/+ mice, a hypothesis that we are currently in the process of investigating with *in vivo* studies..

Ultimately, the overarching goal of this research is to reduce doxorubicin-induced cardiomyopathy to a level at which doxorubicin administration is not dose-limited by off-target cardiotoxicity. Doxorubicin continues to be and will likely remain a widely used chemotherapeutic central to numerous chemotherapy regimens [1]. Despite the discovery and use of targeted, less toxic therapies for specific cancer types (e.g., Trastuzumab), little progress has been made in reducing off-target cardiotoxicity induced by anthracyclines since their clinical introduction nearly 40 years ago [1,19]. Our findings not only implicate CBR3 in doxorubicin metabolism, but underscore the potential importance of CBR3 inhibition in the context of doxorubicin-containing therapies. Finally, if validated in appropriate pre-clinical models, such inhibition would represent a novel advancement in the treatment of a wide variety of cancers.

Funding Information

This work was supported by National Institutes of Health grants P30ES007033 and T32AG000057, a grant to TJK from the University of Washington Department of Environmental and Occupational Health Sciences, and a grant to GFM from the Medical Research Foundation of Oregon.

Acknowledgements

We wish to thank members of the Kavanagh laboratory, and Drs. Chad Weldy, Trevor Penning, Edmund Maser, and Udo Oppermann, for their encouragement and helpful suggestions, and Brian Phillips and the laboratory of Dr. Danny Shen, UW Department of Pharmaceutics, for assistance with LC/MS analysis.

References

1. Lipshultz, S.E., Cochran, T.R., Franco, V.I., and Miller, T.L. (2013). Treatment-related cardiotoxicity in survivors of childhood cancer. *Nat. Rev. Clin. Oncol.* **10(12),** 697-710.
2. Singal, P.K., and Iliskovic, N. (1998). Doxorubicin-induced cardiomyopathy. *N. Engl. J. Med*. **339(13),** 900-905.
3. Blanco, J.G., Sun, C.L., Landier, W., Chen, L., Esparza-Duran, D., Leisenring, W., Mays, A., Friedman, D.L., Ginsberg, J.P., Hudson, M.M., Neglia, J.P., Oeffinger, K.C., Ritchey, A.K., Villaluna, D., Relling, M.V., and Bhatia, S. (2012). Anthracycline-related cardiomyopathy after childhood cancer: role of polymorphisms in carbonyl reductase genes—A report from the Children's Oncology Group. *J. Clin. Oncol.* **30(13),** 1415-1421.
4. Kremer, L.C.M., and Caron, H. (2004). Anthracycline cardiotoxicity in children. *N. Engl. J. Med.* **351,** 120-121.
5. Boucek, R. J., Olson, R. D., Brenner, D. E., Ogunbunmi, E. M., Inui, M., and Fleischer, S. (1987). The major metabolite of doxorubicin is a potent inhibitor of membrane-associated ion pumps. A correlative study of cardiac muscle with isolated membrane fractions. *J. Biol. Chem*. **262(33)**, 15851-15856.
6. Olson, R.D., Mushlin, P.S., Brenner, D.E., Fleischer, S., Cusack, B.J., Chang, B.K., and Boucek, R.J. (1988). Doxorubicin cardiotoxicity may be caused by its metabolite, doxorubicinol. *Proc. Natl. Acad. Sci. USA*. **85(10),** 3585-3589.

7. Kassner, N., Huse, K., Martin, H.J., Gödtel-Armbrust, U., Metzger, A., Meineke, I., Brockmöller, J., Klein, K., Zanger, U.M., Maser, E., and Wojnowski, L. (2005). Carbonyl reductase 1 is a predominant doxorubicin reductase in the human liver. *Drug Metab. Dispos*. **36(10),** 2113-2120.
8. Oppermann, U. (2007). Carbonyl reductases: the complex relationships of mammalian carbonyl- and quinone-reducing enzymes and their role in physiology. *Annu. Rev. Pharmacol. Toxicol.* **47,** 293-322.
9. Fan, L., Goh, B.C., Wong, C.I., Sukri, N., Lim, S.E., Tan, S.H., Guo, J.Y., Lim, R., Yap, H.L., Khoo, Y.M., Iay, F., Lee, H.S., and Lee, S.C. (2008). Genotype of human carbonyl reductase CBR3 correlates with doxorubicin disposition and toxicity. *Pharmacogenetics and Genomics.* **18(7),** 623-631.
10. Lubieniecka, J.M., Liu, J., Heffner, D., Graham, J., Reid, R., Hogge, D., Grigliatti, T.A., and Riggs, W.K. (2012). Single-nucleotide polymorphisms in aldo-keto and carbonyl reductase genes are not associated with acute cardiotoxicity after daunorubicin chemotherapy. *Cancer Epidemiol Biomarkers Prev*. **21(11),** 2118-2120.
11. Bains, O.S., Karkling, M.J., Lubieniecka, J.M., Grigliatti, T.A., Reid, R.E., and Riggs, K.W. (2010). Naturally occurring variants of human CBR3 alter anthracycline in vitro metabolism. *J Pharmacol Exp Ther.* **332(3),** 755-763.
12. McConnachie, L.A., Mohar, I., Hudson, F.N., Ware, C.B., Ladiges, W.C., Fernandez, C., Chatterton-Kirchmeier, S., White, C.C., Pierce, R.H., and Kavanagh, T.J. (2007). Glutamate cysteine ligase modifier subunit deficiency and gender as determinants of acetaminophen-induced hepatotoxicity in mice. *Toxicol. Sci.* **99(2),** 628-636.
13. Haque, J.A., McMahan, R.S., Campbell, J.S., Shimizu-Albergine, M., Wilson, A.M., Botta,D., Bammler, T.K., Beyer, R.P., Montine, T.J., Yeh, M.M., Kavanagh, T.J., and Fausto, N. (2010). Attenuated progression of diet-induced steatohepatitis in glutathione-deficient mice. *Lab Invest.* **90(12),** 1704-1717.
14. Bondareva, A.A., Capecchi, M.R., Iverson, S.V., Li, Y., Lopez, N.I., Lucas, O., Merrill, G.F., Prigge, J.R., Siders, A.M., Wakamiya, M., Wallin, S.L., and Schmidt, E.E. (2007). Effects of thioredoxin reductase-1 deletion on embryogenesis and transcriptome. *Free Radic. Biol. Med.* **43(6),** 911-23.
15. Carmichael, J., Degraff, W.G., Gazdar, A.F., Minna, J.D., and Mitchell, J.B. (1987). Evaluation of a Tetrazolium-based Semiautomated Colorimetric Assay: Assessment of Chemosensitivity Testing. *Cancer Res*. **47**, 936.
16. Blanco, J.G., Leisenring, W.M., Gonzalez‐Covarrubias, V.M., Kawashima, T.I., Davies, S.M., Relling, M.V., Robison, L.L., Sklar, C.A., Stovall, M., and Bhatia, S. (2008). Genetic polymorphisms in the carbonyl reductase 3 gene CBR3 and the NAD(P)H: quinone oxidoreductase 1 gene NQO1 in patients who developed anthracycline‐related congestive heart failure after childhood cancer. *Cancer.* **112(12),** 2789-2795.
17. Jamieson, D., and Boddy, A.V. (2011). Pharmacogenetics of genes across the doxorubicin pathway. *Expert Opin. Drug Metab. Toxicol.* **7(10),** 1201-1210.
18. Ebert, B., Kisiela, M., Malátková, P., El-Hawari, Y., and Maser, E. (2010). Regulation of human carbonyl reductase 3 (CBR3; SDR21C2) expression by Nrf2 in cultured cancer cells. *Biochemistry*. **49(39),** 8499-8511.

19. Hudis, C.A. (2007). Trastuzumab--mechanism of action and use in clinical practice. *N. Engl. J. Med.* **357(1),** 39–51.

Figures

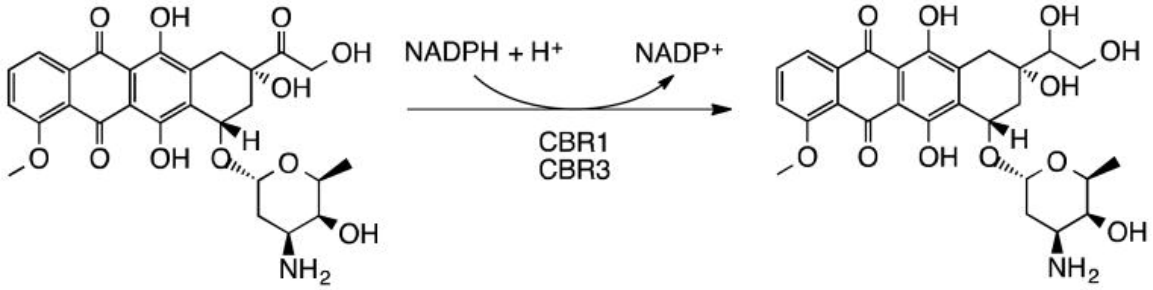

Figure 1. Two-electron reduction of doxorubicin to the putative cardiotoxic alcohol metabolite, doxorubicinol, at the 13th carbon. NADPH-dependent monomeric carbonyl reductase CBR1 is known to mediate this reaction. Here, we demonstrate that this reaction is also carried out by a protein that shares high sequence identity with Cbr1, carbonyl reductase 3.

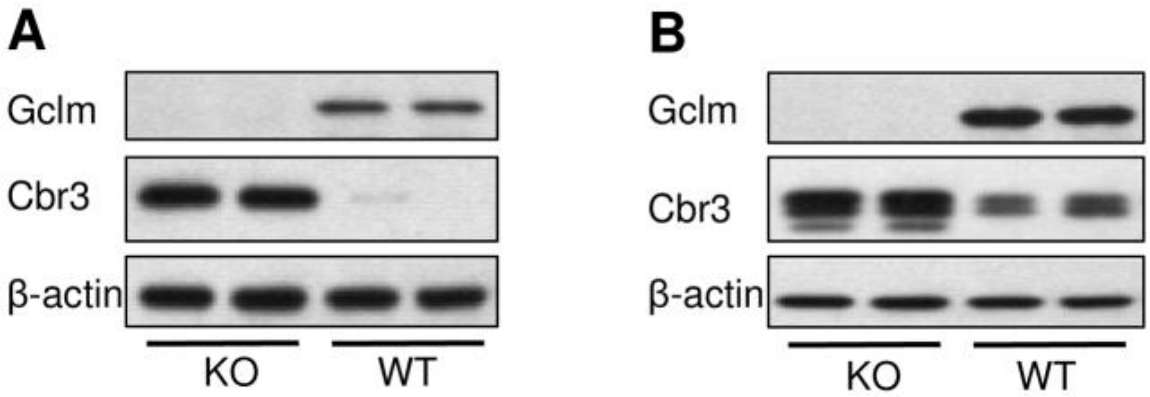

Figure 2. Representative Western blot analyses of GCLM, CBR3, and β-actin (loading control) proteins in (A) primary murine hepatocytes and (B) dialyzed liver homogenates from *Gclm* -/- and *Gclm* +/+ mice.

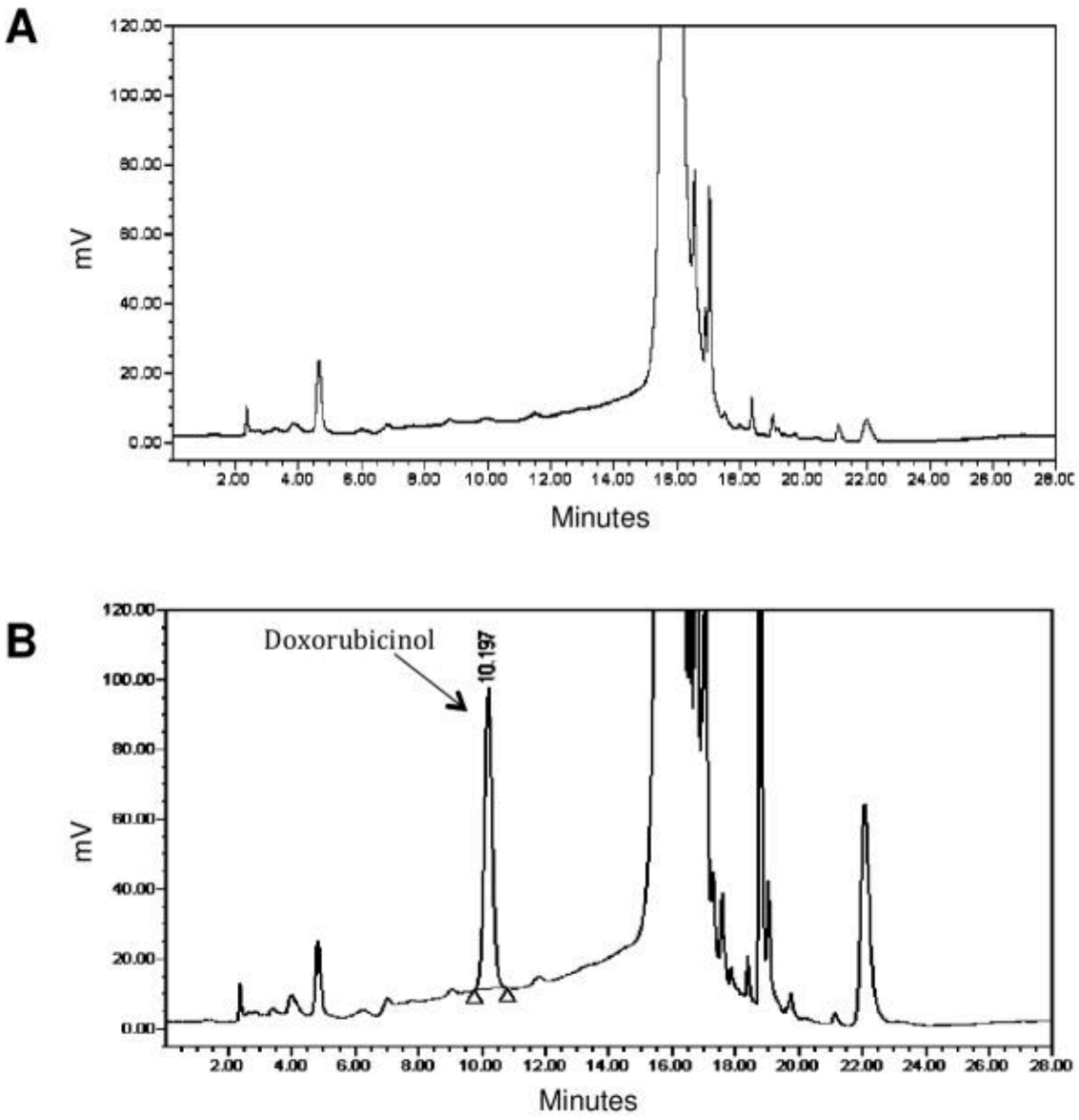

Figure 3. HPLC chromatograms showing doxorubicinol formation with (A) catalytically inactive and (B) catalytically active purified mCBR3. Doxorubicinol eluted at ~10 minutes, while doxorubicin eluted at ~15 minutes.

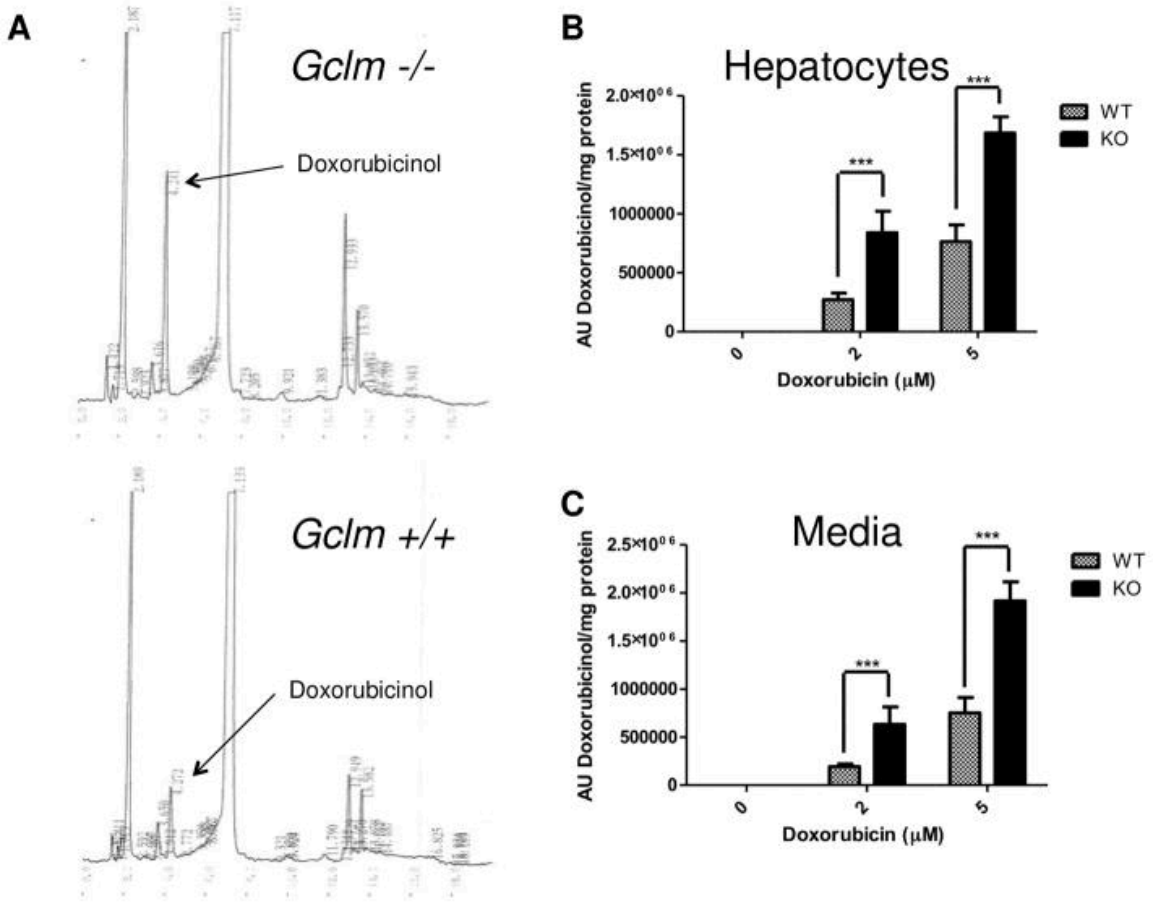

Figure 4. Doxorubicinol formation in *Gclm -/-* and *Gclm +/+* hepatocytes. (A) Representative HPLC chromatograms of doxorubicinol formation in *Gclm -/-* (top panel) and *Gclm +/+* (bottom panel) hepatocytes. (B) Quantification by HPLC of doxorubicinol formation (area units, AU) in hepatocytes and (C) media taken from doxorubicin treatments; n=12 for each treatment. *** indicates $p < 0.001$ for Student's *t*-test relative to wild-type for each dose.

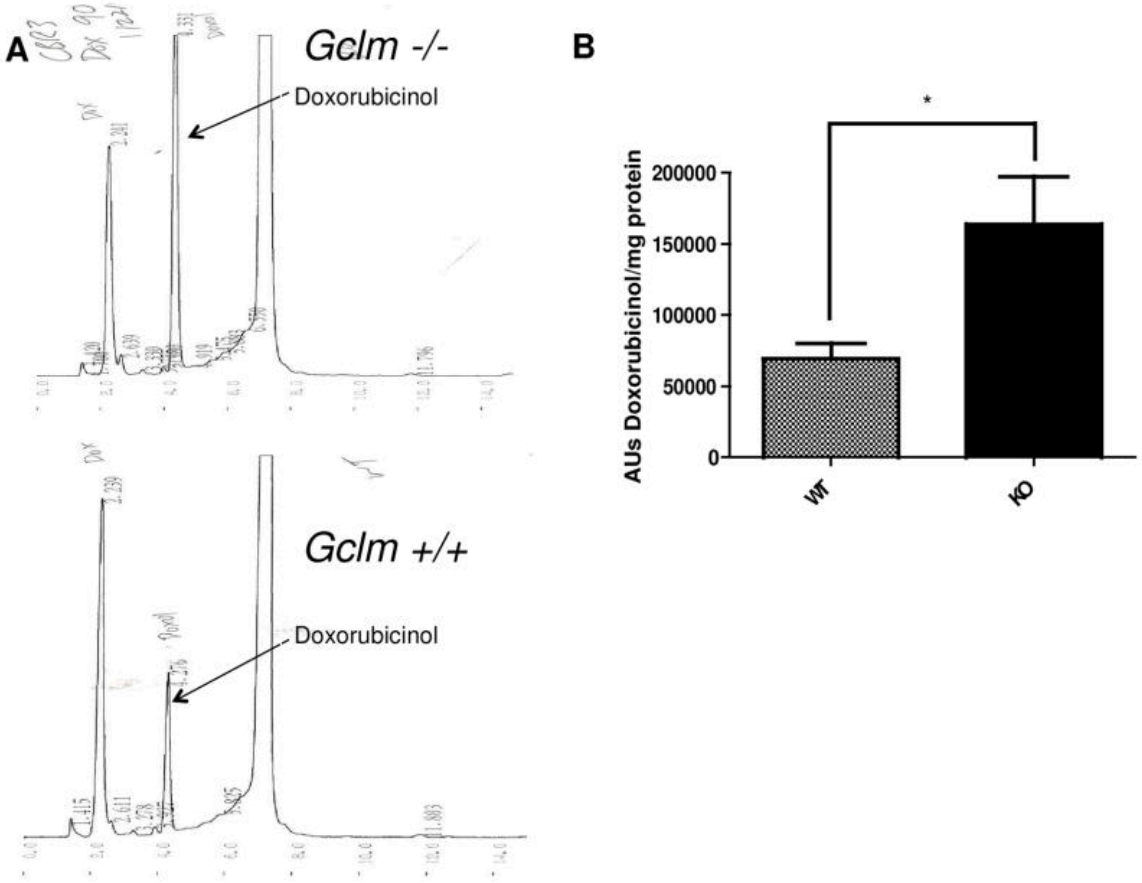

Figure 5. Doxorubicinol formation by *Gclm -/-* and *Gclm +/+* liver homogenates. (A) Representative HPLC chromatograms of doxorubicinol formation in *Gclm -/-* (top panel) and *Gclm +/+* (bottom panel) dialyzed liver homogenates. (B) Quantification by HPLC of doxorubicinol formation (area units, AU) in dialyzed liver homogenates following incubation with 50 mM doxorubicin; n=4 per genotype. *indicates $p < 0.05$ for Student's *t*-test relative to wild-type.

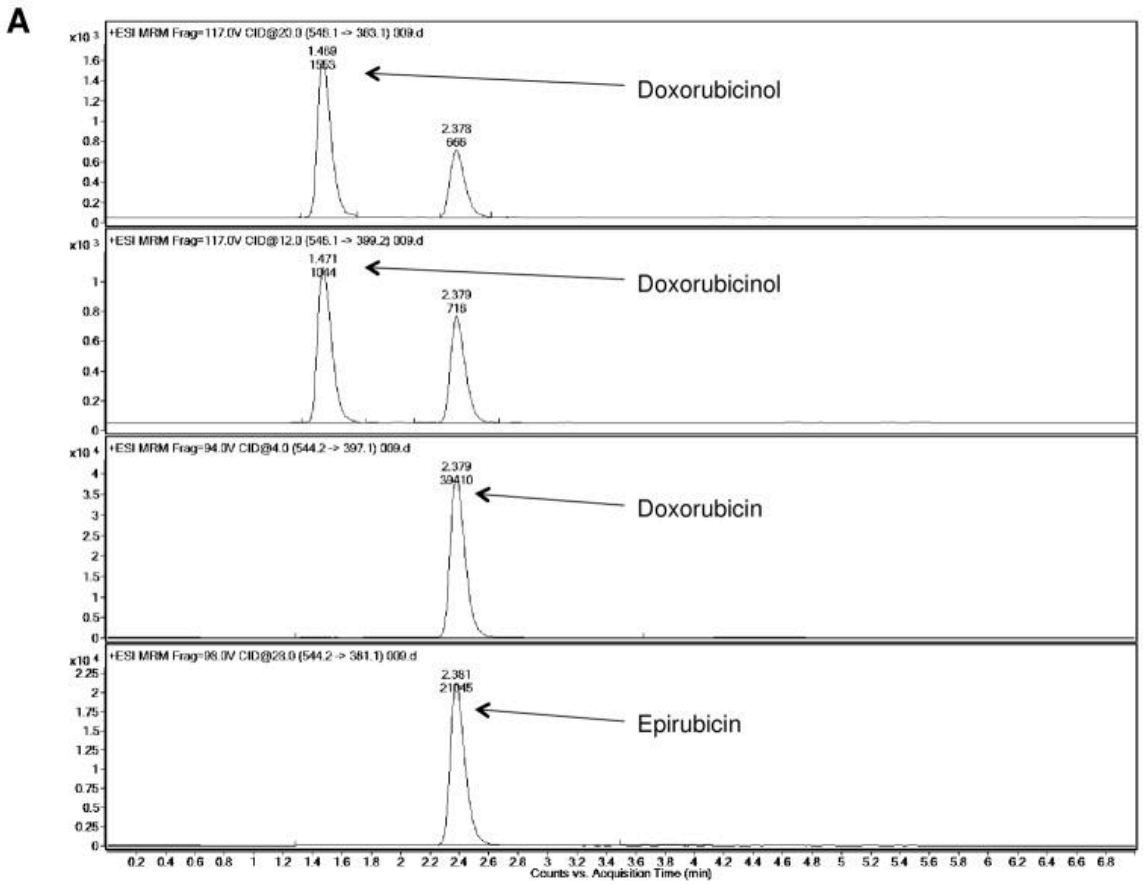

Figure 6. LC/MS analysis of liver homogenate-doxorubicin incubations. Confirmation of doxorubicinol formation in (A) *Gclm* +/+ and (B) *Gclm* -/- liver homogenates. Precursor ions for doxorubicin and epirubicin had a m/z of 544.2, while the precursor ion for doxorubicinol had a m/z of 546.1. The mass-to-charge ratio of the product ions for doxorubicin and epirubicin were 397.1 and 361.1, respectively, while doxorubicinol had two product ions with m/z ratios of 399.2 and 363.1.

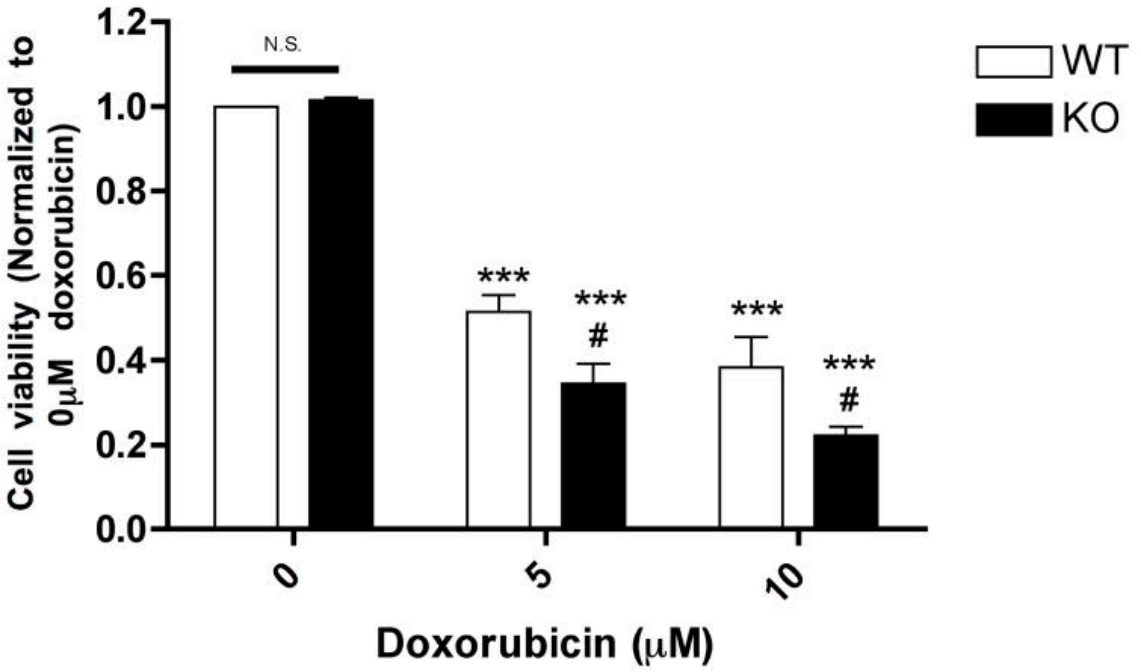

Figure 7. Cytotoxicity in C2C12 cells following co-culturing with either *Gclm -/-* or *Gclm +/+* primary hepatocytes. Two-way ANOVA analysis, *** indicates $p < 0.001$ relative to controls, # indicates $p < 0.001$ relative to wild-type at each; representative of two independent experiments, n=3 per dose and genotype per experiment; n.s. - not significant.